

**Modulation of Bioavailability of Selected Anti-tuberculosis drugs
by Herbal Preparations of *Cuminum cyminum* and *Carum carvi*.**

THESIS

**Submitted in partial fulfilment
of the requirements for the degree of
DOCTOR OF PHILOSOPHY**

By

SACHIN S. BHUSARI

Under the Supervision of

Dr. R. K. Johri



BIRLA INSTITUTE OF TECHNOLOGY AND SCIENCE

PILANI (RAJASTHAN) INDIA

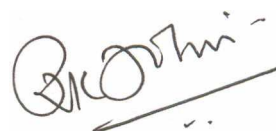
2010

BIRLA INSTITUTE OF TECHNOLOGY AND SCIENCE

PILANI (RAJASTHAN)

CERTIFICATE

This is to certify that the thesis entitled “**Modulation of Bioavailability of Selected Anti-tuberculosis drugs by Herbal Preparations of *Cuminum cyminum* and *Carum carvi***” submitted by SACHIN SHIVLING BHUSARI, ID. No. 2005PHX403 for the award of Ph.D. Degree of the Institute embodies original work done by him under my supervision.



Dr. R.K. JOHRI
Deputy Director & Scientist G
PK/PD Toxicology Division
IIM, (CSIR) Jammu

Date: 06-05-2010

Acknowledgement

It is proud privilege to acknowledge the help I have received from various sources during my Ph.D.

I am immensely thankful to Prof. L. K. Maheshwari, Vice-Chancellor, BITS, Pilani for providing me this opportunity to pursue the off-campus Ph.D. of the Institute. I express my gratitude to Prof. Ravi Prakash, Dean, Research and Consultancy Division (RCD), BITS, Pilani for his constant official support, encouragement and making the organization of my research work through the past few years easy.

I thank Dr. Hemanth Jadav, Mr. Dinesh Kumar, Ms. Monica Sharma, Mr. Sharad Shrivastava, Mr. Gunjan Soni, Mr. Amit Kumar and Ms. Sunita Bansal, nucleus members of RCD, BITS, Pilani, without whose cooperation and guidance it would not have been possible for me to pursue such goal oriented research during each of the past few semesters.

I also express my gratitude to the office staff of RCD whose secretarial assistance helped me in submitting the various evaluation documents in time and give pre-submission seminar smoothly.

I thank my Doctoral Advisory Committee (DAC) members, Dr. R. Mahesh and Dr. Hemanth Jadhav, who spared their valuable time to go through my draft thesis and were audience to my pre-submission seminar in order to provide several valuable suggestions that immensely helped in improving the quality of my Ph.D. thesis report.

I express my profound gratitude to my esteemed brilliant and erudite guide Dr. R. K. Johri for making me fortunate enough to get the opportunity to work under his able guidance and supervision. Present thesis work is the outcome of his efforts, keen

interest, constructive criticism, kind cooperation and time-to-time help. His guidance, appreciation and encouragement always inspired me to pursue the investigation.

I am highly thankful to Dr. Ram Vishwakarma, honorable director of IIM Jammu for allowing me to continue my Ph.D. work.

The natural product chemistry part of present work is the result of inputs received from Dr. K. A. Suri, Dr. N. K. Satti and Dr. B. D. Gupta (Natural Product Chemists, IIM, Jammu). The isolation and characterization of phyto-constituents was possible only because of their constant and restless efforts. The knowledge and experience of the natural product chemists made my work smooth and easy. I will be always thankful for their major contribution in developing my vision towards natural product chemistry and thesis work.

Dr. Ravi Khajuria (Instrumentation Division) helped me in all manners while developing the HPLC finger-print profiles of phyto-constituents. His sound analytical knowledge resulted in establishment of quality finger-printing method and spectrums of phyto-constituents.

I must mention the names of people who contributed a lot in developing my experimental skills in pharmacology. The kind of guidance I received from Ms. Anita Khosa, Ms. Supriya Koul, Ms. Rinku Bhat, Rashmi Madam, Dr. G.D. Singh, Dr. Surjeet Singh and Dr. Anamika is simply unforgettable.

I shall always remember the kind blessings and moral support that Mr. Ashok Tikoo, Mr. Manoj Tikoo, Dr. Subhash Sharma and Dr. Sarojini Johri has given me. They have played the role of my guardians in a place like Jammu, which was new for me altogether.

I must place on record special thanks to Dr. R. K. Raina (PME Division), Dr. S. Koul (Bio-Organic Chemistry Division), Dr. H. M. S. Sampathkumar, Mr. S. D.

Sawant, Mr. Parvinder Singh (Synthetic Organic Chemistry Division), Dr. Saxena, Dr. Shashank Kumar Singh (Pharmacology Division) for their constant help.

I am thankful to my colleagues Meenakshi Koul and Vandhna Bhat for their encouragement throughout this work.

I am touched by the support of Arpita, her parents and their moral encouragement which kept me working in my difficult times.

The senior research fellowship granted by CSIR is highly acknowledged.

Lastly I would like to thank all the people who have criticized me, making me work much harder and thus contributing to the perfection of my work.

And now, due to incapability to express my gratitude towards my parents and god in words, I would just bow my head in their honour.....

Sachin

Abstract

The present investigation highlights a novel drug bioavailability enhancing profile of two related herbs, cumin (white jeera) and caraway (black jeera). In wistar rat, it was found to that the absolute oral bioavailability of rifampicin was decreased when administered in combination with isoniazid and pyrazinamide. The herbal products from cumin seed (solvent-derived extracts/fractions) prominently enhanced the plasma levels of rifampicin (either alone or in combination with isoniazid and pyrazinamide) when co-administered. This activity was found to be located in a molecule, identified as 3', 5'-dihydroxyflavone-7-O- β -D-galacturonide-4'-O- β -D-glucopyranoside from cumin. On the other hand, herbal products from caraway (solvent-derived extracts/fractions) showed a promising enhancement of plasma levels of all the 3 anti-TB drugs, RIF, INH and PZA (when administered in combination).

Further studies were also undertaken to evaluate the involvement of known biochemical regulators of oral bioavailability in the mode of action profile of cumin/caraway bioactive moieties. It was found that a flavonoid glycoside (identified as the bioactive molecule from cumin), increased the absorption of rifampicin across intestinal absorptive surface, while herbal products from caraway increased the absorption of all the 3 anti-TB drugs. Additionally flavonoid glycoside inhibited (a) P-gp mediated intestinal efflux, (b) P-gp dependent intestinal ATPase activity and (c) Hepatic CYP 3A4 activity (hydroxylation). The bioactive moieties have not shown any mucosal toxicity. In acute, sub-acute (4- week), and sub-chronic (8-week) toxicity study, no adverse effects of the bioactive moieties were observed.

Contents

S. No.	Particulars	Page
1	Introduction	1
2	Aims and Objectives	6
3	Review of Literature	7
4	Materials and Methods	
	Materials	48
	Development and validation of HPLC protocols	52
	SOP for determination of anti-TB drugs in plasma	59
	Preparation of herbal test materials	60
	HPLC method for finger printing	63
	Bio-evaluation of parent extracts from cumini/caraway	64
	Activity guided fractionation of cumini	65
	Isolation of active principle from CM-1(2)	67
	Spectral analysis	68
	Bio-evaluation of FG molecules	73
	Activity guided fractionation of caraway	75
	Isolation of marker(s) from CR-1(1)	79
	Pharmacokinetic study of anti-TB drugs (Oral/i.v.) alone and in presence of active test material(s)	82
	<i>In-vitro/ex-vivo</i> mode of action studies	
	Passive transport (PAMPA)	84
	Active transport (Gut sac studies)	85
	Active transport (In-situ studies)	87
	Active transport (Epithelial cells)	89
	P-glycoprotein ATPase activity (Intestinal membrane)	91
	CYP 3A4 enzyme (Liver microsomes)	92
	Toxicity studies	
	Mucosal membrane integrity studies	95
	Acute toxicity studies	95
	Sub-acute toxicity studies	96
	Sub-chronic toxicity studies	97

	Statistical analysis	98
5	Results	100
6	Discussion	148
7	Conclusion	173
8	Specific contribution of present work	176
9	Future scope of the work	177
10	Appendices	
	Annexure-I: Patent Mapping	
	Annexure-II: Lowry Method	
	Annexure-III: Fiske-Subbarow Method	
	Annexure-IV: PK software Data	
11	List of Publications and Presentations	
12	Biography	

List of Tables

	Description	Pg. No.
Table 1	Normal and reverse phase chromatography	20
Table 2	Documented HPLC analysis of anti-TB drugs (1977-2007)	24
Table 3A	Bioactivity profile of <i>Carum carvi</i>	32
Table 3B	Bioactivity profile of <i>Cuminum cyminum</i>	32-33
Table 4	Preparation of standard solutions (RIF)	55
Table 5	Preparation of standard solutions (INH+PZA)	56
Table 6	System suitability test	101
Table 7	Details of parameters and linearity data of calibration curves	103
Table 8	Accuracy data of RIF, INH and PZA	104
Table 9	Precision data of RIF, INH and PZA	105
Table 10	Stability data of RIF	108
Table 11	Stability data of INH and PZA	109
Table 12	Effect of CM test materials on plasma levels of RIF, INH and PZA	111
Table 13	Effect of CR test materials on plasma levels of RIF, PZA and INH	113
Table 14A	Pharmacokinetic parameters of RIF, INH and PZA (oral)	118
Table 14B	Pharmacokinetic parameters of RIF	121
Table 15	Absolute/relative bioavailability	123
Table 16	Mucosal to serosal transfer of RIF	125
Table 17	Serosal to mucosal transfer of Rho123	128
Table 18	Effect of FG-3, RIF and verapamil on Rho123 clearance under steady state plasma conc. of Rho123	132
Table 19	Effect of FG-3 on the ³ H-benzopyrene transport (Guinea pig intestinal epithelial cells)	133
Table 20	Effect of test materials on mucosal (luminal) protein content of un-everted sac	138
Table 21A	Hematological values of rats treated with FG-3 (4-weeks sub-acute toxicity study)	142
Table 21B	Hematological values of rats treated with FG-3 (8-weeks sub-chronic toxicity study)	143
Table 22A	Biochemical parameters of rats treated with FG-3 (4-week sub-acute toxicity study)	144
Table 22B	Biochemical parameters of rats treated with FG-3 (8-week sub-chronic toxicity study)	145
Table 23A	Organ to body weight ratio (4-week sub-acute toxicity study)	146
Table 23B	Organ to body weight ratio (8-weeks sub-chronic toxicity study)	147

List of Figures

	Description	Pg. No.
Fig. 1	Compartmental Models	9
Fig. 2	Relationship between the drug levels in blood plasma and the possible effects after oral administration	9
Fig. 3	Log plasma conc. vs. Time curve	12
Fig. 4A	Three patterns for the same drug in which the rate of absorption varied while the total amount absorbed (AUC) was unchanged	16
Fig. 4B	Three patterns for the same drug in which the rate of absorption was same but the extent of absorption varied	16
Fig. 5	HPLC components	19
Fig. 6A	Rifampicin	25
Fig. 6B	Isoniazid	26
Fig. 6C	Pyrazinamide	27
Fig. 7	Cumin and Caraway Herbs-Seeds	30
Fig. 8A	Flow chart-A	61
Fig. 8B	Flow chart-B	62
Fig. 8C	Flow chart-CI	66
Fig. 8D	Flow chart-CII	66
Fig. 9A	Chemical structure of FG-1 molecule	69
Fig. 9B	Chemical structure of FG-2 molecule	70
Fig. 9C	Chemical structure of FG-3 molecule	71
Fig. 9D	Chemical structure of FG-4 molecule	72
Fig. 10A	HPLC Chromatogram of CM-1(2)	73
Fig. 10B	HPLC Chromatogram of FG-3 (Pure molecule from cumin)	74
Fig. 11	Flow chart-D	75
Fig. 12	HPLC finger print of CR-1(1)	76
Fig. 13A	Finger print of CR-1(1) Sub-Fr.2	77
Fig. 13B	Finger print of CR-1(1) Sub-Fr.2D	77
Fig. 13C	Finger print of CR-1(1) Sub-Fr.3	78
Fig. 14A	Finger print of TF-1(Trifolin)	80
Fig. 14B	Kaempferol-3- β -D galactoside (Trifolin, TF-1)	80
Fig. 15	PAMPA system (Millipore)	84
Fig. 16	Experimental design of <i>in-situ</i> Rho123 efflux study	88
Fig. 17	HPLC Chromatogram of Testosterone	94
Fig. 18A	Chromatogram of blank rat plasma	106
Fig. 18B	Chromatogram of mobile phase	106
Fig. 18C	Chromatogram of plasma sample spiked with RIF	107
Fig. 18D	Chromatogram of plasma sample spiked with INH and PZA	107
Fig. 19A	Pharmacokinetic profile of RIF (ORAL)	115
Fig. 19B	Pharmacokinetic profile of INH (ORAL)	116

Fig. 19C	Pharmacokinetic profile of PZA (ORAL)	117
Fig. 19D	Pharmacokinetic profile of RIF (I.V.)	122
Fig. 20	Parallel Artificial membrane permeability assay (PAMPA)	124
Fig. 21A	RIF	126
Fig. 21B	PZA	126
Fig. 21C	INH	127
Fig. 22	Effect of test substances on Rho123 efflux	129
Fig. 23	Effect of FG-3 on intestinal clearance and intestinal exsorption rate of Rho123	131
Fig. 24	Effect of test substances on P-gp ATPase activity	134
Fig. 25	Effect of test substances on testosterone hydroxylase activity	135
Fig. 26	Effect of test substances on erythromycin demethylase activity	136
Fig. 27	Effect of FG-3 on inducible erythromycin demethylase activity	137
Fig. 28A	Weekly body weight (Sub-acute toxicity study in male rats)	139
Fig. 28B	Weekly body weight (Sub-acute toxicity study in female rats)	139
Fig. 28C	Weekly body weight (Sub-chronic toxicity study in male rats)	140
Fig. 28D	Weekly body weight (Sub-chronic toxicity study in female rats)	140

List of Abbreviations

Abbreviation	Description
Anti-TB	Anti-tuberculosis
AB	Absolute bioavailability
ACE	Active constituent extract
Alcol.	Alcoholic
ALT	Alanine amino transferase
Aq.	Aqueous
AST	Aspartate amino transferase
AUC	Area under curve
AUMC	Area under moment curve
Bil	Bilirubin
CAL	Calibration
Chol	Cholesterol
Cl	Clearance
CL _{Int.Ex.}	Intestinal exsorption clearance
Cl _p	Plasma clearance
CL _t	Total plasma clearance
CM	Cumin
CM-1	Aqueous extract of cumin
CM-1(1)	Butanolic extract of CM-1
CM-1(2)	Remaining aqueous portion of CM-1 after Butanolic extraction
CM-1(3)	Alcoholic extract of CM-1
CM-1(4)	50 % aqueous alcoholic extract of residue remaining after alcoholic extract of CM-1
CM-1(5)	Portion remaining after 50 % aqueous alcoholic extract of residue remaining after alcoholic extract of CM-1
CM-2	50 % aqueous alcoholic extract of cumin
CM-3	95 % alcoholic extract of cumin
C _{max}	Peak plasma concentration
Conc.	Concentration
C _p	Plasma concentration
cpm	Counts per minute
C _{pss}	Steady-state plasma concentration
CR	Caraway
CR-1	Aqueous extract of caraway
CR-1(1)	Butanolic extract of CR-1
CR-1(1) Sub-Fr. 2	Sub-fraction of CR-1(1)
CR-1(1) Sub-Fr. 2D	Sub-fraction of CR-1(1)
CR-1(1) Sub-Fr. 3	Sub-fraction of CR-1(1)
CR-1(2)	Remaining aqueous portion of CR-1 after Butanolic extraction
CR-2	50 % aqueous alcoholic extract of caraway
CR-3	95 % alcoholic extract of caraway
Creat	Creatinine
CYP	Cytochrome P

d.w.	Distilled water
Diff.	Difference
Exsorption Rate Int.	Intestinal exsorption rate
F	Bioavailability
FDC	Fixed dose combination
FG-1	apigenin-7-glucoside
FG-2	luteolin-7-glucoside
FG-3	3',5-dihydroxyflavone-7-O- β -D-galacturonide-4'-O- β -D-glucopyranoside
FG-4	apigenin-7-galacturonyl glucoside
Fig.	Figure
G.I.	Gastro-intestinal
GIT	Gastro-intestinal tract
GMP	Good manufacturing practice
Gr	Group
Gra.	Granulocytes
h	Hour/s
Hb	Haemoglobin
HMP	Herbal medicinal products
HPLC	High performance liquid chromatography
I.I.I.M.	Indian Institute of Integrative Medicine
i.p.	Intra-peritoneal
i.v.	Intravenous
ICH	International Conference on Harmonization
IR	Infra-red spectroscopy
k_{ab}	Absorption rate constant
k_{el}	Elimination rate constant
LCMS	Liquid chromatography mass spectrometry
LLE	Liquid liquid extraction
LOD	Limit of detection
LOQ	Limit of quantification
Lym.	Lymphocytes
m.p.	Melting point
M/F	Male/Female
m/z	Mass to charge ratio
ME	Marker extract
min	Minute/s
MRT	Mean residential time
MTB	Mycobacterium tuberculosis
MW	Molecular weight
NMR	Nuclear magnetic resonance
OD	Optical density
ODS	Octadecyl silane
p.o.	Per oral
PAMPA	Parallel artificial membrane permeability assay
P_{app}	Apparent permeability coefficient
P-gp	P-glycoprotein
Pi	In-organic phosphate

PK	Pharmacokinetics
pKa	Dissociation constant
Plt	Platelet
POA	Pyrazinoic acid
PXR	Pregnane X Receptor
QC	Quality control
R.T.	Retention time
RB	Relative bioavailability
RBC	Red blood cells
Ref.	Reference
Rf	Retention factor
Rho	Rhodamine
RP	Reverse phase
rpm	Rotations per minute
RSD	Relative standard deviation
S.D.	Standard deviation
S/N	Signal to noise
SEM	Standard error of mean
SGOT	Serum glutamate oxaloacetate transaminase
SGPT	Serum glutamate pyruvate transaminase
SLP	Solid lipid particles
SOP	Standard operating procedure
SPE	Solid phase extraction
SS	System suitability
$t_{1/2}$	Half-life
TB	Tuberculosis
Temp.	Temperature
TF-1	Kaempferol-3- β -D galactoside (Trifolin)
TG	Triglyceride
TLC	Thin layer chromatography
T_{max}	Time of peak plasma concentration
UA	Uric acid
UV	Ultra-violet
V_c	Volume of central compartment
V_d	Volume of distribution
Vol.	Volume
vs.	Versus
WBC	White blood cells
WHO	World health organization

Note: Abbreviations of chemicals are appended in “Chemicals and reagents” Section 4.5

INTRODUCTION

1. Introduction

The goal of a drug delivery system is to achieve and sustain therapeutic blood levels of a drug. Various routes of administration are used for efficient delivery of drugs in which, peroral route is predominant. Oral chemotherapy holds great promise as a cost-effective and patient-friendly method of administration. However peroral delivery poses many hurdles starting from drug dissolution in gastrointestinal fluid to first pass metabolism due to various physicochemical and biopharmaceutical problems. With the result oral therapy is limited by a large variability in the rate and extent of absorption into the systemic circulation.

Considerable evidence is accumulating to suggest that many clinically important drugs are not optimally utilized. If systemic availability of a drug averages 20 %, for example, then 80 % of a dose is simply wasted. For drugs that are expensive to produce and beyond the reach of millions, wasting 80 % of the precious substance is not comprehensible. There is, thus, a need to search for alternative drug forms having better action profile in terms of systemic availability and efficacy. Besides cost-effective reformulation of known drugs for resource poor countries of the world is indeed a great need of the hour.

Improving the bioavailability of major clinical drugs which exhibit poor/variable bioavailability is now increasingly being viewed as a medical need of great interest. Maximizing oral bioavailability is therapeutically important because the extent of bioavailability directly influences plasma conc. as well as therapeutic and toxic outcomes. Poorly bioavailable drugs are inefficient because a major portion of a dose never reaches the plasma or exerts its pharmacological effect. The inter-subject variability in bioavailability also remains correlated with the extent of bioavailability.

Therefore low oral bioavailability leads to high variability and poor control of plasma conc. and effects. Inter-subject variability is particularly of concern for a drug with a narrow therapeutic margin or a steep dose vs. effect profile [1].

Advances in the pharmaceutical sciences have led to the establishment of a number of approaches for addressing poor/variable oral bioavailability. These strategies include, (a) micronization i.e., controlling the particle size, to produce increased surface area for dissolution, (b) use of salt forms with enhanced dissolution profiles, (c) polymorphism of crystal size or form selection, (d) solubilization of lesser soluble drugs by way of chemical modification and/or complexation using cyclodextrins, (e) use of co-solvents for higher solubilization, (f) targeted delivery of drugs at the site of action, (g) micellar solutions, (h) use of lipid systems for the delivery of lipophilic drugs, (i) controlled drug delivery by film coating or use of polymeric matrices for sustained release of drugs, (j) prodrug approach, (k) microencapsulation such as liposomes, (l) crystal engineering approaches, (m) use of permeation enhancers such as, surfactants, fatty acids, medium chain glycerides, steroidal detergents, acyl carnitine and alkanoylcholines, N-acetylated α -amino acids, N-acetylated non- α -amino acids, chitosans and other mucoadhesive polymers, and (n) use of excipients that inhibit secretory transport [2, 3]. Although several of these approaches seemed to have potential to improve oral bioavailability of poorly bioavailable drugs, many of these which have been tried as an adjunct to produce a better drug profile, have put another burden - these synthetic agents are, by and large, toxic in short/long term use. This has created utmost medical need to devise new strategies in order to improve the action profile of existing/new drugs.

During past 20 years, extensive experimental research has been conducted at Indian Institute of Integrative Medicine (CSIR), Jammu (formerly known as Regional

Research Laboratory, Jammu) to address the problem of poor/variable oral bioavailability of clinically important drugs, based on the clues from Ayurvedic literature - a journey from traditional wisdom to modern therapeutic approach. Traditional Ayurvedic medicines often comprise of several poly-herbal formulations. A frequent and consistent repetition of certain herbals individually or as group was noticed in large number of Ayurvedic prescriptions recommended for variety of indications. One and foremost group of such herbals which has been documented very frequently as essential part of about 70 % prescriptions was 'Trikatu'. 'Trikatu' (the three acrids) comprise of long pepper, black pepper and dry ginger in equal proportions. According to Ayurveda, these three acrids collectively act as "kapha-vatta-pitta-haratvam" which means "correctors of the three humours (doshas) of the human organism". Out of 370 compound formulations listed in the Handbook of Domestic Medicines and Common Ayurvedic Remedies, 210 contain either trikatu or its individual ingredients [4].

Systematic and scientific investigations in combinations with several modern drugs revealed the important role of 'Trikatu' as enhancer of oral drug bioavailability [5]. Further while investigating influence of components of 'Trikatu', experimental evidences revealed that this property was located in *Piper* sp. A single major alkaloidal constituent, piperine, from black pepper was found to be responsible for bioavailability enhancing effect. In 1995, IIM, Jammu secured a US Patent for 'a process for preparation of a new pharmaceutical composition with enhanced activity for the treatment of tuberculosis and leprosy' (**Annexure I**). To describe this action profile a new term 'bioenhancer' was coined by the scientist at I.I.M, Jammu.

The basic concept of bioenhancers was also captured elsewhere, and several studies validated it for wide categories of drugs/pharmacologically active substances.

A patent mapping revealed that from the year 1995 (when first patent was granted to IIM, Jammu) to the year 2008, 55 US patents have been filed and granted worldwide on the preparation and use of bioenhancers (**Annexure I**).

During the last 5 years, extensive brain storming sessions were held at the Division of Pharmacology, IIM, Jammu, and inputs received from herbalists/traditional healers, modern cell biology experts, and also from documented *Materia Medica*, coupled with evidences for prior use by humans, it was envisaged that Indian spice herbs could be a potential source for bioenhancers. It has been hypothesized that a bioenhancer could act as a '*biological response modifier*' essentially via modulating 'synergy', and this may be one of the hallmarks of action profile of indigenous drugs using multi-herb compositions [6]. During the course of these investigations many experimental evidences have revealed that a bioenhancer may act by (a) modifying gastrointestinal tract permeation properties (b) inhibiting the rate of CYP 450 enzymes mediated degradation of drug in liver/intestine, and/or (c) reducing the P-gp-mediated intestinal efflux mechanism. Subsequently a large number of herbal products (in the form of solvent-derived extract/fractions/subfractions/pure isolates) continued to be investigated for their possible bioavailability enhancing profile when co-administered with wide categories of drugs such as anti-tuberculosis (anti-TB), anti-cancer and antifungals.

Among such herbs, seeds of one spice herb, *Cuminum cyminum* showed a promising bioavailability enhancing effect on rifampicin (RIF). In a collateral exploratory study the seeds of another related spice herb, *Carum carvi* showed a promising bioavailability enhancing effect on 3 drugs, when co-administered with a combination of RIF, pyrazinamide (PZA), and isoniazid (INH).

The object of the present investigation was to extend the activity spectrum of both cumin and caraway seed (since they bear a phylogenetic relationship, parsley variety), with respect to bioavailability enhancement of orally co-administered anti-TB drugs. The work components included (a) preparation of solvent-derived herbal product(s), (b) chemical standardization of the active moieties, (c) isolation and identification of active constituent(s), (d) pharmacokinetic interactions and bioavailability assessment, and (e) identification of the mode of action.

Bibliography

- [1] Aungst B.J. Intestinal Permeation Enhancers. *Journal of Pharmacy & Pharmacology*. 2000, 89: 429-441.
- [2] Aungst B.J. Novel formulation strategies for improving oral bioavailability of drug with poor membrane permeation or presystemic metabolism. *Journal of Pharmaceutical Sciences*. 1993, 82: 979-987.
- [3] Blagden N., De Matas M., Gavan P.T., York P. Crystal engineering of active pharmaceutical ingredients to improve solubility and dissolution rates. *Advanced Drug Delivery Reviews*. 2007, 59:617-630.
- [4] CCRIM (Central Council of Research in Indian medicine and Homeopathy) 1979. Handbook of domestic medicine and common Ayurvedic remedies. New Delhi.
- [5] Johri R.K., Zutshi U. An Ayurvedic formulation 'Trikatu' and its constituents. *Journal of Ethnopharmacology*. 1992, 37: 85-91.
- [6] Williamson E.M. Synergy and other interactions in phytomedicines, *Phytomedicine*. 2001, 8: 401-407.

AIMS & OBJECTIVES

2. Aims and Objectives of the Present Investigation

- **To study the effect of oral administration of herbal preparation of *Cuminum cyminum* on oral bioavailability of RIF alone and in presence of INH and PZA.**
- **To study the effect of oral administration of herbal preparation of *Carum carvi* on oral bioavailability of RIF, INH and PZA.**
- **To isolate and standardize bioactive natural product (s) (herbal/ molecule)**
- **To investigate the mode of action**

REVIEW OF LITERATURE

3. Review of Literature

3.1 Pharmacokinetics

The science of pharmacokinetics (PK) deals with the important aspects of selecting a drug, dosing regimen, and monitoring the dosing for appropriate therapeutic or toxic effects for an individual. PK explores what the body does to the drug, and essentially describes the fate of a drug after administration to a living being and involves several features like the extent and rate of absorption, distribution, metabolism and excretion referred to as the ADME. These four criteria influence the drug levels and kinetics of drug exposure to the tissues and hence influence the performance and pharmacological action of a drug.

Absorption is the movement of a drug into the bloodstream and is of primary importance since the drug must be absorbed before any medicinal effects can take place. A drug's pharmacokinetic profile may be altered by adjusting factors that affect absorption. Stomach is the first place where in its aqueous environment an orally administered drug will dissolve. The rate of dissolution is a key target for controlling the duration of a drug's effect. Absorption is also influenced by gut motility, food intake and presence of other drugs.

Distribution is the dispersion or dissemination of drug from intravascular space to extra vascular space (body tissues). It describes the reversible transfer of drug from one space to another within the body and is dependent on certain physiological and physicochemical factors. Physicochemical factors are partition coefficient, degree of ionization and molecular size of the drug. Physiological factors are the permeability between tissues, blood flow, perfusion rate of tissue and plasma protein binding.

A drug begins to be broken down as soon as it enters the body.

Metabolism is this irreversible transformation of a drug. The majority of small-molecule drug metabolism is carried out in the liver by redox enzymes, termed cytochrome P450 (CYP 450) enzymes (biotransformation). Biotransformation is thus the process which terminates the drug action and facilitates its excretion.

Excretion is the elimination of the drug from the body. Unless excretion is complete, accumulation of foreign substances can adversely affect normal metabolism. Absorption, biotransformation and elimination are first-order: rate depending upon the conc. of the drug. When body's capacity to process the drug limits the rate, saturated, zero order kinetics is observed.

A. Compartment models

Compartmental schemes are generally made by fitting kinetic models to conc. vs. time course. A compartment is a distinguishable pool of the drug and refers to those organs and tissues for which the rates of uptake and subsequent clearance of a drug are similar. It is different from anatomic compartments, which are bounded by fasciae. There are five major body compartments: blood plasma, interstitial fluid, fat tissue, intracellular fluid, and trans-cellular fluid. The trans-cellular compartment includes fluids in the pleural and peritoneal cavity. If the distribution of the drug between blood and tissues is sufficiently rapid and the equilibrium is attained instantaneously, body is regarded as single homogenous compartment. This is one-compartment model. However most of the drugs initially distributes at different rates in various fluids and tissues. Consequently the kinetic behavior of such drugs can be depicted more realistically by considering the body as two-compartment model (**Fig. 1**).

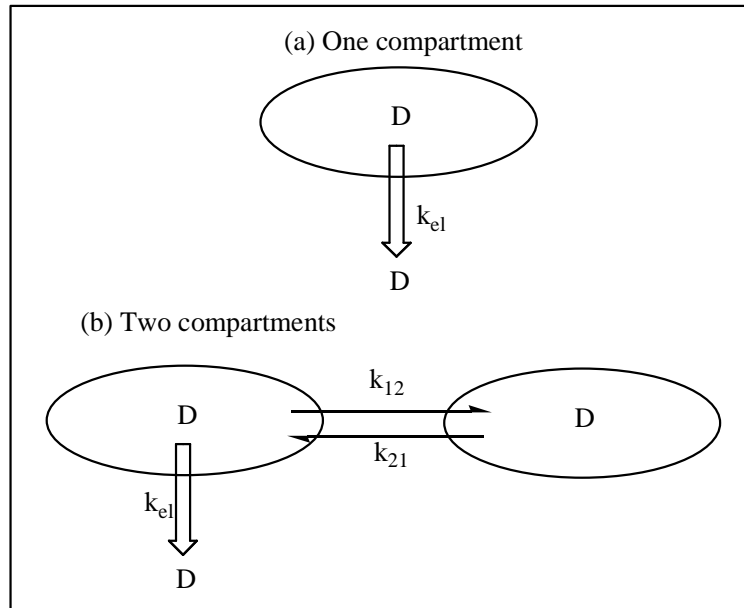


Fig. 1. Compartment models

B. Oral dosing

Non-compartmental PK analysis is dependent on estimation of total drug exposure and is estimated by the area under the curve of a plasma conc. -time graph (AUC). **Fig. 2** describes the plasma conc. of a drug versus (vs.) time curve after single oral dosing.

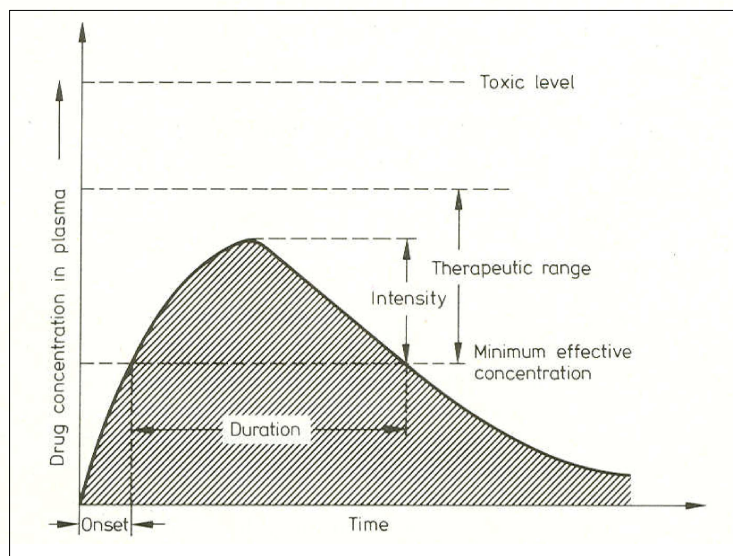


Fig. 2. Relationship between the drug levels in blood plasma and the possible effects after oral administration

The absorption phase may also be depicted as the absorbed drug or eliminated drug. During the rising part of the curve the rate of absorption is greater than the rate of elimination. During the declining phase of the curve, rate of elimination is greater than the rate of absorption. The faster the absorption of a drug, the larger is the peak conc. in plasma vs. time curve.

From these curves important information is generated with respect to (a) absorption rate constant (k_{ab}) and the elimination rate constant (k_{el}), taking into account whether the data fits into one-, or two- compartment model, and whether $k_{ab} \gg k_{el}$, or vice versa, (b) the time at which the peak plasma conc. occurs (T_{max}), which is determined by the value of the rate constants and (c) area under the curve (AUC) which is a useful measure of the amount of drug absorbed and eliminated. The constants namely peak plasma conc. (C_{max}), T_{max} and AUC are the kinetic determinants of oral bioavailability of a drug. The total area under $Ct \times t$ vs. time is defined as the area under the first moment curve (AUMC). $AUMC/AUC$ is the mean retention time (MRT). MRT gives a quantitative estimate of the persistence time of a drug in the body and is a function both of distribution and elimination.

An effective dose is the smallest amount of a drug required to produce a measurable effect and the dosing refers to the process of administering a measured amount of a drug. A route of administration is the path by which a drug is brought into the systemic circulation. It can be topical for local effect, enteral (oral), or parenteral (non-oral).

Therapeutic window is the range of the amount of a drug that gives an effect (effective dose) and the amount that gives an adverse effect. Narrow therapeutic index is when the ratio of toxic dose/therapeutic dose is less than ten.

A conc. vs. time profile of a drug in the blood is the net result of several processes. A \log_{10} plasma conc. vs. time plot yields a linear plot in which the straight line may be extrapolated back to obtain the conc. of the drug in plasma at time zero. This theoretical conc. is otherwise not measurable by sampling since mixing of the drug is not instantaneous. The half-life ($t_{1/2}$) is the time taken for the conc. of the blood or plasma to decline to half of its original value and remains constant over the entire period. For first order reaction:

$$\begin{aligned} dc/dt &= -k_1 x, \\ \text{or, } dc/c &= -k_1 dt; \\ \text{or } \ln ct &= \ln c_0 - k_1 t; \\ \text{or } \ln ct/c_0 &= -k_1 t, \text{ where } t = \ln c_1/c_0 \end{aligned}$$

$$\begin{aligned} \text{At } t_{1/2}, c_1/c_0 &= 0.5, \text{ so that} \\ \ln 0.5 &= -0.693. \end{aligned}$$

Therefore, $t_{1/2} = 0.693/k_1$. k_1 is the elimination rate constant (k_{el}) and is a proportionality constant representing the fraction of drug eliminated per unit of time. For example if k_{el} is 0.1/min, 10 percent of the drug at any instant time would be eliminated in one minute. It is a constant and independent of initial conc. and values will be uniform throughout the entire process. $t_{1/2} = 0.693/k_{el}$ describes the relationship between these two constants. With first order elimination, at a certain point in therapy, the amount of drug administered during a dosing interval exactly replaces the amount of drug excreted. When this equilibrium occurs (rate in = rate out), steady-state is reached. For zero order process

$$\begin{aligned} dc/dt &= -k_0 \\ \text{or } ct &= c_0 - k_0 t, \\ \text{so that } 0.5 c_0 &= c_0 - k_0 t_{1/2}, \text{ and} \\ t_{1/2} &= 0.5 c_0/k_0; \end{aligned}$$

here, $t_{1/2}$ is not dependent of conc. From the $t_{1/2}$ of a drug or elimination rate constant one can predict a dosing regimen. If the drug is given every $t_{1/2}$, the accumulation at steady state will be two-fold relative to the first dose. In such cases the loading dose is two-times the maintenance dose. When a drug is given by oral route, it requires 4 times the $t_{1/2}$ of drug to reach an average conc. within 10 % of the steady-state conc.

C. Intravenous dosing

Fig. 3 represents a semi-logarithmic plot of plasma conc. measured after an intravenous (i.v.) dose (solid line).

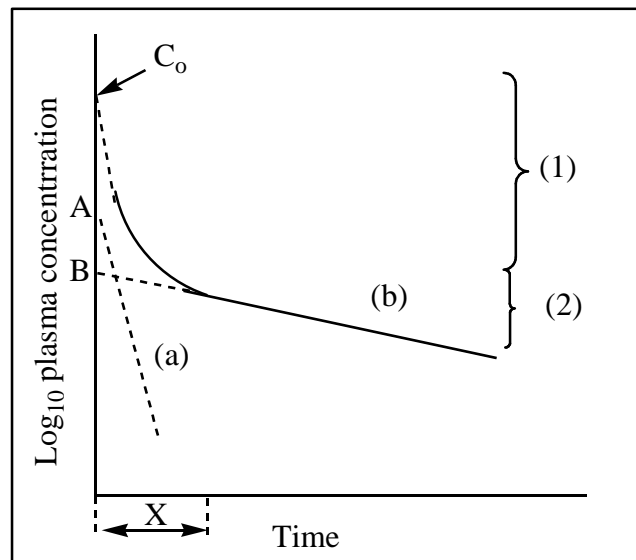


Fig. 3. Log plasma conc. vs. time curve

The plasma level decline can be divided into two phases, (1) and (2). Phase (1) shows the distribution of drug from the central compartment (plasma and rapidly distributed tissues), into the second compartment. After a certain time period, equilibrium will be attained and the two compartments will behave as one: the plot therefore becomes log/linear (2) (Line b).

This log/linear phase represent elimination from the central compartment which is now in equilibrium with the second compartment. The slope of line (b) is used to

determine a rate constant (β), which is a hybrid rate constant which governs the overall elimination rate of the drug. The $t_{1/2}$ which is calculated using this rate constant (β), is the biological $t_{1/2}$. The zero time intercept (B) represents the conc. of the drug distributed instantaneously in both the compartments. Line (a) represents the difference of C_p values which lie on line (b) from the real values of C_p . Slope of this line gives rate constant (α) which governs the distribution of the drug in the second compartment. The intercept (A) when added to intercept (B) gives the C_0 , theoretical conc. of the drug at time zero. From this plot many useful parameters are derived:

$$\text{Biological } t_{1/2} = 0.693/\beta;$$

$$\text{Volume of distribution (V}_d\text{)} = \text{Dose}/\text{B, or}$$

$$V_d = \text{Cl}_p/\beta;$$

$$\text{Volume of central compartment (V}_c\text{)} = \text{Dose}/ \text{A}+\text{B};$$

$$C_p = A e^{-\alpha t} + B e^{-\beta t};$$

$$\text{AUC} = \text{A}/\alpha + \text{B}/\beta.$$

D. Volume of distribution (V_d) and Clearance (Cl)

Drug dosage regimens are determined by two basic parameters; (i) V_d , which determines the amount of drug required to achieve a target conc. and (ii) Cl, which determines the dosage rate to maintain an average steady state conc. A drug's V_d is that volume of body fluid into which a drug dose is dissolved. It does not refer to any identifiable compartment in the body. It is simply the size of a compartment necessary to account for the amount of drug in the body. Generally drug conc. are analyzed in blood, plasma or serum, representing the apparent volume throughout which the amount of drug would need to distribute in order to produce the measured conc. This relationship is described by the equation $V_d = \text{Dose}/C_p$. Variability between drug with respect to V_d is because of proportional differences of the drug remaining in plasma. Water soluble drugs or drugs with high plasma binding have a high plasma conc.

relative to the dose, so that their V_d is low. On the other hand, lipid soluble drugs or the drugs which have high tissue binding have a low plasma conc. relative to the dose, so that their V_d is high. V_d , multiplied by the known effective conc. of a drug in plasma determines the loading dose.

A drug starts to be eliminated as soon as it is absorbed. Cl defines how a dose is to be given, at a rate that balances its clearance rate. It is not an indicator of how much drug is being removed, but only represents the theoretical volume of blood or plasma which is totally cleared of drug per unit time. It is related to the volume in which the drug is dissolved (V_d) and the rate at which it goes out (related to $t_{1/2}$ or k_{el}). Therefore Cl is defined as the product of $V_d \times k_{el}$. For intravenous route, the clearance, $Cl_p = \text{Dose} / \text{AUC}$ [7, 8].

3.2 Bioavailability

Bioavailability (expressed as the letter F) describes the fraction of an administered dose of unchanged drug that reaches the systemic circulation and is available at the site of action. When a drug is administered via i.v. route, its bioavailability is 100%. However, when it is administered via other routes (such as orally), its bioavailability decreases (due to incomplete absorption and first pass metabolism). Bioavailability is one of the essential tools in pharmacokinetics and is critically regulated by a drug's absorption pattern.

A. Absolute bioavailability: It is the fraction of the drug absorbed through non-i.v. route compared with the corresponding i.v. route of the same drug. The comparison is generally dose normalized if different doses are used. A drug given by the i.v. route will have an absolute bioavailability of 1 ($F=1$) while drugs given by other routes usually have an absolute bioavailability of <1 .

B. Relative bioavailability: It measures the bioavailability of a certain drug when compared with another formulation of the same drug, usually an established standard, or through administration via a different route. Relative bioavailability is one of the measures used to assess bioequivalence between two drug products. Identical drugs can produce different results depending on the route of administration. Various factors reduce the availability of drugs when administered by non-i.v. routes. These include physical properties of the drug (hydrophobicity, pKa, solubility), drug formulation (immediate release, excipients used, manufacturing methods, modified release - delayed release, extended release, sustained release, etc.), fed or fasting conditions, gastric emptying rate, circadian differences, interactions with other drugs/foods, GIT factors, individual variation in metabolic differences, age, gender, disease conditions, phenotypic differences, entero-hepatic circulation and diet patterns [9].

C. Bioavailability indices: (AUC and C_{max})

The absorption process influences the quantitative action of all xenobiotics. Bioavailability is quantified by the determination of the conc. of the drug in the blood plasma at given time intervals following administration. From the **Fig. 2**, following information can be obtained (i) C_{max} , (ii) The rate of absorption, i.e., the time between the administration and the achievement T_{max} and (c) Total amount absorbed. This is measured from the area under the plasma conc.–time curve and is expressed as AUC.

Fig. 4A-B shows how the variations of these parameters affect the quantitative action of the drug.

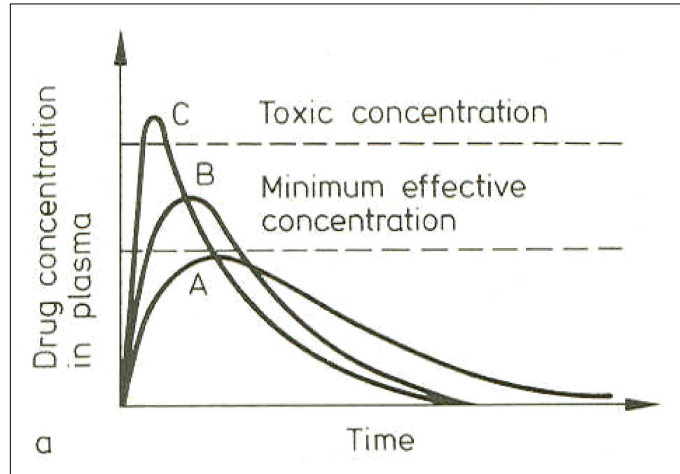


Fig. 4A. Three patterns for the same drug in which the rate of absorption varied while the total amount absorbed (AUC) was unchanged. A, Therapeutic level not attained; B, Therapeutic level attained; C, Toxic level attained.

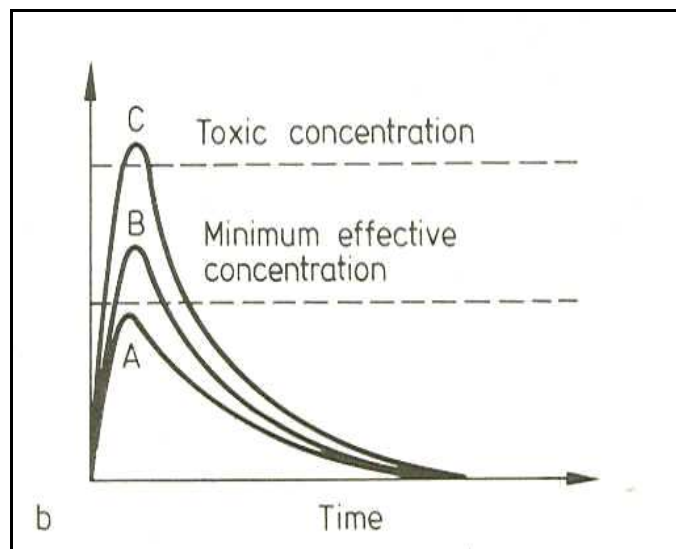


Fig. 4B. Three patterns for the same drug in which the rate of absorption was same but the extent of absorption varied. A, Therapeutic levels not attained; B, Therapeutic level attained; C, Toxic level attained.

Fig. 4A depicts three hypothetical examples for the same drug in which the rate of absorption varied while the AUC remained unchanged. **Fig. 4B** depicts three examples in which rate remained the same, but the fraction of the amount absorbed

varied. These examples show that for a rapid action drug or for drugs with a narrow safety margin, the rate of absorption is important, while for long acting and with repeated dosing of a drug, the amount absorbed remains important [10].

D. Site of drug absorption: The Intestine

In the gastro-intestinal tract (GIT) the small intestine represents the largest absorptive surface, about 200 m² in an adult human and is endowed with an abundant blood supply and thus because of its much larger surface and better supply, plays a greater role in the absorption of xenobiotics. Intestine is a complex biological membrane and is composed essentially of the mucosal epithelial cells, the tight junction and inter-cellular spaces, the glycocalyx covering the luminal face of the brush border, and the unstirred water layer immediately adjacent to the luminal face of the glycocalyx.

The overall permeability of the gut is therefore a composite of the permeability properties of its constituents and favours directional transport from the lumen into the sub-epithelial tissue.

The term 'intestinal permeation' refers to the process of passage of various substances across the gut wall, either from the lumen into the blood or lymph, or in the opposite direction. 'Permeability' is the condition of the gut which governs the rate of this complex two-way process.

Majority of orally administered drugs are absorbed from the intestine via diffusion. The kinetics of this process is determined by the factors expressed in Fick's law. According to this law the rate of diffusion dn/dt , i.e., the number of solutes (dn), crossing the area A in time dt over a distance (dx) is proportional to the concentration difference dc/dx ; $dn/dt = DA \times dc/dx$, where D is the diffusion coefficient. Since a

lipid membrane is interposed in the path of diffusion and represents a lipid barrier, it follows that the lipid solubility of the solute will play a significant role in the trans-cellular intestinal transport.

Since the luminal surface of the intestine is lined with a 'leaky' epithelium, membrane itself does not offer any resistance, the flow of solutes is essentially by diffusion.

By knowing the diameter of the membrane, the term dx is included in a new coefficient, the 'permeability coefficient' P and has the dimensions of velocity. Fick's law in terms of the permeability constant P is generally expressed as: $dn/dt = PA dc$. Intestinal permeation is essentially a two-way process: flow of substances from the lumen into the blood stream (absorption) and the flow from the blood stream into the lumen (exsorption) [10].

3.3 Bio-analytical Aspects

A pharmacokineticist is mainly concerned with the determination of drug levels in plasma for establishing a conc. vs. time profile. In order to measure accurate drug conc., the usefulness of high performance liquid chromatography (HPLC) cannot be overstated.

Today, the most important bio-analytical tool is HPLC, due to its superior qualitative and quantitative results, reproducibility, high detection sensitivity and unsurpassed reliability.

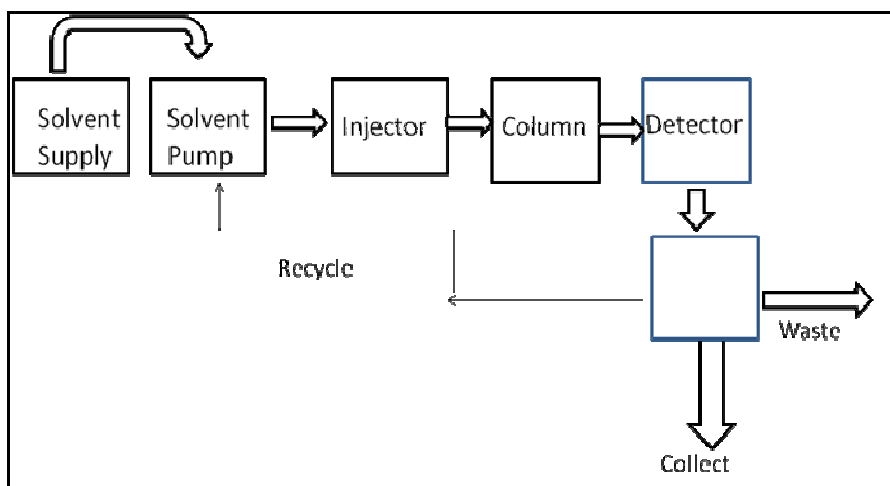


Fig. 5. HPLC components

In an elution chromatographic separation analytes differ from each other only in their residence time in or at the stationary phase, and produces features related to peak width, peak symmetry (measured at 10 % of the peak height) and retention times.

A. Normal phase chromatography: It is employed for the separation of non-ionic, non-polar to medium polar substances, which is achieved by interaction of stationary phase's polar surface with polar parts of the sample molecules. The stationary phase is usually SiO_2 , Al_2O_3 , $-\text{NH}_2$, $-\text{CN}$, $-\text{Diol}$, $-\text{NO}_2$, while the mobile phase solvents are heptane, hexane, cyclo-hexane, chloroform (CHCl_3), di-chloromethane (CH_2Cl_2), dioxane and methanol (MeOH).

B. Reversed phase (RP) chromatography: It is employed for separation of non-ionic and ion-forming non-polar to medium polar substances (carboxylic acids – hydrocarbons). If ion forming substances (as carboxylic acids) are to be separated, a pH control by buffers is necessary. RP-HPLC is most frequently used liquid chromatographic technique and in comparison with normal phase applications, has several advantages; (i) It is more stable and reproducible (ii) allows the use of various mobile phases and buffer additives, and (iii) can be easily controlled either isocratically or in the gradient mode. The stationary phase is usually C-8 or C-18

while the mobile phase solvents are acetonitrile (ACN), MeOH, tetrahydrofuran (THF) with organic modifiers like acetic acid, formic acid, phosphate, acetate, citrate, and formet buffer.

Table 1. Normal and reverse phase chromatography

	Normal Phase	Reversed Phase
Polarity of stationary phase	High	Low
Polarity of mobile phase	Low to medium	Medium to high
Sample elution order	Least polar first	Most polar first
Retention can be increased By:	Increasing surface of stationary phase	Increasing surface of stationary phase
	Reducing polarity of mobile phase	Increasing n-alkyl-chain length of stationary phase
	Reducing water content of mobile phase (with non-polar eluents)	Increasing polarity of mobile phase (increasing water content)
	Increasing polarity of sample molecules	Reducing polarity of sample molecules

C. Sample preparation : The common methods employed in sample preparation are weighing, dilution, filtration, evaporation, pH adjustment, vortexing, internal standards addition, conc., centrifugation, liquid-liquid extraction and solid-phase extraction.

D. Liquid liquid extraction (LLE): LLE partitions a sample between two immiscible phases to separate analytes from interfering matrix. Out of the two phases, one is usually aqueous and the other is organic. Analytes extracted into the organic phase are easily recovered by evaporation of the solvent, while analytes extracted into the aqueous phase can be injected directly onto a HPLC column.

E. Solid phase extraction (SPE): The advantages of the SPE compared to classical liquid-liquid extraction are the low solvent consumption, the enormous time saving and the potential for automation. SPE offers a multitude of adsorbents for polar,

hydrophobic and/or ionic interactions, while LLE is limited to partition equilibria in the liquid phase. The main objectives of SPE are to prepare selective and specific sample by removing interfering matrix components. Enrichment of samples can increase the detection sensitivity by 100 to 5000 times. The analytes can be either adsorbed on the SPE packing material or directly flow through while the interfering substances are retained. Primary goal of SPE is selective extraction of components of interest from a complex sample or much larger sample volumes prior to actual analysis by HPLC.

F. Mobile phase: Mobile phase is a mixture of aqueous and an organic solvent which is miscible with water. Solvent selectivity is the ability of a solvent to resolve two or more peaks on a given stationary phase. For reversed phase separation, water, acetonitrile, tetrahydrofuran, methanol, or isopropyl alcohol are most commonly used as binary mixtures. Sample retention can be controlled by varying the solvent strength of mobile phase. Time of elution of an analyte depends to a large degree on the water content of the organic solvent and may be adjusted. Higher conc. of the organic solvent will cause shorter retention time. Solvent degassing ensures stability and reproducibility of HPLC operations, as the dissolved oxygen interferes with detector performance. Filtering the mobile phase and samples prevents column blockage by removing particulate substances and make them sufficiently transparent. Solvent delivery system comprises of reciprocating/syringe pump which needs to be optimized for accuracy and gradient linearity.

G. HPLC column: Column selection is based on the type of the sample to determine how the analytes will physically and chemically interact with the packing material. Particle size and column dimensions are the main selection criteria. C18 stationary

phase also named octadecylsilane or ODS is most commonly used in method development and routine analysis.

H. Particle size and efficiency: Short diffusion paths in the pores of the stationary phase are required for achieving high column efficiency. Smaller particles offer shortest diffusion paths. A well-packed 3 μm HPLC column has about twice the separation efficiency of a 5 μm column.

I. Flow rate and inner diameter: Small column size is mostly preferred because it allows much higher detector sensitivity. Simultaneously the consumption of solvent is decreased due to lower flow rates.

J. Signal/noise ratio: Signals (S) refers to the baseline-corrected absorbance of the analyte peak and noise (N) refers to the width of the baseline contributed by interference from light, detector electronics, temperature variations and pump noise etc.

3.4 Validation of Analytical method

Analytical method validation is a critical component. In order to minimize variation, assay of samples are carried out on a single day, relating to standard curve of each day. Also, quality control (QC) samples are run each day. These are samples of known conc. (low, medium and high), prepared by spiking drug-free biological fluid with drug. The QC samples help in determining intra-day accuracy and precision of the analytical method. The standard solutions are at conc. different from QC samples and from lowest to highest conc. that could be anticipated for a particular study. The regression line to fit the linear (straight line) standard curve is based on least squares analysis, weighted or unweighted.

A. Sensitivity. The limit of detection (LOD) is the lowest conc. of drug that will yield an assay response significantly different from that of a sample blank, whereas the

limit of quantitation (LOQ) (sensitivity) is the lowest conc. of drug that can be determined with acceptable precision under the given experimental conditions. Specificity is important for a drug to be determined in order to identify a possible interference at the respective retention time of analyte.

B. Accuracy. The term ‘accuracy’ is a measure of the degree to which a mean (m) obtained from a series of experimental measurements agrees with the value m , which is accepted as the true or correct value for the quantity measured. Absolute accuracy of a mean is defined as $m - \bar{m}$, and of an individual measurement, $x_i - m$. Relative accuracy of a mean is calculated by $(m - \bar{m})/m$, and percent accuracy by $100 \times (m - \bar{m})/m$. Generally from replicate measurements, more reproducible data is obtained and the mean is considered to be the best estimate of the true value (μ). For HPLC protocols accuracy applies to both absolute and relative recovery, and indicated in terms of mean conc., standard deviation and coefficient of variation, of overall individual QC samples at each conc.

C. Precision. The term ‘precision’ describes the reproducibility of measurements within a set. It is used to show scatter or dispersion between numeric values in a set of measurements that have been determined under the same analytical parameters. A small value of σ , indicates higher precision than a large value of σ . Generally ‘standard deviation’(s) is a more reliable expression of precision and is widely used for determining statistical significance. A more meaningful way to compare precision between different samples is to calculate relative standard deviation (RSD), which is equal to $(s)/m$. The standard error of the mean (SEM) determines the limits or the intervals on either side of ‘ m ’ within which there is 68 % probability or confidence of finding the true value (μ), assuming a normal frequency distribution and random sampling [11].

3.5 Documented reports regarding determination of anti-TB drugs by HPLC

A literature survey has revealed several reports which deal with the determination of anti-TB drugs by HPLC in biological samples. These are summarized below.

Table 2. Documented HPLC analysis of anti-TB drugs (1977-2007)

Year	Drug	Investigators	Ref.
1977	INH	Saxena et al.	12
1978	RIF	Lecaillon et al.	13
1986	RIF	Chan et al.	14
1993	RIF+INH+PZA	Seifert et al.	15
1994	RIF+INH+PZA	Walubo et al.	16
1995	INH	Hansen et al.	17
1996	INH	Sedag et al.	18
1998	PZA, INH	Kraemer et al.; Moussa et al.	19, 20
1998	RIF+INH+PZA	Khushawar and Rind.	21
1999	RIF+INH+PZA	Panchgnula et al.; Smith et al.	22, 23
2000	PZA	Conte et al.	24
2002	RIF+INH+PZA	Calleri et al.; Khushawar and Rind.	25, 26
2003	RIF+INH+PZA	Mohan et al.	27
2004	RIF	Hemantha Kumar et al.	28
2005	RIF+INH+PZA	Unsalan et al.	29
2006	RIF+INH+PZA	McIlleron et al.	30
2007	RIF+INH+PZA	Song et al.	31
	+ ETM		
2007	RIF+INH+PZA	Glass et al.	32
2007	RIF	Ruslami et al.	33

3.6 Anti-TB drugs

A. Rifampicin (RIF)

RIF is the most effective drug available for the treatment of tuberculosis. Primary mechanism of action of RIF is via inhibition of DNA-dependent RNA polymerase in susceptible strains of bacteria. Beta-subunit of this complex enzyme is the site of action of this drug.

The oral administration of RIF produces peak conc. in plasma in 2 to 4 h and is rapidly eliminated in bile, and undergoes an entero-hepatic circulation. C_{max} is in the range of 4-32 $\mu\text{g/ml}$ [35].

During next 6 h drug is in de-acetylated form. This metabolite is also anti-bacterial. The half-life of RIF varies from 1.5-5 h and shortened later during 14 days due to hepatic microsomal enzymes. Up to 30 % of the drug is excreted in urine, and up to 65 % in faeces. RIF is distributed well throughout the body. RIF is completely absorbed.

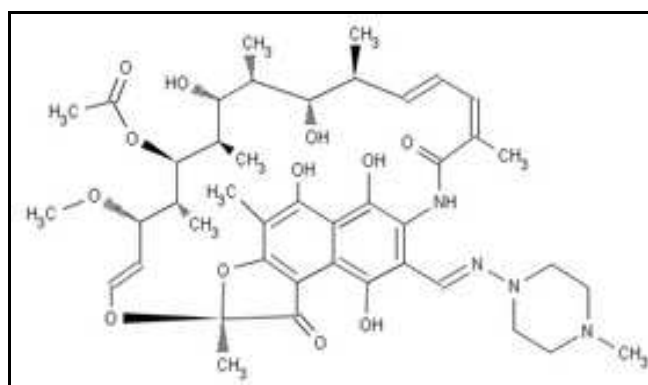


Fig. 6A. Rifampicin

*[2,7-(Eoxypentadeca [1,11,13] trienimino) naphtha [2,]1-b]furan-1,11(2H)-dione,5,6,9,17,19,21-hexahydroxy-23-methoxy-2,4,12,16,18,20,{22-heptam-ethyl-8-[N-(4-methyl-1-piperazinyl) formimidoyl]-,} 21-acetate
(MW, 822.94, m.p. 183°C)*

B. Isoniazid (INH)

INH is considered to be the most important drug for the chemotherapy of tuberculosis (TB). It is the hydrazide of isonicotinic acid and is bacteriostatic for resting bacilli but also inhibits the multiplication of the tubercular bacillus, as it is remarkably selective for mycobacteria.

INH is readily absorbed when administered either orally or parenterally. 75-95 % of a dose is excreted in the urine within 24 h, mostly as metabolites (acetyl INH and isonicotinic acid). Human beings show genetic heterogeneity with regard to the rate of acetylation of INH.

The rate of acetylation affects the conc. of the drug in plasma and its $t_{1/2}$ in the circulation. INH is a prodrug, and its anti-TB function requires in vivo activation by bacterial KatG, an enzyme with dual activities of catalase and peroxidase.

INH activation leads to inhibition of the synthesis of mycolic acids, a long chain fatty acid containing component of the bacterial cell wall. In this pathway Inh A (enoyl ACP reductase) and Kas A (beta-ketoacyl ACP synthase) have been identified as the targets of INH inhibition [35].

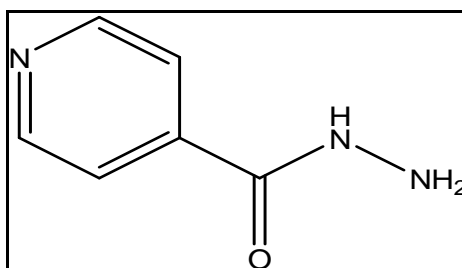


Fig. 6B. Isoniazid

(Isonicotinic acid hydrazide, MW, 137.1, m.p., 171.4°C)

C. Pyrazinamide (PZA)

PZA is the synthetic pyrazine analogue of nicotinamide, is also the pro-drug that requires activation or conversion to its active form, pyrazinoic acid (POA) by the PZase/nicotinamidase enzyme. PZA/POA is more active against semi-dormant organisms than actively growing bacilli. The target of PZA/POA appears to be the membrane. PZA is an important component of the short-term (6 months) multiple-drug therapy of tuberculosis. It is well absorbed from the GIT, and is widely distributed throughout the body. The maximum plasma conc. is achieved at 2 h of oral dosing. The drug is excreted by renal glomerular filtration. It is hydrolyzed to POA and subsequently hydroxylated to 5-hydroxy-POA, which is the main excretory product [35].

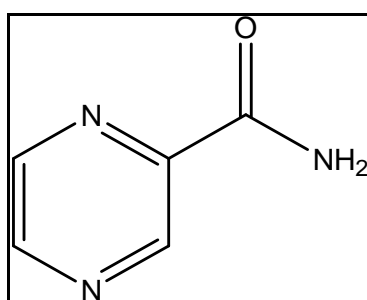


Fig. 6C. Pyrazinamide
(*Pyrazine carboxamide, MW 123.1, m.p. 189-191°C*)

3.7 Bioavailability concerns related to anti-TB drugs

RIF, PZA and INH in a fixed dose combination (FDC) is considered a frontline anti-TB therapy. However, RIF a key drug exhibits variable bioavailability from solid oral dosage forms and this problem is more apparent when it is formulated as FDC in presence of other first-line anti-TB drugs, and this has been a matter of clinical concern [36-37]. In this context various extrinsic and intrinsic factors have been

assessed [38]. Although the origin and cause of the problem is not clearly understood, several underlying reasons are (a) changes in crystalline forms of RIF, (b) manufacturing practices, (c) adsorption by excipients, (d) formulation factors, and (e) drug decomposition in formulations [39].

Evaluation of sources of biopharmaceutic pharmacokinetic variations have been undertaken to facilitate optimization of TB treatment regimens by identification of avoidable sources of variation and of risk factors for low or high drug conc. in patients [40-42].

Among the various physical/chemical factors that can possibly be the reasons for the variable bioavailability of RIF from FDC anti-TB products, one that explains most of the issues is the rapid decomposition of RIF in the presence of INH in stomach acidic conditions: acidic hydrolysis of RIF to 3-formylrifamycin under acid conditions and reaction of the latter with INH leads to formation of isonicotinyl hydrazone [36, 43]. Rate of degradation of RIF in the presence of INH is reported to be about two times more than that of RIF alone. Rifampicin degrades by 12.4% to form 3-formyl RIF while in presence of INH; the degradation is catalyzed to about 21.5% [44]. Several factors independently associated with variations in anti-TB drug conc. were identified: human immunodeficiency virus infection, gender, age, history of previous anti-TB treatment, dosing, fasting and food conditions [39, 45].

3.8 Formulation strategies to improve the bioavailability

In order to improve the oral bioavailability of RIF, many pharmaceutical strategies have been explored, like protecting RIF from exposure to acid by enteric coating, by simultaneous administration of soluble alkalizers, or through use of specific additives in formulation [39].

Several novel drug delivery approaches have been developed in order to address issues of unacceptable RIF bioavailability on co-administration with INH [46, 47]. These include implant-, microparticulate-, and various other carrier-based drug delivery systems like liposomes, incorporating the principal anti-TB agents that either target the site of TB infection or reduce the dosing frequency with the aim of improving patient outcomes.

A multiparticulate drug delivery system is designed for attainment of segregated gastrointestinal delivery of RIF and INH. These are ionotropically cross linked polymeric enterospheres for delivery of INH to the small intestine [48, 49]. A synthetic polymer (poly lactide-co-glycolide)-nanoparticle encapsulated- (RIF + INH + PZA) combination has shown improvement in the pharmacokinetic parameters in a murine TB model. The relative/absolute bioavailability of the 4 anti-TB drugs was enhanced several fold. This polymeric nanoparticle based oral combination showed significant potential to shorten the duration of TB chemotherapy, besides reducing the dosing frequency [50-52].

Chemotherapeutic potential of a nebulized solid lipid particles (SLPs) incorporating RIF, INH and PZA against experimental tuberculosis showed several fold improvement in the mean residence time and drug bioavailability. A similar pharmacokinetic profile was also observed in *Mycobacterium tuberculosis* (MTB)-infected guinea pigs [50, 53-55].

Nano-particle and alginate chitosan microspheres-based drug delivery systems have also been explored [52]. A micelle-forming co-polymer with INH has been evaluated for potential use [56]. Sustained release RIF-loaded microspheres have been reported to effectively treat MTB-infected macrophages in mice and also used along with INH in vivo [57].

3.9 *Cuminum cyminum* L. and *Carum carvi* L.

Cumin Herb

Caraway herb



SEED

SEED

Fig. 7. Cumin and Caraway Herbs-Seeds

Cumin (white jeera) and caraway (black jeera) seeds belong respectively to *Cuminum cyminum* L. and *Carum carvi* L, which are herbaceous, annual, umbelliferous flowering plants, rarely exceeding a foot in height and are native from India to Mediterranean. Cumin and caraway are believed to be one of the earliest cultivated herbs and has been in use since Biblical times both as a spice and a medicine.

Romans used ground cumin much like black pepper is used today. It was introduced to the Americas by Spanish colonists. Caraway is the main ingredient in

the scandinavian "Schnapps" and the German "kummel". Today, cumin/caraway are popular spices all over the world for their distinctive aroma, due to its essential oil content.

The cumin/caraway seed of herbal medicine is a pale green fruit of the parsley family, and their phytochemical analysis has revealed variety of glycosides and its derivatives [58- 66].

A. Ethnomedical/Folklore usage:

In indigenous medicine cumin/caraway seeds have long been considered stimulant, carminative, stomachic, astringent, anti-spasmodic, aphrodisiac, galactagogue and used as, stomachic, stimulant, carminative, and antimicrobial.

It has been shown to be effective in treating indigestion, diarrhea, dyspepsia, flatulence, morning sickness, colic and dyspeptic headache and bloating, and is said to promote the assimilation of other herbs and to improve liver function.

Vapors from caraway seeds are reported to gives relief in patients suffering from lumbago and rheumatism. Caraway water finds use as a vehicle for pediatric medicines. In mixture with alcohol and castor oil, it is used for the treatment of scabies [67-72].

According to Ayurveda, jeera exhibits the following properties.

Guna (properties)	Laghu (light), Ruksha (dry)
Rasa (taste)	Katu (Punjent)
Veerya (potency)	Ushna (Hot)

B. Pharmacological activities:

In several experimental studies botanical products from *Cuminum cyminum* and *Carum carvi* have shown diverse pharmacological effects (**Table 3A-B**).

Table 3A. Bioactivity profile of *Carum carvi*

Activity	Investigators	Ref.
Antibacterial, Antimicrobial	Iacobellis et al., 2005	73
	Mhady et al., 2005	74
Anti-oxidant	Satyanarayana et al., 2004	75
Cholesterol lowering	Lemhadri et al., 2006	76
Diuretic	Lahlou et al., 2007	77
Anti-ulcer	Khayyal et al., 2001	78
Hypoglycaemic	Eddouks et al., 2004	79
Anti-carcinogenic, chemopreventive	Nader-Khalili, 2005	80
	Deeptha et al, 2006	81
	Kamaleeshwari and Nalini, 2006	82
	Mazaki et al., 2006	83

Table 3B. Bioactivity profile of *Cuminum cyminum*.

Activity	Investigators	Ref.
Antibacterial, Antimicrobial	Shetty et al., 1994	84
	Agnihotri and Vaidya, 1996	85
	Ozcan and Erkmén, 2001	86
	Singh et al., 2002	87
	Iacobellis et al., 2005	73
	Singh et al., 2005	88
	Nostro et al., 2005	89
	Manuel et al., 2008	90

Contd.

	Shayegh et al., 2008	91
Antioxidant	Martinez-Tome et al., 2001	92
	Satyanarayana et al., 2004	79
	Thippeswamy and Naidu., 2005	93
	Singh et al., 2005	88
	Topal et al., 2007	94
Anti-hyperlipidemic, Cholesterol lowering	Sambaiah and Srinivasan, 1991	95
	Dhandapani et al., 2002	96
	Kode et al., 2005	97
GIT effects	Vasudevan et al., 2000	98
	Platel and Srinivasan, 2001	99
Ovicidal	Tunc et al., 2000	100
Tyrosinase inhibitor	Kubo and Kinst-Hori et al., 1998	101
Anti-fertility	Garg, 1976	102
Aldose reductase glycosidase inhibitor	Lee, 2005	103
Anti-carcinogenic, chemopreventive	Nalini et al., 2006	104
	Gagandeep et al., 2003	105
	Aruna and Sivaramakrishnan, 1992	106
	Nalini et al., 1998	107
Anti-diabetic, hypoglycaemic	Roman-Ramos et al., 1995	108
	Dhandapani et al., 2002	96
	Srinivasan, 2005	109
Estrogenic	Malini and Vanithakumari, 1987	110
Smooth muscle relaxant	Boskabady et al., 2005	111
Antiepileptic	Janahmadi et al., 2005	112
Cytoprotective	Aruna et al., 2005	113
Antiepileptic	Janahmadi, 2005	112
Anti-platelet aggregatory	Srivastava, 1989	114

Bibliography

- [7] Notari R.E. Biopharmaceutics and clinical pharmacokinetics- An introduction. 3rd ed., New York: Marcel Dekker Inc; 1980.
- [8] Gibaldi M. Biopharmaceutics and clinical pharmacokinetics. 3rd ed., New York: Marcel Dekker; 1984.
- [9] Welling P.G., Tse F.L.S. Pharmacokinetics- Regulatory-Industrial-Academic perspectives. 2nd ed., New York: Marcel Dekker; 1995.
- [10] Csaky T.Z. Pharmacology of Intestinal Permeation. Berlin: Springer-Verlag; 1984.
- [11] Smith R.V., Stewart J.T. Text book of biopharmaceutic analysis- A description of methods for the determination of drugs in biologic fluids. Philadelphia: Lea & Febiger; 1981.
- [12] Saxena S.J., Stewart J.T., Honigberg I.L., Washington J.G., Keene G.R. Liquid chromatography in pharmaceutical analysis VIII: determination of isoniazid and acetyl derivative in plasma and urine samples. *Journal of Pharmaceutical Sciences*. 1977, 66: 813-816.
- [13] Lecaillon J.B., Febvre N., Metayer J.P., Souppart C. Quantitative assay of rifampicin and three of its metabolites in human plasma, urine and saliva by high performance liquid chromatography. *Journal of Chromatography*. 1978, 145: 319-324.
- [14] Chan K., Wong C.L., Lok S. high-performance liquid chromatographic determination of pyrazinamide in cerebrospinal fluid and plasma in the rabbit. *Journal of Chromatography*. 1986, 380: 367-73.

- [15] Seifert H.I., Kruger P.B., Parkin D.P., van Jaarsveld P.P., Donald P.R. Therapeutic monitoring of antituberculosis drugs by direct inline extraction on a high-performance liquid chromatography system. *Journal of Chromatography*. 1993, 619: 285-290.
- [16] Walubo A., Smith P., Folb P.I. Comprehensive assay for pyrazinamide, rifampicin and isoniazid with its hydrazine metabolites in human plasma by column liquid chromatography. *Journal of Chromatography B: Biomedical Sciences and Applications*. 1994, 658: 391-396.
- [17] Hansen E.B., Dooley K.L., Thompson H.C. High-performance liquid chromatography analysis of the antituberculosis drugs aconiazide and isoniazid. *Journal of Chromatography B: Biomedical Sciences and Applications*. 1995, 670: 259-266.
- [18] Sedag N., Pertat N., Dutertre H., Dumontet M. Rapid, specific and sensitive method for isoniazid determination in serum. *Journal of Chromatography B: Biomedical Sciences and Applications*. 1996, 675: 113-7.
- [19] Kraemer H.J., Feltkamp U., Breithaupt H. Quantification of pyrazinamide and its metabolites in plasma by ionic-pair high-performance liquid chromatography. Implication for the separation mechanism. *Journal of Chromatography B: Biomedical Sciences and Applications*. 1998, 706: 319-328.
- [20] Moussa L.A., Khassouani C.E., Soulaymani R., Jana M., Cassanas G., Alric R., Hüb B. Therapeutic isoniazid monitoring using a simple high-performance liquid chromatographic method with ultraviolet detection. *Journal of Chromatography B: Analytical Technologies in the Biomedical and Life Sciences*. 2002, 766: 181-184.
- [21] Khuhawar M.Y., Rind F.M. High performance liquid chromatographic determination of isoniazid, pyrazinamide and rifampicin in pharmaceutical preparations. *Pakistan Journal of Pharmaceutical Sciences*. 1998, 11: 49-54.

- [22] Panchgnula R., Sood A., Sharda N., Kaur K., Kaul C.L. Determination of rifampicin and its main metabolite in plasma and urine in presence of pyrazinamide and isoniazid by HPLC method. *Journal of Pharmaceutical and Biomedical Analysis*. 1999, 18: 1013-1020.
- [23] Smith P.J., Van D.J., Fredricks A. Determination of rifampicin, isoniazid and pyrazinamide by high performance liquid chromatography after their simultaneous extraction from plasma. *International Journal of Tuberculosis and Lung Diseases*. 1999, 11: S325-328.
- [24] Conte J.E., Lin E., Zurlinden E. High-performance liquid chromatographic determination of pyrazinamide in human plasma, bronchoalveolar lavage fluid, and alveolar cells. *Journal of Chromatographic Sciences*. 2000, 38: 33-7.
- [25] Calleri E., De Lorenzi E., Furlanetto S., Massolini G., Caccialanza G. Validation of a RP-LC method for the simultaneous determination of isoniazid, pyrazinamide and rifampicin in a pharmaceutical formulation. *Journal of Pharmaceutical and Biomedical Analysis*. 2002, 29: 1089-96.
- [26] Khuhawar MY, Rind FM. Liquid chromatographic determination of isoniazid, pyrazinamide and rifampicin from pharmaceutical preparations and blood. *Journal of Chromatography B: Analytical Technologies in the Biomedical and Life Sciences*. 2002, 766: 357-63.
- [27] Mohan B., Sharda N., Singh S. Evaluation of the recently reported USP gradient HPLC method for analysis of anti-tuberculosis drugs for its ability to resolve degradation products of rifampicin. *Journal of Pharmaceutical and Biomedical Analysis*. 2003, 31: 607-12.
- [28] Hemantha Kumar A.K., Chandra I., geetha R., Chelvi K.S., Lalitha V., Prema G. A. Validated high-performance liquid chromatography method for the determination of rifampicin and desacetyl rifampicin in plasma and urine. *Indian Journal of Pharmacology*. 2004, 36: 231-233.

- [29] Unsalan S., Sancar M., Bekce B., Clark P.M., Karagoz T., Izzettin F.V., Rollas S. Therapeutic monitoring of Isoniazid, Pyrazinamide and Rifampicin in tuberculosis patients using LC. *Chromatographia*. 2005, 61: 595-598.
- [30] McIlleron H., Wash P., Burger A., Norman J., Folb P.I. Smith P. Determinants of rifampin, isoniazid, pyrazinamide, and ethambutol pharmacokinetics in a cohort of tuberculosis patients. *Antimicrobial Agents and Chemotherapy*. 2006, 50: 1170-1177.
- [31] Song S.H., Jun S.H., Park K.U., Yoon Y., Lee J.H., Kim J.Q., Song J. Simultaneous determination of first-line anti-tuberculosis drugs and their major metabolic ratios by liquid chromatography/tandem mass spectrometry. *Rapid Communications in Mass Spectrometry*. 2007, 21(7): 1331-1338.
- [32] Glass B.D., Agatonovic-Kustrin S., Chen Y.J., Wisch H. Optimization of a stability-indicating HPLC method for the simultaneous determination of rifampicin, isoniazid, and pyrazinamide in a fixed-dose combination using artificial neural networks. *Journal of Chromatographic Sciences*. 2007, 45: 38-44.
- [33] Ruslami R., Nijland H.M., Alisjahbana B., Parwati I., van Crevel R., Aarnoutse R.F. Pharmacokinetics and tolerability of a higher rifampin dose vs. the standard dose in pulmonary tuberculosis patients. *Antimicrobial Agents Chemotherapy*. 2007, 51: 2546-2561.
- [34] Kruijtzter C.M.F., Beijen J.H., Schellens J.H.M. Improvement of oral drug treatment by temporary inhibition of drug transporters and or cytochrome P450 in the gastrointestinal tract and liver: an overview. *The Oncologist*. 2007, 7: 516-530.
- [35] Hardman J.G., Limbird L.E., Molinoff P.B., Ruddon R.W. Goodman & Gilman's *The pharmacological basis of therapeutics*. 9th ed., New York: McGraw Hill, 1996.

- [36] Shishoo C.J., Shah S.A., Rathod I.S., Savale S.S., Vora M.J. Impaired bioavailability of rifampicin in presence of isoniazid from fixed dose combination (FDC) formulation. *International Journal of Pharmaceutics*. 2001, 228: 53-67.
- [37] Agrawal S., Singh I., Kaur K.J., Bhade K.J., Kaul C.L., Panchgnula R. Comparative bioavailability of rifampicin, isoniazid and pyrazinamide from a four drug fixed dose combination with separate formulations at the same dose levels. *International Journal of Pharmacognosy*. 2004. 276: 41-49.
- [38] Agrawal S., Singh I., Kaur K.J., Bhade S., Kaul C.L., Panchagnula R. Bioequivalence trials of rifampicin containing formulations: extrinsic and intrinsic factors in the absorption of rifampicin. *Pharmacological Research*. 2004. 50: 317-327.
- [39] Singh S., Mariappan T.T., Sankar R., Sarda N., Singh B. A critical review of the probable reasons for the poor/variable bioavailability of rifampicin from anti-tubercular fixed-dose combination (FDC) products, and the likely solution to the problem. *International Journal of Pharmaceutics*. 2001, 228: 5-17.
- [40] Panchagnula R., Agrawal S. Agrawal S. Biopharmaceutic and pharmacokinetic aspects of variable bioavailability of rifampicin. *International Journal of Pharmaceutics*. 2004, 271 :1-4.
- [41] Agrawal S., Panchgnula R. Implication of biopharmaceutics and pharmacokinetics of rifampicin in variable bioavailability from solid oral dosage forms. *Biopharmaceutics and Drug Disposition*. 2005, 26:321-334.
- [42] Agrawal S., Ashokraj Y., Bharatam P.V., Pillai O., Panchgnula R. Solid-state characterization of rifampicin samples and its biopharmaceutic relevance. *European Journal of Pharmaceutical Sciences*. 2004, 22: 127-144.

- [43] Prasad B., Bhutani H., Singh S. Study of the interaction between rifapentine and isoniazid under acid conditions. *Journal of Pharmaceutical and Biomedical Analysis*. 2006, 16: 1438-41.
- [44] Shishoo C.J., Shah S.A., Rathod I.S., Savale S.S., Kotecha J.S., Shah P.B. Stability of rifampicin in dissolution medium in presence of isoniazid. *International Journal of Pharmaceutics*. 1999, 190: 109-123.
- [45] Panchgnula R., Rungta S., Sancheti P., Agrawal S., Kaul C.L. In-vitro evaluation of food effect on the bioavailability of rifampicin from antituberculosis fixed dose combination formulation. *Farmaco*. 2003, 58: 1099-1103.
- [46] Singh S., Mariappan T.T., Bhutani H. Novel anti-tuberculosis FDC formulations without reduced bioavailability of rifampicin: from concept to market. *International Journal of Tuberculosis and Lung Diseases*. 2005, 9: 701-702.
- [47] Du Toit L.C., Pillay V., Danckwerts M.P. Tuberculosis chemotherapy: current drug delivery approaches. *Respiratory Research*. 2006, 19: 118-120.
- [48] Pandey R., Khuller G.K. Chemotherapeutic potential of alginate-chitosan microspheres as anti-tubercular drug carriers. *Journal of Antimicrobial Chemotherapy*. 2004. 53: 635-640.
- [49] Du Toit L.C., Pillay V., Danckwerts M.P., Penny C., Formulation and statistical optimization of a novel crosslinked polymeric anti-tuberculosis drug delivery system. *Journal of Pharmaceutical Sciences*. 2007, 97: 2176-2207.
- [50] Sharma A., Pandey R., Sharma S., Khullar G.K. Chemotherapeutic efficacy of poly (DL-lactide-co-glycolide) nanoparticle encapsulated antitubercular drugs at sub-therapeutic dose against experimental tuberculosis. *International Journal of Antimicrobial Agents*. 2004, 24: 599-604.

- [51] Pandey R., Sharma S., Khullar G.K. Chemotherapeutic efficacy of nanoparticle encapsulated antitubercular drugs. *Drug Delivery*. 2006, 13: 287-294.
- [52] Pandey R., Khullar G.K. Oral nanoparticle-based antituberculosis drug delivery to the brain in an experimental model. *Journal of Antimicrobial Chemotherapy*. 2006, 57: 1146-1152.
- [53] Pandey R., Sharma A., Zhoor A., Sharma S., Khullar G.K., Prasad B. Poly (DL/Lactide/co/glycolide) nanoparticle based inhalable sustained drug delivery system for experimental tuberculosis. *Journal of Antimicrobial Chemotherapy*. 2003, 52: 981-986.
- [54] Pandey R., Khullar G.K., Solid lipid particle-based inhalable sustained drug delivery system against experimental tuberculosis. *Tuberculosis*. 2005; 85: 227-234.
- [55] Pandey R., Khuller G.K. Subcutaneous nanoparticle-based antitubercular chemotherapy in an experimental model. *Journal of Antimicrobial Chemotherapy*. 2004, 54: 266-268.
- [56] Silva M., Lara A.S., Leite C.Q., Ferreira E.I. Potential tuberculostatic agents: micelle-forming copolymer poly (ethylene glycol)-poly(aspartic acid) prodrug with isoniazid, *Archives of Pharmacology*. 2001, 334: 189-193.
- [57] Quenelle D.C., Winchester G.A., Staas J.K., Barow E.L., Barow W.W. Treatment of tuberculosis using a combination of sustained release rifampicin microspheres and oral dosing with isoniazid. *Antimicrobial Agents and Chemotherapy*. 2001, 45: 1637-1644.
- [58] El-Negoumy S.I., Mansour R.M.A. Flavone glycosides of *Cuminum cyminum* seeds. *Fasc*. 1989, 40: 87-89.

- [59] Khafagy S.M., Sarg T.M., Abdel Salem N.A., Gabr O. Isolation of two flavone glycosides from the fruits of *Cuminum cyminum* grown in Egypt. *International Journal of Pharmaceutical Sciences*. 1978, 33: 296-297.
- [60] Ishikawa T., Takayanagi T., Kitazima J. Water soluble constituents of cumin:monoterpene glucosides. *Chemical and Pharmaceutical Bulletin*. 2002, 50: 1471-1478.
- [61] Kitazima J., Ishikawa T., Fuzimatu E., Kondho K., Takayanagi T. Glycosides of 2-C-methyl-D-erythritol from the fruits of anise, coriander and cumin. *Phytochemistry*. 2003, 62: 115-120.
- [62] Takayanagi T., Ishikawa T., Kitazima J. 2003. Sesquiterpene lactone glucosides and alkyl glucosides from the fruit of cumin. *Phytochemistry*. 63: 479-484.
- [63] Zheng G.Q., Kenney P.M., Lam L.K. Anethofuran, carvone and limonene: potential cancer chemopreventive agents from dill weed oil and caraway oil. *Planta Medica*. 1992, 58: 338-341.
- [64] Matsumura T., Ishikawa T., Kitazima J. Water soluble constituents of caraway: aromatic compound, aromatic compound glucoside and glucides. *Phytochemistry*. 2002, 61: 455-459.
- [65] Kunzenmann J., Herrmann K. Isolation and identification of flavon(ol)-O-glycosides in caraway (*Carum carvi* L.), fennel (*Foeniculum vulgare* Mill.), anise (*Pimpinella anisum* L.) and coriander (*Coriandrum sativum* L.) and of flavon-C-glycosides in anise. I. Phenolics of spices. *Z Lebensm Unters Forsch*. 1997, 164: 194-200.
- [66] Bouwmeester H.J., Gershenzon J., Konings M.C., Croteau R. Biosynthesis of the monoterpenes limonene and carvone in the fruit of caraway. I. Demonstration of enzyme activities and their changes with development. *Plant Physiology*. 1998, 117: 901-912.

- [67] Chopra R.N., Nayar. S.L., Chopra. I.C. Glossary of Indian Medicinal Plants (Including the Supplement). New Delhi: Council of Scientific and Industrial Research, New Delhi. 1986.
- [68] Mhaskar K.S., Blatter E. and Caius J.F. Kiritikar & Basu's Illustrated Indian Medicinal Plants. New Delhi: Satguru Publications; 2000.
- [69] Tahraoui A., El-Hilaly J., Israili Z.H., Lyoussi B. Ethnopharmacological survey of plants used in the traditional treatment of hypertension and diabetes in south-Eastern Morocco (Errachidia province). *Journal of Ethnopharmacology*. 2007, 110: 1105-1117.
- [70] Khan S., Balick M.J. Therapeutic plants of Ayurveda: A review of selected clinical and other studies for 166 species. *Journal of Alternative and Complementary Medicine*. 2001, 7: 405-415.
- [71] Bown D. *Encyclopaedia of Herbs and their Uses*. London: Dorling Kindersley; 1995.
- [72] Chevallier A. *The Encyclopedia of Medicinal Plants*. London: Dorling Kindersley; 1996.
- [73] Iacobellis N.S., Lo Cantore P., Capasso F., Senatore F. Antibacterial activity of *Cuminum cyminum* L. and *Carum carvi* L. essential oils. *Journal of Agricultural and Food Chemistry*. 2005, 53: 57-61.
- [74] Mahady G.B., Pendland S.L., Stoia A., Hamill F.A., Fabricant D., Dietz B.M., et al. *In vitro* susceptibility of *Helicobacter pylori* to botanical extracts used traditionally for the treatment of gastrointestinal disorders. *Phytotherapy Research*. 2005, 19: 988-91.
- [75] Satyanarayana S., Sushruta K., Sarma G.S., Srinivas N., Subba Raju G.V. Antioxidant activity of the aqueous extracts of spicy food additives evaluation

and comparison with ascorbic acid in in-vitro systems. Journal of Herbal Pharmacotherapy. 2004, 4: 1-10.

- [76] Lemhadri A., Hajji L., Michel J.B., Eddouks M. Cholestrol and triglycerides lowering activities of caraway fruits in normal and streptozotocin diabetic rats. Journal of Ethnopharmacology. 2006, 106: 321-326.
- [77] Lahlou S., Tahraoui A., Israili Z., Lyoussi B. Diuretic activity of the aqueous extracts of *Carum carvi* and *Tanacetum vulgare* in normal rats. Journal of Ethnopharmacology. 2007, 110: 458-463.
- [78] Khayyal M.T., el-Ghazaly M.A., Kenaway S.A., Seif-el-Nasr M., Mahran L.G., Kafafi Y.A. Antiulcerogenic effect of some gastrointestinally acting plant extracts and their combination. *Arzneimittelforschung*. 2001, 51: 545-553.
- [79] Eddouks M., Lemhadri A., Michel J.B. Caraway and caper: potential anti-hyperglycaemic plants in diabetic rats. Journal of Ethnopharmacology. 2004, 94: 143-148.
- [80] Naderi-Kalali B., Allameh A., Rasaei M.J., Bach H.J., Behehti A., Doods K., et al. Suppressive effects of caraway (*Carum carvi*) extracts on 2,3,4,7,8-tetrachlorodibenzo-p- dioxindependent gene expression of cytochrome P450 1A1 in the rat H4IIE cells. *Toxicology in Vitro*. 2005, 19: 373-377.
- [81] Deeptha K., Kamaleeswari M., Sengottuvelan M., Nalini N. Dose dependent inhibitory effect of dietary caraway on 1,2-dimethylhydrazine-induced colonic aberrant crypt foci and bacterial enzyme activity in rats. *Investigational New Drugs*. 2006, 24: 479-488.
- [82] Kamaleeswari M., Deeptha K., Sengottuvelan M., Nalini N. Effect of dietary caraway (*Carum carvi* L.) on aberrant crypt foci development, fecal steroids, and intestinal alkaline phosphatase activities in 1,2-dimethylhydrazine-

- induced colon carcinogenesis. *Toxicology and Applied Pharmacology*. 2006, 214: 290-296.
- [83] Mazaki M., Kataoka K., Kinouchi T., Vinitketkumnuen U., Yamada M., Nohmi T., et al. Inhibitory effects of caraway (*Carum carvi* L.) and its component on N-methyl-N'-nitro-N-nitrosoguanidine-induced mutagenicity. *Journal of Medical Investigation*. 2006, 53: 123-133.
- [84] Shetty R.S., Singhal R.S., Kulkarni P.R. Antimicrobial properties of cumin. *World Journal of Microbiology and Biotechnology*. 1994, 10: 232-233.
- [85] Agnihotri S., Vaidya A.D. A novel approach to study antibacterial properties of volatile components of selected Indian medicinal herbs. *Indian Journal of Experimental Biology*. 1996, 34: 712-715.
- [86] Ozcan M., Erkmen O. Antimicrobial activity of the essential oils of Turkish plant spices. *European Food Research Technology*. 2001, 212: 658-660.
- [87] Singh G., Kapoor I.P., Pandey S.K., Singh U.K., Singh R.K. Studies on essential oils: part 10; antibacterial activity of volatile oils of some spices. *Phytotherapy Research*. 2002, 16: 680-682.
- [88] Singh G., Marimuthu P., Murali H.S., Bawa A.S. Antioxidative and antibacterial potentials of essential oils and extracts isolated from various spice materials, *Journal of Food Safety*. 2005, 25: 130-145.
- [89] Nostro A., Cellini L., Di Bartolomeo S., Di Campli E., Grande R., Cannatelli M.A., Marzio L., Alonzo V. Anti-bacterial effect of plant extracts against *Helicobacter pylori*. *Phytotherapy Research*. 2005, 19: 198-202.
- [90] Manuel V.M., Yolanda R.N., Perez-Alvarez F.L., Juana J.A. Antibacterial activity of different essential oils obtained from spices widely used in Mediterranean diet. *International Journal of Food Sciences and Technology*. 2008, 43: 526-531.

- [91] Shayegh S., Rasooli I., Taghizadeh M., Astaneh S.D. Phytotherapeutic inhibition of supragingival dental plaque. Antimicrobial activities properties of *Cuminum cyminum* essential oils against *Streptococcus mutans* and *Streptococcus pyogenes*. *Natural Products Research*. 2008, 22: 429-440.
- [92] Martinez-Tome M., Jimenez A.M., Ruggieri S., Frega N. , Strabbioli R. , Murcia M.A. Antioxidant properties of Mediterranean spices compared with common food additives. *Journal of Food Protection*. 2001, 64: 1412-1419.
- [93] Thippeswamy N.B., Naidu K.A. Antioxidant potency of cumin varieties--cumin, black cumin and bitter cumin on antioxidant systems. *European Food Research Technology*. 2005, 220: 472-476.
- [94] Topal U., Sasaki M., Goto M., Otles S. Chemical compositions and antioxidant properties of essential oils from nine species of Turkish plants obtained by supercritical carbon dioxide extraction and steam distillation. . *International Journal of Food Sciences and Nutrition*. 2007, 18: 1-16.
- [95] Sambaiah K., Srinivasan K. 1991. Effect of cumin, cinnamon, ginger, mustard and tamarind -induced hypercholesterolemic rats. *Nahrung*. 35: 47-51.
- [96] Dhandapani S., Subramanian V.R., Rajagopal S., Namasivayam N. Hypolipidemic effect of *Cuminum cyminum* L. on alloxan-induced diabetic rats. *Pharmacology Research*. 2002, 46: 251-255.
- [97] Kode A., Rajagopalan R., Penumathsa S.V., Menon V.P. Effect of ethanol and thermally oxidized sunflower oil ingestion on phospholipid fatty acid composition of rat liver: protective role of *Cuminum cyminum* L. *Annals of Nutrition and Metabolism*. 2005, 49: 300-303.
- [98] Vasudevan K., Vembar S., Veeraraghavan K., Haranath P.S. Influence of intragastric perfusion of aqueous spice extracts on acid secretion in anesthetized albino rats. *Indian Journal of Gastroenterology*. 2000, 19: 53-56.

- [99] Platel K., Srinivasan K. Studies on the influence of dietary spices on food transit time in experimental rats. *Nutrition Research*. 2001, 21: 1309-1314.
- [100] Tunc I., Berger B.M., Erler F., Dagli F. Ovicidal activity of essential oils from five plants against two stored-product insects. *Journal of Stored Products Research*. 2000, 36: 161-166.
- [101] Kubo I., Kinst-Hori I. Tyrosinase inhibitors from cumin. *Journal of Agricultural and Food Chemistry*. 1998; 46: 5338-5341.
- [102] Garg S.K. Antifertility screening of plants--effect of four indigenous plants. *Indian Journal of Medical Research*. 1976, 64: 1133-1135.
- [103] Lee H.S. Cuminaldehyde: Aldose Reductase and alpha-Glucosidase Inhibitor Derived from *Cuminum cyminum* L. Seeds. *Journal of Agricultural and Food Chemistry*. 2005, 53: 2446-2450.
- [104] Nalini N., Manju V., Menon V.P. Effect of spices on lipid metabolism in 1,2-dimethylhydrazine-induced rat colon carcinogenesis. *Journal of Medicinal Food*. 2006, 9: 237-245.
- [105] Gagandeep, Dhanalakshmi S., Méndiz E., Rao A.R., Kale R.K. Chemopreventive effects of *Cuminum cyminum* in chemically induced forestomach and uterine cervix tumors in murine model systems. *Nutrition and Cancer*. 2003, 47: 171-180.
- [106] Aruna K., Sivaramakrishnan V.M. Anticarcinogenic effects of some Indian plant products. *Food and Chemical Toxicology*. 1992, 30: 953-956.
- [107] Nalini N., Sabitha K., Vishwanathan P., Menon V.P. Influence of spices on the bacterial (enzyme) activity in experimental colon cancer. *Journal of Ethnopharmacology*. 1998, 62: 15-24.

- [108] Roman-Ramos R., Flores-Saenz J.L., Alarcon-Aguilar F.J. Anti-hyperglycemic effect of some edible plants. *Journal of Ethnopharmacology*. 1995, 48: 25-32.
- [109] Srinivasan K. Plant foods in the management of diabetes mellitus: spices as beneficial antidiabetic food adjuncts. *International Journal of Food Science and Nutrition*. 2005, 56: 399-414.
- [110] Malini T., Vanithakumari G. Estrogenic activity of *Cuminum Cyminum* in rats. *Indian Journal of Experimental Biology*. 1987, 25: 442-444.
- [111] Boskabady M., Kiani S., Azizi H. Relaxant effect of *Cuminum cyminum* on guinea pig tracheal chains and its possible mechanism. *Indian Journal of Pharmacology*. 2005, 37: 111-115.
- [112] Janahmadi M., Niazi F., Danvali S., Kamalinejad M. Effects of the fruit essential oil of *Cuminum cyminum* Linn. (Apiaceae) on pentylenetetrazole induced epileptiform activity in F1 neurons of *Helix aspersa*. *Journal of Ethnopharmacology*. 2005,104: 278-282.
- [113] Aruna K., Rukkumani R., Varma P.S., Menon V.P. Therapeutic role of *Cuminum cyminum* on ethanol and thermally oxidized sunflower oil- induced toxicity. *Phytotherapy Research*. 2005, 19: 416-421.
- [114] Srivastava K.C. Extracts from two frequently consumed spices--cumin (*Cuminum cyminum*) and turmeric (*Curcuma longa*) inhibit platelet aggregation and alter eicosanoid biosynthesis in human blood platelets. *Prostaglandins Leukotrienes Essential Fatty Acids*. 1989, 37: 57-64.

MATERIALS & METHODS

4. Material and Methods

4.1 Plant Materials

Following types of seeds were identified and authenticated by Dr. B.K. Kapahi, Senior Taxonomist of IIM, Jammu.

Type	Herb	Source
Cumin- White jeera	<i>Cuminum cyminum</i>	Hot, semi-arid region of Gujarat (Unjha)
Caraway- Black jeera	<i>Carum carvi</i>	Cold dessert area of Lahaul

Seed samples were dried in tray drier to remove the moisture and kept in self-sealing polythene bags and stored in vacuum chambers.

4.2 Animals

Inbred animals were procured from the Animal House of IIM, Jammu. Animals were kept (3 animals/cage) under regulated environmental conditions. (Temp. $26 \pm 2^{\circ}\text{C}$, relative humidity $50 \pm 5\%$; 12 h light/dark cycle) and maintained on pelleted rodent diet (Ashirwad Industries Ltd. Chandigarh, India). Water was provided *ad libitum*. The Institutional Animal Ethics Committee approved the animal handling and other protocols. The animals were fasted for 16 h before use unless otherwise indicated.

Animal	Strain	Sex	Weight Range (gm)
Rats	Wistar	M/F	160-180
Mice	Swiss albino C57BL/6	M/F	25-30
		M/F	25-30
Guinea Pig	English	M/F	350-450

4.3 Statistics/PK Software

Statistical comparisons were made by using SPSS 12.0 Data Editor. A PK software (PK solutions 2.0, Summit research services, Montrose, CO, USA) was used for determination of PK parameters.

4.4 Equipments

System	Model/Make	Manufacturer
Analytical Balance	Genius	Sartorius, Germany
Bath Sonicator	RK510H	Sonorex, Germany
Beta scintillation counter	1450 Microbeta Trilux	Perkin-Elmer, USA
Deep freeze	Scientemp	Adrian, USA
Elisa Plate Reader	Multiskan Spectrum	Thermo Electron, USA
Freeze drier	Virtis	Biopharma Process Sys., UK
Homogenizer	RW-20 DZM	IKA-WERK, Japan
HPLC system	LC-10 ATVP	Shimadzu, Japan
	Series 1100	Agilent, USA
Ice Maker Machine	Massa Martana-PG	Angelantoni Industries, Italy
Incubator	Climacell	BMT Group, Germany
IR	Vector 22	Brucker Daltonics, Germany
LCMS	Esquire 3000	Brucker Daltonics, Germany
NMR	DPX-200	Brucker Daltonics, Germany
Peristaltic Pump	Minipulse 2 & 3	Gilson, France
Pipettes	Finnpipette	Thermo Electron, USA
Refrigerated Centrifuge	3K30	Sigma, USA
Rota-vapor	R-114	Buchi, Germany
Solid phase extraction system	Visiprep	Supelco, USA
Solvent Evaporator	SPD 111V	Thermo Electron USA
Spectrofluometer	LS 50B	Perkin Elmer, USA
Tray Drier	PMD	Biochem. Engg., India
UV-Visible Spectrophotometer	UV-1601PC	Shimadzu, Japan
Vortex Mixer	Vortex Genie-2	Scientific Ind., USA
Water Bath Shaker	C76	Edison, USA
Water Purif. System	Elix	Millipore, USA

4.5 Chemicals and reagents

Identity	Abbreviation	Grade	Source
Acetic acid		AR	Qualigens, India
Acetonitrile	ACN	HPLC	Rankem, India
Adenosine triphosphate	ATP	AR	Sigma, USA
2-Aminoethyl diphenylborinate		AR	Qualigens, India
Barium hydroxide	Ba(OH) ₂	AR	Qualigens, India
³ H Benzopyrene	³ H BP	AR	Sigma, USA
Bovine serum albumin	BSA	AR	Sigma, USA
n- Butanol	n-BuOH	HPLC	Rankem, India
Calcium chloride	CaCl ₂	Extra-pure	Sigma, USA
Chloroform	CHCl ₃	HPLC	Rankem, India
Creatinine phosphokinase		AR	Sigma, USA
Di-chloromethane	DCM	HPLC	Rankem, India
Di-methyl sulfoxide	DMSO	HPLC	Rankem, India
Di-potassium hydrogen phosphate	K ₂ HPO ₄	Extra-pure	Qualigens, India
Di-sodium hydrogen phosphate	Na ₂ HPO ₄	Extra-pure	Qualigens, India
Dithiothreitol		AR	Sigma, USA
Dulbecco's phosphate buffered saline		AR	Sigma, USA
Ethanol	EtOH	HPLC	Qualigens, India
Erythromycin			Sigma, USA
Ethyl acetate		HPLC	Rankem, India
Ethylenediamine tetra-acetic acid	EDTA	AR	Sigma, USA
Ethylene glycol tetra-acetic acid	EGTA	AR	Sigma, USA
Folin's reagent		AR	Qualigens, India
Formaldehyde	HCHO	AR	Qualigens, India
Glucose		AR	Hi-media, India
L-Glutamine		AR	Sigma, USA
Heparin		AR	Sigma, USA
Hexane		HPLC	Rankem, India
Hexadecane		AR grade	Sigma, USA
4-(2-hydroxyethyl)-1-piperazineethanesulfonic acid	HEPES	AR	Sigma, USA
Isoniazid	INH	AR	Sigma, USA
Isopropyl alcohol	IPA	HPLC	Rankem, India

List contd.

Magnesium chloride	MgCl ₂	AR	Hi-media, India
Mannitol		AR	Hi-media, India
Methanol	MeOH	HPLC	Rankem, India
Nicotine adenine di-nucleotide phosphate (Reduced)	NADPH	AR	Sigma, USA
Ouabain		AR	Sigma, USA
Phenobarbital		AR	Sigma, USA
Phenol Red		LR	Qualigens, India
Phosphate buffered saline		Extra-pure	Hi-media, India
Phosphocreatinine		AR	Sigma, USA
<i>o</i> -phosphoric acid		AR	Qualigens, India
Picric acid		LR	Qualigens, India
Piperine	PIP	AR	Sigma, USA
Poly ethylene glycol 4000	PEG	AR	Hi-media, India
Potassium chloride	KCl	Extra-pure	Hi-media, India
Potassium Dihydrogen phosphate	KH ₂ PO ₄	Extra-pure	Qualigens, India
Propylene glycol		LR	Qualigens, India
Pyrazinamide	PZA	AR	Sigma, USA
Rifampicin	RIF	AR	Sigma, USA
Rhodamine 123	Rho123	AR	Sigma, USA
Silica gel		AR	Merck, USA
Sodium acetate		Extra-pure	Hi-media, India
Sodium azide	NaN ₃	AR	Sigma, USA
Sodium bicarbonate	NaHCO ₃	Extra-pure	Hi-media, India
Sodium chloride	NaCl	Extra-pure	Hi-media, India
Sodium carboxy methyl cellulose	NaCMC	LR	Hi-media, India
Sodium Dihydrogen Phosphate	NaH ₂ PO ₄	Extra-pure	Qualigens, India
Sodium dodecyl sulphate	SDS	AR	Sigma, USA
Sodium citrate		Extra-pure	Hi-media, India
Sodium pentobarbital		AR	Sigma, USA
Sucrose		Extra-pure	Hi-media, India
Testosterone		AR	Sigma, USA
Tris buffer		AR	Hi-media, India
<i>o</i> -vanadate		AR	Sigma, USA
Verapamil		AR	Sigma, USA
Water		HPLC	Millipore, USA
Zinc sulphate	ZnSO ₄	AR	Hi-media, India

4.6 Development and validation of HPLC protocols for the determination of anti-TB drugs in rat plasma.

4.6.1 Instrumentation: Chromatographic analysis was performed on Shimadzu HPLC system equipped with a diode array detector (SPD-M10AVP), solvent delivery module (LC-10ATVP), online degasser (DGU-14A), an auto-injector (SIL-10ADVP), flow channel system (FCV-14AH) and system controller (SCL-10AVP) using a reversed-phase HPLC column (RP-18, 250×4.6 mm, 5µm particle size, Sigma, USA). (Software for data analysis: VP V6.12 SP2).

4.6.2 Selection of columns (stationary phases) and mobile phases: On the basis of physico-chemical properties of each analyte (RIF, INH and PZA), various mobile phases were tested on the lipophilic stationary phases for best possible resolution. The columns (stationary phases) of various packing materials and particle sizes from different manufacturers were used. The organic solvents like MeOH, acetonitrile (ACN) and isopropyl alcohol (IPA) along with organic modifier such as acetate, citrate, and phosphate buffers were investigated as mobile phase composition for their ability to resolve the analytes.

4.6.3 General: The solutions were prepared by weighing suitable quantity of individual drug using aluminium foil. The weighed quantity was transferred to volumetric flask and solubilized using HPLC grade ACN. The HPLC column was equilibrated with mobile phase composition for at least 2 h before start of analysis. The external standard method was utilized for quantitation.

4.6.4 Preparation of reference solutions: Initially, 50 mg of RIF was exactly weighed using pre-calibrated analytical balance and transferred in a 50 ml volumetric flask and dissolved using sonication. Dilutions were made with ACN to achieve 1mg/ml strength (Stock-I). The reference solution containing flask was covered with foil and sealed with paraffin film to avoid degradation and loss due to evaporation. In a similar manner, reference solutions of INH and PZA were prepared and stored. In case of PZA reference solution, HPLC grade water was used as solvent.

4.6.5 Preparation of calibration standards (CAL STD): The Stock-I solutions were diluted to different working stock solutions with the HPLC grade ACN (for RIF and INH) and water (for PZA). 50 µl of each RIF working stock was spiked in blank plasma to achieve conc. of the analytical range 0.1-20 µg/ml for RIF (**Table 4**). The 50 µl of each working stock solution of INH and PZA was spiked to achieve the conc. range of 0.1-10 µg/ml and 0.05-30 µg/ml in combination for INH and PZA respectively (**Table 5**).

4.6.6 Preparation of quality control standards (QC STD): Stock-II (1mg/ml) solutions were prepared by weighing, dissolving and diluting suitable quantity of RIF, INH and PZA as described above in **Section 4.6.4**. The stock-II solutions were diluted everyday of experiment and 3 quality control standards (0.10 µg/ml, 10.00 µg/ml and 20.00µg/ml of RIF and 0.1 µg/ml + 0.05 µg/ml, 2.5 µg/ml + 10.0 µg/ml and 10.0 µg/ml + 30.0 µg/ml of INH + PZA) were prepared (**Table 4-5**).

4.6.7 Preparation of system suitability standards (SS STD): Stock-III (1mg/ml) solutions were prepared by weighing, dissolving and diluting suitable quantity of RIF,

INH and PZA as described above in **Section 4.6.4**. The stock-III solutions were diluted on the day of experiment and SS STD of 1.00 µg/ml were prepared (**Table 4-5**).

4.6.8 Recovery procedure: The SPE technique was used to recover the RIF from plasma. A semi-automated vacuum chamber and vacuum pump system (Supelco, USA) were used for the extraction of RIF using following steps: (a) conditioning of the SPE cartridge (C18, 3 ml capacity, 100 mg bed, Samprep-Ranbaxy, Mumbai, India) with 2 ml MeOH followed by 2 ml HPLC grade water and 2 ml 50 mM phosphate buffer (pH 5.0), (b) dispensing 2 ml of diluted (1:5 dilution with HPLC grade water) spiked plasma (RIF added externally to achieve 0.1, 10 and 20 µg/ml conc. in plasma) into SPE cartridge and drying under positive pressure, (c) washing with 2 ml HPLC grade water followed by 2 ml 50 mM phosphate buffer (pH 5.0), and (d) eluting the samples with 2 ml of HPLC grade ACN. The eluents were carefully collected in clean glass tubes and 50 µl of each sample was injected into HPLC system for analysis.

The LLE technique was optimized for simultaneous recovery of INH and PZA from plasma. To the 500 µl spiked plasma samples (INH+PZA added externally to achieve 0.1 µg/ml + 0.05 µg/ml, 2.5 µg/ml + 10.0 µg/ml and 10.0 µg/ml + 30.0 µg/ml conc. in plasma), 3 ml mixture of HPLC grade IPA and dichloromethane (DCM) (1:2 v/v) was added using micro-pipettes and the samples were vortexed for 2 min. The organic layer was separated and collected by using glass syringe and needle. The separated organic layer was allowed to dry using solvent evaporator (Thermo Electron Corporation, USA). The dry samples thus obtained were reconstituted in 300 µl mobile phase, filtered through 0.45 µm syringe filters (Millipore, USA) and injected into HPLC system for analyzing its contents.

Table 4. Preparation of standard solutions (RIF)

	Strength (µg/ml)	RIF Ref. stock solution (mg/ml)	RIF working stock solution (µg/ml)	Vol. of working stock solution (µl)	Vol. of blank plasma solution (µl)	Total Vol. (µl)
CAL STD 1	0.1	1	2	50	950	1000
CAL STD 2	0.5	1	10	50	950	1000
CAL STD 3	1.0	1	20	50	950	1000
CAL STD 4	2.5	1	50	50	950	1000
CAL STD 5	5.0	1	100	50	950	1000
CAL STD 6	10.0	1	200	50	950	1000
CAL STD 7	20.0	1	400	50	950	1000
QC STD 1	0.1	1	2	50	950	1000
QC STD 2	10.0	1	200	50	950	1000
QC STD 3	20.0	1	400	50	950	1000
SS STD 1	1.0	1	20	50	-	1000*

*CAL STD; Calibration standards, QC STD; Quality control standards, SS STD; System suitability standards; *with mobile phase*

Table 5. Preparation of standard solutions (INH+PZA)

	Strength (µg/ml)	Ref. stock solution (mg/ml)		Working stock solution (µg/ml)		Vol. of working stock solution (µl)		Vol. of blank plasma (µl)	Total Vol. (µl)
	(INH + PZA)	INH	PZA	INH	PZA	INH	PZA		
CAL STD 1	0.1 + 0.05	1	1	2	1	50	50	900	1000
CAL STD 2	0.5 + 1.0	1	1	10	20	50	50	900	1000
CAL STD 3	1.0 + 5.0	1	1	20	100	50	50	900	1000
CAL STD 4	2.5 + 10.0	1	1	50	200	50	50	900	1000
CAL STD 5	5.0 + 20.0	1	1	100	400	50	50	900	1000
CAL STD 6	10.0 + 30.0	1	1	200	600	50	50	900	1000
QC STD 1	0.1 + 0.05	1	1	2	1	50	50	900	1000
QC STD 4	2.5 + 10.0	1	1	50	200	50	50	900	1000
QC STD 6	10.0 + 30.0	1	1	200	600	50	50	900	1000
SS STD 6	1.0 + 1.0	1	1	20	20	50	50	-	1000*

*CAL STD; Calibration standards, QC STD; Quality control standards, SS STD; System suitability standards; *with mobile phase*

4.6.9 Validation: The method was validated in accordance with guidelines of International Conference on Harmonization (ICH). The parameters assessed were linearity, range, accuracy, precision, specificity, limit of quantitation and robustness.

A. System suitability: The SS STD (1 µg/ml) were utilized for the test. The system suitability test was performed using nine replicate injections before analysis of samples. The acceptance parameters were less than 0.5 % and 1.5 % relative standard deviation (R.S.D.) for retention time and peak area respectively along with more than 3500 plates.

B. Recovery: The spiked plasma samples of RIF and INH+PZA were analyzed and the peak area obtained for each sample was fitted mathematically into amount vs. peak area co-relation.

C. Linearity and range: Seven and six point calibration curves were constructed over a pre-defined conc. range of RIF and INH+PZA respectively. The peak areas vs. conc. plots were subjected to linear least square regression analysis. The intra and inter-day linearity was established.

D. Accuracy and precision: The accuracy and precision of method was estimated by analyzing QC standards. The intra and inter-day accuracy was established by evaluating nominal and mean measured conc. of QC STD which were compared and expressed as difference% (diff.%). The diff.% was calculated by using following formula. $\text{Diff.\%} = [(\text{Mean measured conc.} - \text{Nominal conc.}) / \text{Nominal conc.}] \times 100$. The intra and inter-day precision was established by analyzing nine replicates each of 3 QC STD at 3 different time intervals in a day and on three consecutive days respectively. It was expressed in terms of % RSD.

E. Limit of quantitation (LOQ): The lowest conc. of calibration curves with acceptable accuracy and precision were reported as LOQ for all the 3 analytes.

Further, it was confirmed by signal to noise (S/N) ratio values. The signal 3 times noise value was treated as limit of detection (LOD) and 9 times noise value as LOQ.

F. Robustness: The robustness of both the methods was evaluated by analyzing quality control standards after varying the mobile phase composition and pH of aqueous buffer. The ACN volume in total mobile phase was modified in between 55-65 %. The pH range selected for study was from 4.5 to 5.5. The acceptance criteria were less than 2 % variation in the final results after modification in mobile phase composition and pH.

G. Specificity: The specificity of both the methods was assessed using spiked plasma samples. The INH+PZA working solutions were spiked into RIF -containing plasma samples so as to check their interference in RIF estimation. The specificity of INH+PZA estimation method was assessed by spiking RIF into plasma samples containing INH+PZA.

H. Stability: The stability of RIF and INH+PZA in plasma was demonstrated using spiked plasma samples of different conc. after (a) 24 h storage at room temperature (protected from light), (b) three freeze-thaw cycles and (c) 1 month frozen storage at -80⁰C. The stability of the processed samples in the autosampler (10⁰C) was confirmed after 24 h storage.

4.7 Standard operating procedure for determination of anti-TB drugs in rat plasma.

A. Dose calculation: Rat doses of RIF, INH and PZA were derived as follows.

Drug	Human dose (mg/70kg)	x Factor	Rat dose (mg/200 gm)	Dose (mg/kg)
RIF	450	0.018	8.1	40
INH	300	0.018	5.4	30
PZA	1000	0.018	18	90

B. Dosing volume:

Oral	1.0 ml/100 gm
Intravenous	0.5 ml/100 gm

C. Preparation of drug solution for oral administration: The required quantity of each drug was weighed accurately by using analytical balance and was transferred to glass mortar and pestle. The sodium carboxy methyl cellulose (Na-CMC) (2 % of total volume of formulation) was added as suspending agent. The weighed material was triturated and aqueous fine suspension was prepared by using HPLC grade water.

D. Solution/ suspensions for oral dosing: Extracts/fractions (obtained as described in **Section 4.8**) of aqueous nature were dissolved in distilled water, whereas extracts/fractions of non-aqueous nature were formulated as aq. suspensions using 2 % Na-CMC. The pure molecules were dissolved in the distilled water.

E. Preparation of drug solution for intravenous administration: The 10 mg of RIF was dissolved in 150 μ l mixture of dimethyl sulfoxide (DMSO), ethanol (EtOH) and propylene glycol (1:1:1 v/v) and diluted with 1 % poly ethylene glycol (PEG) 4000 in sterile normal saline upto 1000 μ l.

F. Storage: Solutions were prepared fresh on each day of experiment, and stored in amber colored glass vial (20 ml capacity) away from direct light exposure.

G. Procedure for blood samples collection: The animals were marked with marking solution (5 % picric acid) for individual identification, and weights were recorded using an animal weighing balance. The required volumes of drug solutions with or without a test material was administered orally using oral feeding cannula. The exact time of formulation administration (drug with or without test material) was noted. At pre-defined time intervals, the blood samples (500 µl) were collected from individual animal via retro-orbital plexus using glass capillaries in heparinized glass tubes. The blood samples were centrifuged at 5000 rpm for 10 min and the plasma was collected. The plasma samples (100 µl each) were processed for the recovery of drug(s) according to pre-optimized procedure as described in **Section 4.6.8**.

H. HPLC analysis: The recovered and dry samples were reconstituted in respective mobile phases (300 µl), filtered through 0.45 µm syringe filter and analyzed for anti-TB drugs by HPLC.

4.8 Preparation of herbal test materials.

Seeds of cumin and caraway were ground to a coarse powder using grinder mixer. The powdered materials were processed to obtain the following test materials as per the scheme depicted in **Fig. 8A-B: Flow Charts A- B**.

Seed	Herbal Product	Sample Identity
<i>Cumin</i>	Aq. Extract	CM-1
	50 % Aq. Alcol. Extract	CM-2
	95 % Alcol. Extract	CM-3
Caraway	Aq. Extract	CR-1
	50 % Aq. Alcol. Extract	CR-2
	95 % Alcol. Extract	CR-3

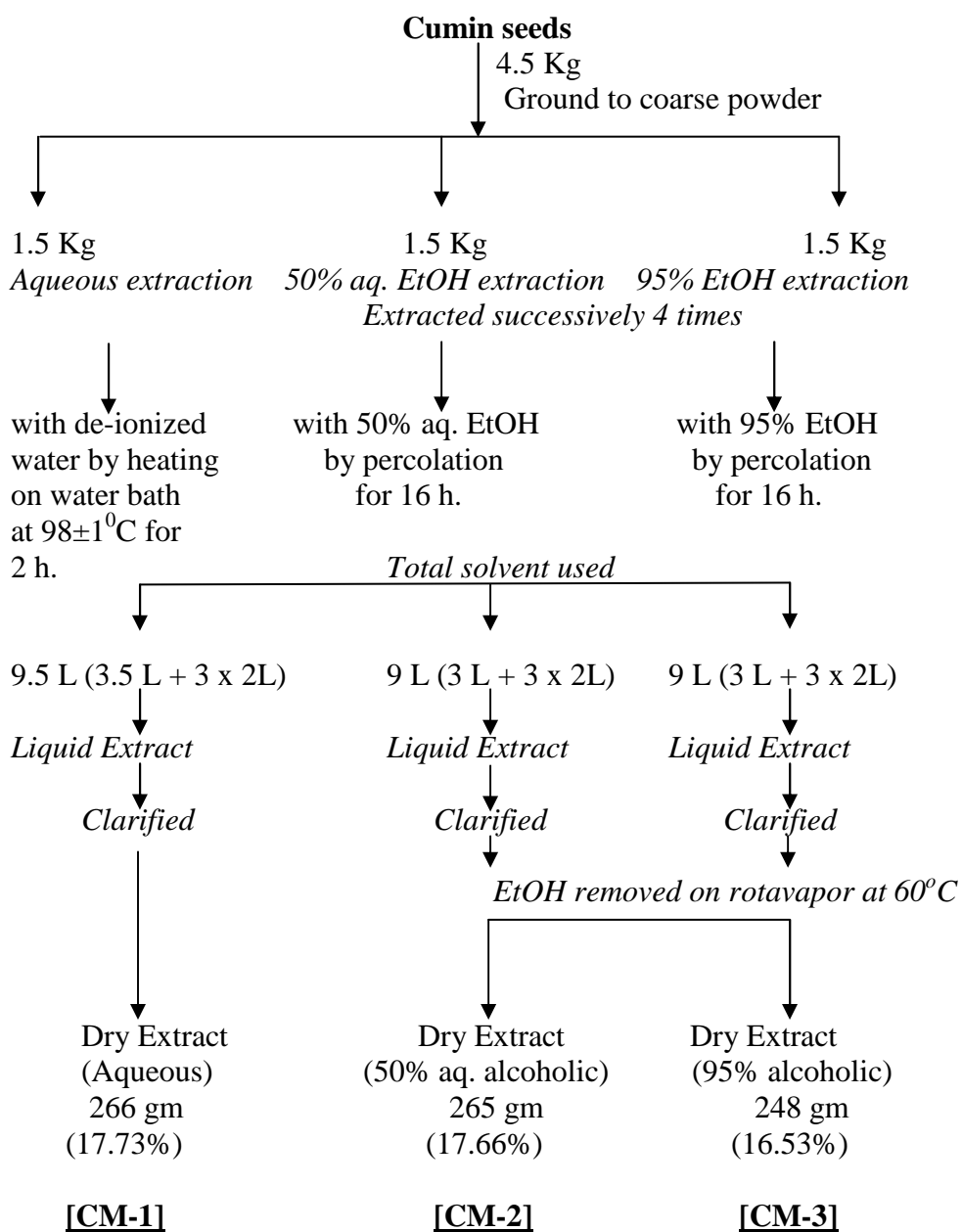


Fig. 8A. Flow Chart-A

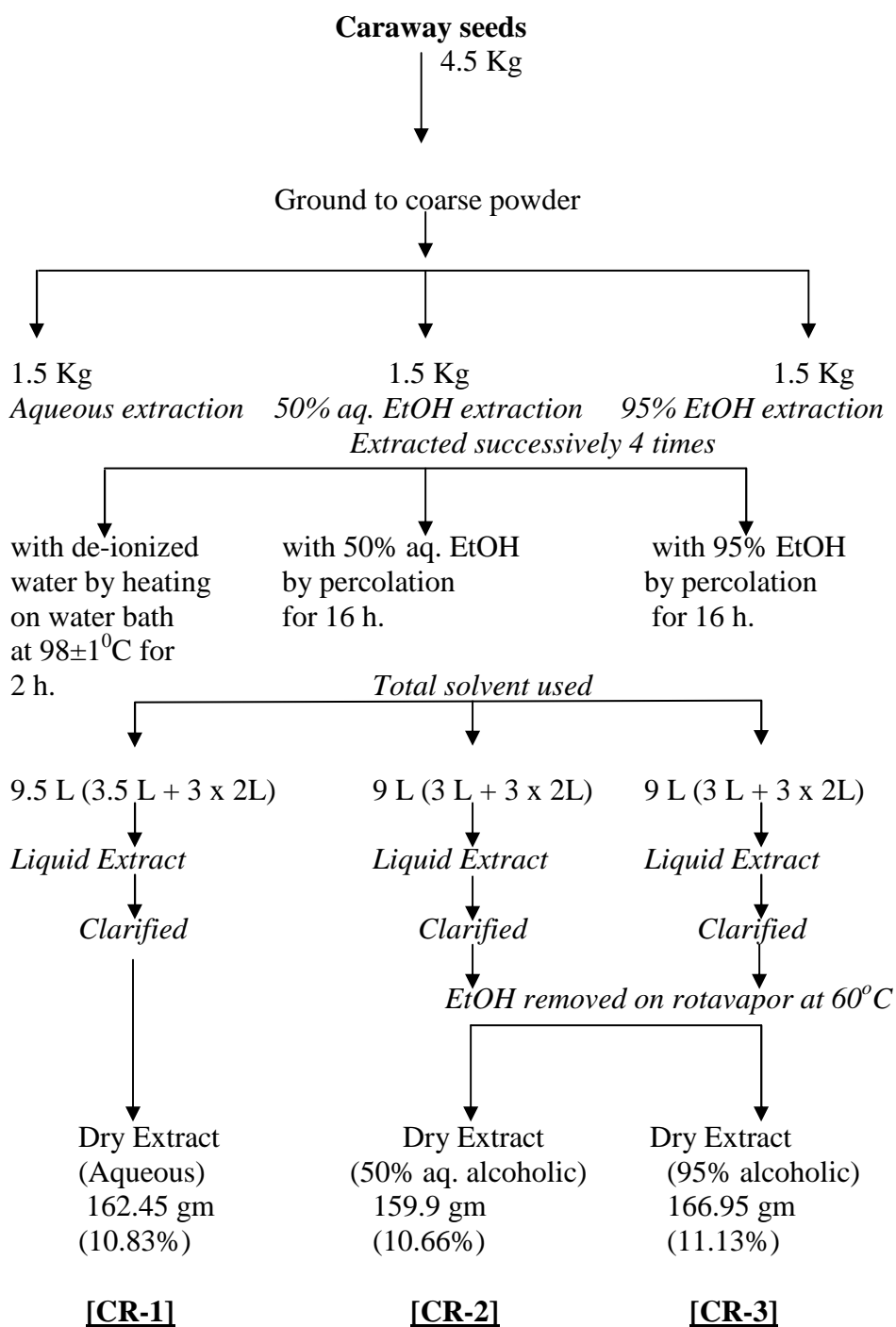


Fig. 8B. Flow Chart-B

Optimized HPLC conditions for Finger printing of test materials.

Mobile phase: ACN: water containing 2 % acetic acid (17:83 v/v)

Flow rate: 1 ml/min.

Column: RP-18 (250 x 4.6 mm, 5 μ m (Merck)

Oven temp.: 30°C

Detection wavelength: 254 nm

HPLC Finger print Method validation.

On the basis of FG-3 and TF-1 [R.T. = 7.58 for CM-1(2), and 20.77 for CR-1(1)], the validation study was performed.

A. Linearity and range: The calibration curves were linear ($r^2 > 0.99$) over the low-to-high conc. range of 1-10 μ g/ml for both CM-1(2) and CR-1(1).

The intra-day and inter-day accuracy (diff.%) and precision (%RSD) was calculated using three conc. [1, 5 and 10 μ g/ml each of CM-1(2) and CR-1(1)].

B. Accuracy: The intra-day diff.% for CM-1(2) was between -1.3 and 3.2 % whereas for CR-1(1), it was between -2.1 and 4.7 %. The inter-day diff.% for CM-1(2) was between -2.6 and 5.2 % whereas for CR-1(1), it was between -3.4 and 6.1 %.

C. Precision: The intra-day % RSD for CM-1(2) was between 2.5 and 4.7 % whereas for CR-1(1), it was 1.9 and 3.7 %. The inter-day % RSD for CM-1(2) was between 3.1 and 5.7 % whereas for CR-1(1), it was between 3.1 and 5.9 %.

D. Stability: The stability of CM-1(2) and CR-1(1) at 5 μ g/ml strength was demonstrated after 1, 6 and 15 day storage at room temperature. The % RSD of CM-1(2) was 1.2 (day 1), 3.7 (day 6) and 4.2 (day 15) whereas that of CR-1(1) was 3.1 (day 1), 4.3 (day 6) and 5.9 (day 15).

4.9 Bioevaluation of parent extracts from cumin/caraway.

Initially for proof of efficacy and activity guided fractionation the effect of test materials was investigated during the peak time window of the drugs (1-4 h) post-administration.

Study 1A. Effect of CM/CR extracts on the plasma levels of anti-TB drugs.

Experimental design: A total of 42 rats were divided into 7 groups (6 rats/group). Test drugs (RIF, INH and PZA) along with CM/CR test materials (arbitrary dose of 100 mg/kg) were administered per orally to various groups as follows:

Gr	Treatment (p.o.)
I	RIF, 40 mg/kg + INH, 30 mg/kg+ PZA, 90 mg/kg
II	RIF, 40 mg/kg + INH, 30 mg/kg+ PZA, 90 mg/kg + CM-1 (100 mg/kg)
III	RIF, 40 mg/kg + INH, 30 mg/kg+ PZA, 90 mg/kg + CM-2 (100 mg/kg)
IV	RIF, 40 mg/kg + INH, 30 mg/kg+ PZA, 90 mg/kg + CM-3 (100 mg/kg)
V	RIF, 40 mg/kg + INH, 30 mg/kg+ PZA, 90 mg/kg + CR-1 (100 mg/kg)
VI	RIF, 40 mg/kg + INH, 30 mg/kg+ PZA, 90 mg/kg + CR-2 (100 mg/kg)
VII	RIF, 40 mg/kg + INH, 30 mg/kg+ PZA, 90 mg/kg + CR-3 (100 mg/kg)

Blood samples were collected during the peak time window (1, 2, 3 and 4 h post-dosing), and processed to obtain plasma. Drug conc. was determined as described in **Section 4.6.8**.

The results as summarized in **Table 12-13 (Section 5.2.1)** showed that CM-1 and CR-1 were the active samples, which were taken up for further dose -dependent investigation.

Study 1B. Dose-dependent study.

Experimental design: A total of 24 rats were divided into 4 groups (6 rats/group), and treated as per the following schedule:

Gr	Treatment (p.o.)
I	RIF, 40 mg/kg + INH, 30 mg/kg+ PZA, 90 mg/kg + CM-1 (40 mg/kg)
II	RIF, 40 mg/kg + INH, 30 mg/kg+ PZA, 90 mg/kg + CM-1 (16 mg/kg)
III	RIF, 40 mg/kg + INH, 30 mg/kg+ PZA, 90 mg/kg + CR-1 (40 mg/kg)
IV	RIF, 40 mg/kg + INH, 30 mg/kg+ PZA, 90 mg/kg + CR-1 (16 mg/kg)

Collection and analysis of plasma samples was done as described in **Study 1A**.

The results as summarized in **Table 12-13 (Section 5.2.1)** showed that CM-1 and CR-1 produced optimum effect at a dose of 16 mg/kg.

- The activity guided fractionation of CM-1 and its bioevaluation was continued.

The results are described in **Section 4.9.1**.

- The activity guided fractionation of CR-1 and its bioevaluation was continued.

The results are described in **Section 4.9.2**.

4.9.1 Activity guided fractionation of cumin (CM-1).

CM-1 (active aqueous extract of cumin seed) was partitioned into 5 fractions as per the scheme depicted in **Fig. 8C-D: Flow Chart C I-II**. Following fractions were obtained.

CM-1(1)	Butanolic
CM-1(2)	Aqueous
CM-1(3)	Ethanolic
CM-1(4)	50 % aqueous-ethanolic
CM-1(5)	Marc (remaining residue)

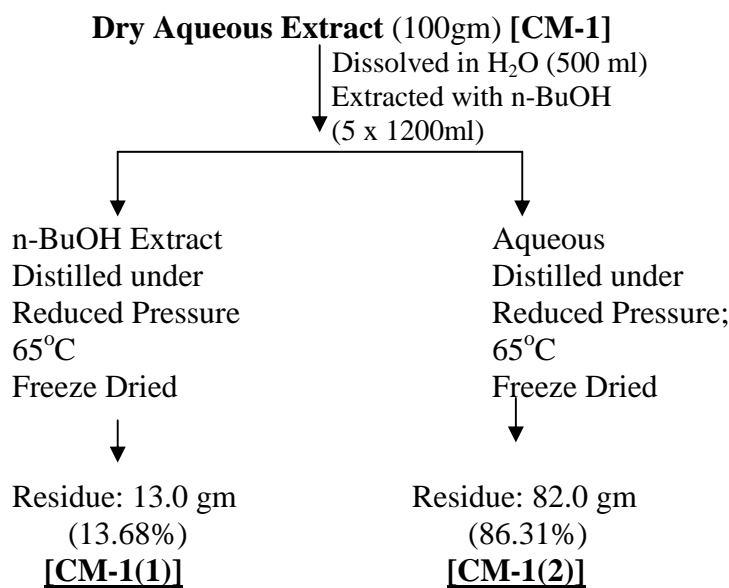


Fig. 8C. Flow Chart-CI

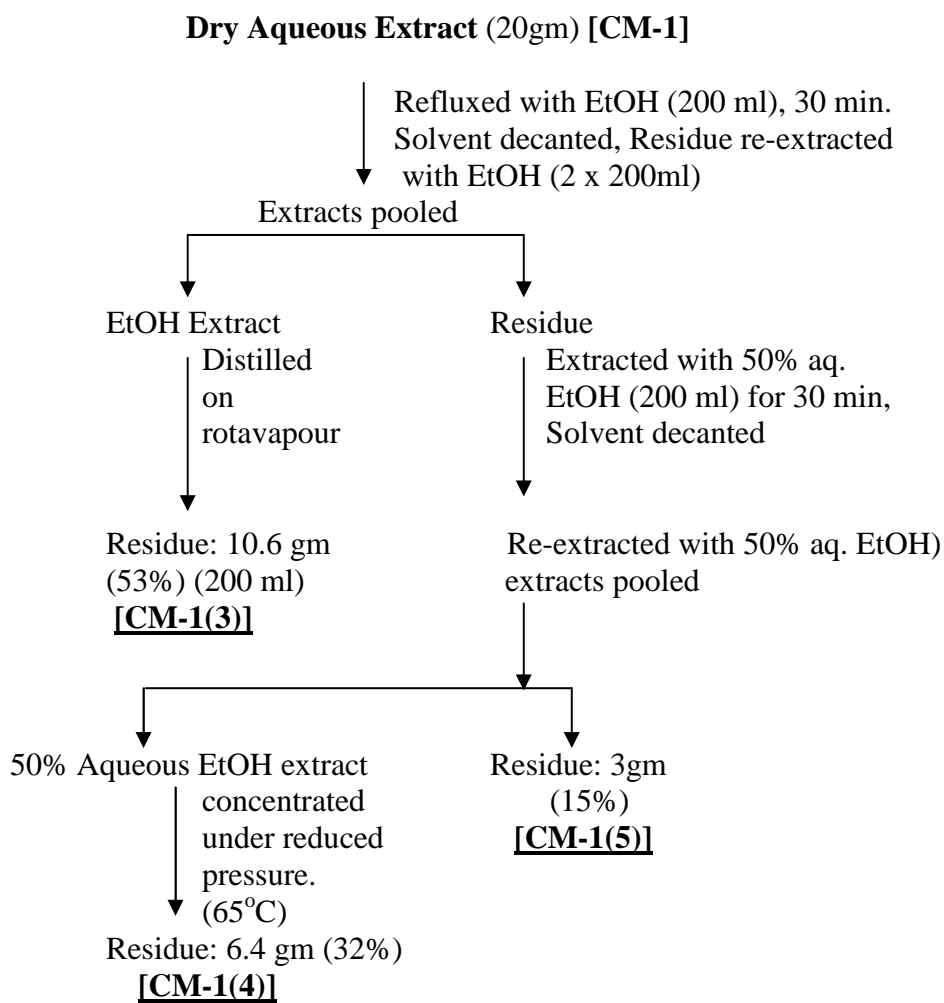


Fig. 8D. Flow Chart-CII

Activity profile of each fraction was investigated as described below:

Study 2. Effect of CM-1 fractions on plasma levels of RIF.

Experimental design: A total of 30 rats were divided into 5 groups (6 rats/group) and treated as follows.

Gr	Treatment (p.o.)
I	RIF, 40 mg/kg + INH, 30 mg/kg+ PZA, 90 mg/kg + CM-1(1) (2 mg/kg)
II	RIF, 40 mg/kg + INH, 30 mg/kg+ PZA, 90 mg/kg + CM-1(2) (13 mg/kg)
III	RIF, 40 mg/kg + INH, 30 mg/kg+ PZA, 90 mg/kg + CM-1(3) (8 mg/kg)
IV	RIF, 40 mg/kg + INH, 30 mg/kg+ PZA, 90 mg/kg +CM-1(4) (5 mg/kg)
V	RIF, 40 mg/kg + INH, 30 mg/kg+ PZA, 90 mg/kg +CM-1(5) (2.5 mg/kg)

Test dose of CM-1 fractions were adjusted on the basis of their extractive yield from parent extract. Collection and analysis of plasma samples was done as described in **Study 1A**.

From the results as summarized in **Table 12**, CM-1(2) was found to be the active fraction, and was further processed.

Isolation of Active Principle from CM-1(2).

CM-1(2) was dissolved in minimum quantity of de-ionized water and adsorbed on silica gel (60-120 mesh) The free flowing material was charged onto a glass column (4 cm diameter) packed with silica gel (60-120 mesh in ethyl acetate).

The column was eluted first with ethyl acetate and then with EtOH by gradually increasing the percentage of water in EtOH.

In all 420 fractions were collected. TLC was run in n-BuOH (B): acetic acid (A): water (W) 4:1:5) and patterns were visualized by freshly prepared borinate-PEG solution (2-aminoethyl diphenylborinate, 1 % in methanol: polyethylene glycol 4000, 5 % in ethanol, 1:1 v/v).

Fractions 43-49, 56-60, 81-167 and 180-198 showed identical TLC patterns with a single spot in solvent system B: A: W (4:1:5). The fractions with identical R_f values were pooled. Crystallization was carried out in EtOH and the residues (a yellow powder) collected. These were designated as FG-1, FG-2, FG-3 and FG-4.

Spectral analysis.

The NMR and IR analysis was performed using DPX 200 and Vector 22 models respectively (Bruker).

LC-Mass spectroscopy was conducted on ion-trap (Bruker, Esquire 3000) mass spectrometer equipped with an ionization source in the positive mode and connected to an Agilent 100 series HPLC binary pump equipped with an Agilent 100 series diode array detector.

The ion source was operated in the positive electrosprey ionization (ESI) mode at 340°C at 35 psi for the nebulizer with nitrogen flow of 10 L/min. The scan range was 100-900 m/z and ICC target value 8000 whereas the maximum acquisition time was 200 milliseconds.

The samples were chromatographed at 30°C on a Merck RP-18 column (5 µm, 250 x 4.6 mm) by UV detector at 340 nm. The mobile phase consisted of 1.5 % acetic acid in water: ACN (83:17, v/v) and was delivered at a flow rate of 1 ml/min.

Spectral analysis of FG-1.

FG-1 is a yellow powder soluble in water; m.p. 227-228°C.

^1H NMR (DMSO- d_6). δ 3.20-3.71 (m, sugar proton), δ 5.05 (d, 1H, $J=7.2$ Hz, H-1''), δ 6.85 (s, 1H, H-3), δ 6.48 (d, 1H, $J=2.1$ Hz, H-6), δ 6.86 (d, 1H, $J=2.1$ Hz, H-8), δ 6.96 (d, 2H, $J=8.8$ Hz, H-3' and H-5'), δ 7.96 (d, 2H, $J=8.8$ Hz, H-2' and H-6').

^{13}C NMR (DMSO- d_6). δ 164.3 (C-2), 102.9 (C-3), 161.0 (C-4), 161.5 (C-5), 99.5 (C-6), 162.8 (C-7), 94.9 (C-8), 156.8 (C-9), 105.4 (C-10), 120.8 (C-1'), 128.3 (C-2' and C-6'), 117.3 (C-3' and C-5'), 100.2 (C-1''), 73.1 (C-2''), 76.5 (C-3''), 69.8 (C-4''), 77.1 (C-5''), 60.8 (C-6'').

The LC-MS spectrum of FG-1 gave $[\text{M}+\text{H}]^+$ ion at m/z 426.

Based on the above data the FG-1 had the molecular formula $\text{C}_{21}\text{H}_{13}\text{O}_{10}$ (MW 425) and was identified as “apigenin-7-glucoside”.

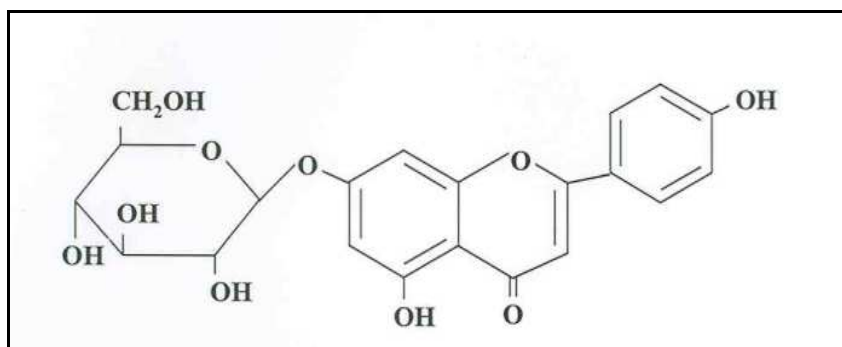


Fig. 9A. Chemical structure of FG-1 molecule

Spectral analysis of FG-2.

FG-2 is a yellow powder soluble in water; m.p. 230-245°C.

^1H NMR (DMSO- d_6). δ 3.23-3.69 (m, sugar proton), δ 5.0 (d, 1H, $J=7.1$ Hz, H-1 $'''$), δ 6.45 (d, 1H, $J=2.1$ Hz, H-6), δ 6.75 (s, 1H, H-3), δ 6.79 (d, 1H, $J=2.1$ Hz, H-8), δ 6.92 (d, 1H, $J=8.2$ Hz, H-5 $'$), δ 7.43 (d, 1H, $J=2.1$ Hz, H-2 $'$), δ 7.45 (dd, 1H, $J=2.1$ and 8.1 Hz, H-6 $'$).

^{13}C NMR (DMSO- d_6). δ 164.6 (C-2), 103.3 (C-3), 181.8 (C-4), 161.1 (C-5), 99.8 (C-6), 163.0 (C-7), 95.0 (C-8), 156.9 (C-9), 105.5 (C-10), 113.7 (C-2 $'$), 145.7 (C-3 $'$), 149.8 (C-4 $'$), 116.1 (C-5 $'$), 119.1 (C-6 $'$), 100.4 (C-1 $''$), 73.3 (C-2 $''$), 76.6 (C-3 $''$), 70.0 (C-4 $''$), 77.3 (C-5 $''$), 61.0 (C-6 $''$).

The LC-MS spectrum of FG-2 gave $[\text{M}+\text{H}]^+$ ion at m/z 443.1.

Based on the above data the FG-2 had the molecular formula $\text{C}_{21}\text{H}_{14}\text{O}_{11}$ (MW 442) and was identified as “luteolin-7-glucoside”.

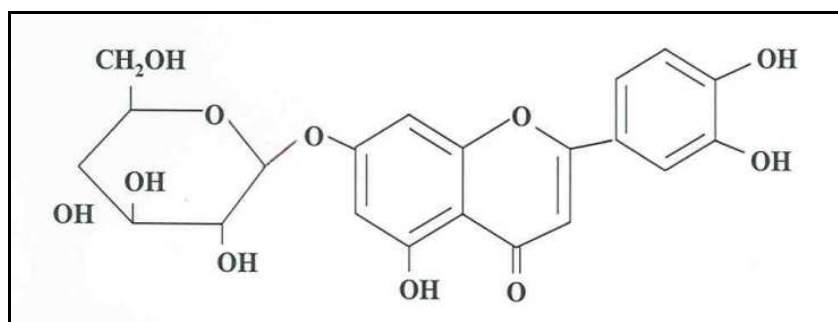


Fig. 9B. Chemical structure of FG-2 molecule

Spectral analysis of FG-3.

FG-3 is a yellow powder soluble in water; m.p. 268-270°C.

^1H NMR (DMSO- d_6). δ 3.08-3.75 (m, 17H, sugar protons), 4.50 (d, 1H, $J= 7.21$ Hz, H-1'''), 5.21 (d, 1H, $J= 6.82$ Hz, H-1''), 6.42 (bs, 1H, H-6), 6.65 (bs, 1H, H-8), 6.81 (d, 1H, $J=8.42$, H-5'), 7.09 (s, 1H, H-3), 7.35 (q, 1H, $J= 8.42$ and 1.8 Hz, H-6'), 7.80 (bs, 1H, H-2').

^{13}C NMR ($\text{H}_2\text{O}-\text{CD}_3\text{OD}$). δ 165.36 (C-2) , 104.01 (C-3), 183.19 (C-4), 160.87 (C-5), 99.41 (C-6), 163.09 (C-7), 96.31 (C-8), 157.65 (C-9), 106.50 (C-10), 122.36 (C-1') ,114.10 (C-2'), 145.37 (C-3'), 148.74 (C-4') ,116.81 (C-5'), 120.75 (C-6'), 101.21 (C-1''), 73.25 (C-2''), 77.23 (C-3''), 70.72 (C-4''), 76.89 (C-5'') , 62.02 (C-6''), 103.39 (C-1'''), 75.02 (C-2''' and C-4'''), 77.71 (C-3''') 82.07 (C-5''') ,176.44 (C-6''').

The LC-MS spectrum of FG-3 gave $[\text{M}+\text{H}]^+$ ion at m/z 625.1, $[\text{M}+\text{H-galacturonic acid}]^+$ at m/z 449.1 and $[\text{M}+\text{H-galacturonic acid- glucose}]^+$ at m/z 287 and the presence of galacturonic acid and glucose moieties.

Based on the above data the FG-3 had the molecular formula $\text{C}_{27}\text{H}_{28}\text{O}_{17}$ (MW 624) and was identified as 3',5-dihydroxyflavone-7-O- β -D-galacturonide-4'-O- β -D-glucopyranoside.

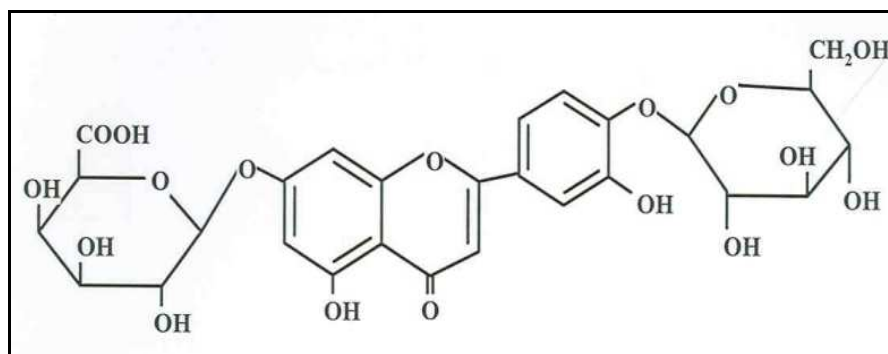


Fig. 9C. Chemical structure of FG-3 molecule

Spectral analysis of FG-4.

FG-4 is a yellow powder soluble in water; m.p. 239-241°C.

^1H NMR (DMSO- d_6). δ 3.75 (m, sugar proton), δ 5.01 (d, 1H, $J= 7.21$ Hz, H-1 $'''$), δ 5.21 (d, 1H, $J= 6.82$ Hz, H-1 $''''$), δ 6.48 (bs, 1H, H-6), δ 6.86 (bs, 1H, H-8), δ 6.96 (d, 2H, $J= 8.8$ Hz, H-3 $'$ and H-5 $'$), δ 7.96 (d, 2H, $J= 8.8$ Hz, H-2 $'$ and H-6 $'$).

^{13}C NMR ($\text{H}_2\text{O}-\text{CD}_3\text{OD}$). δ 165.3 (C-2), 103.01 (C-3), 161.0 (C-4), 161.05 (C-5), 99.41 (C-6), 162.8 (C-7), 94.9 (C-8), 156.8 (C-9), 106.50 (C-10), 120.8 (C-1 $'$), 128.3 (C-2 $'$ and C-6 $'$), 117.3 (C-3 $'$ and C-5 $'$), 161.8 (C-4 $'$), 100.2 (C-1 $''$), 73.1 (C-2 $''$), 76.5 (C-3 $''$), 69.8 (C-4 $''$), 77.1 (C-5 $''$), 60.8 (C-6 $''$), 103.3 (C-1 $'''$), 74.1 (C-2 $'''$), 77.7 (C-3 $'''$), 75.02 (C-4 $'''$), 82.0 (C-5 $'''$), 176.4 (C-6 $'''$).

The LC-MS spectrum of FG-4 gave $[\text{M}+\text{H}]^+$ ion at m/z 602.

Based on the above data the FG-4 had the molecular formula $\text{C}_{27}\text{H}_{21}\text{O}_{16}$ (MW 601) and was identified as “apigenin-7-galacturonyl glucoside”.

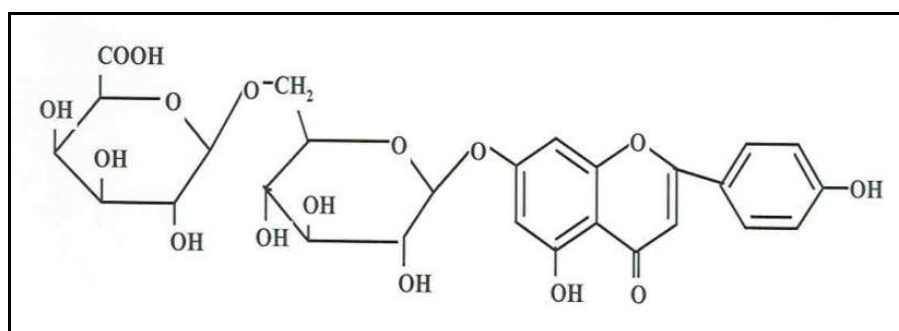


Fig. 9D. Chemical structure of FG-4 molecule

Study 3. Bioevaluation of FG molecules.

Experimental design: A total of 24 rats were divided into 4 groups (6 rats/group) and treated with an arbitrary dose of 5 mg/kg.

Gr	Treatment (p.o.)
I	RIF, 40 mg/kg + INH, 30 mg/kg+ PZA, 90 mg/kg + FG-1, 5 mg/kg
II	RIF, 40 mg/kg + INH, 30 mg/kg+ PZA, 90 mg/kg + FG-2, 5 mg/kg
III	RIF, 40 mg/kg + INH, 30 mg/kg+ PZA, 90 mg/kg + FG-3, 5 mg/kg
IV	RIF, 40 mg/kg + INH, 30 mg/kg+ PZA, 90 mg/kg + FG-4, 5 mg/kg

Collection and analysis of plasma samples was done as described in **Study 1A**.

The results as summarized in **Table 12** have revealed that FG-3 was the active molecule. The FG-3 was further taken up for dose dependent investigation. The HPLC finger print profile of active parent fraction CM-1(2) is shown in **Fig. 10A** and of FG-3 is shown in **Fig. 10B**.

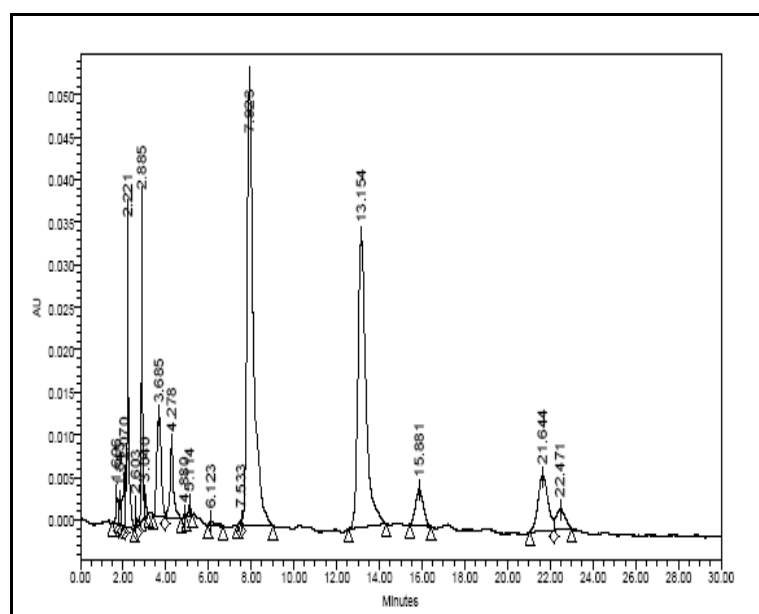


Fig. 10A. HPLC Chromatogram of CM -1(2)

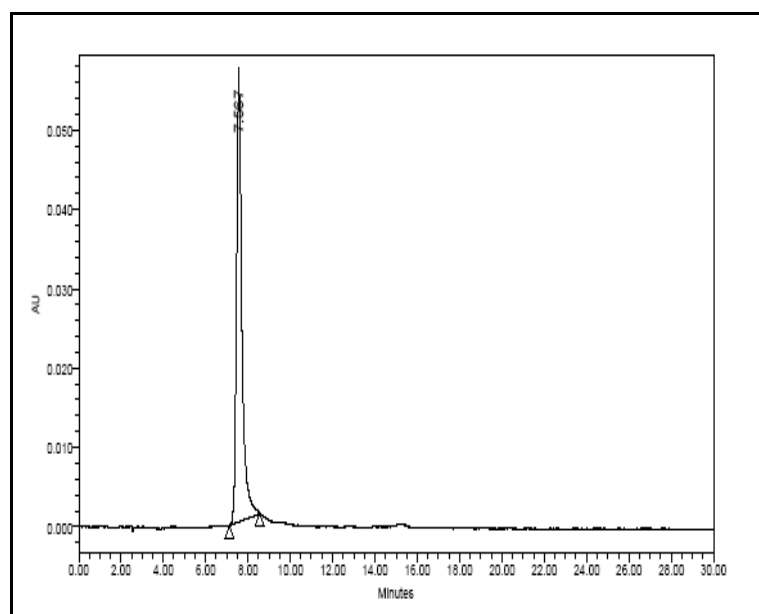


Fig. 10B. HPLC Chromatogram of FG-3 (pure molecule from cumin)

Study 4. Dose-dependent effect of FG-3.

Experimental design: A total of 24 rats were divided into 4 groups (6 rats/group) and treated as follows.

Gr	Treatment (p.o.)
I	RIF, 40 mg/kg + INH, 30 mg/kg+ PZA, 90 mg/kg + FG-3, 10 mg/kg
II	RIF, 40 mg/kg + INH, 30 mg/kg+ PZA, 90 mg/kg + FG-3, 7.5 mg/kg
III	RIF, 40 mg/kg + INH, 30 mg/kg+ PZA, 90 mg/kg + FG-3, 2.5 mg/kg
IV	RIF, 40 mg/kg + INH, 30 mg/kg+ PZA, 90 mg/kg + FG-3, 1.25 mg/kg

Collection and analysis of plasma samples was done as described in **Study 1A**.

The results are summarized in **Table 12**. It was found that FG-3 was most active at 5 mg/kg dose.

4.9.2 Activity guided fractionation of caraway (CR-1).

CR-1 (active aqueous extract of caraway seed) was partitioned into 2 fractions as per the scheme depicted in **Fig. 11-Flow Chart D**. Following fractions were obtained.

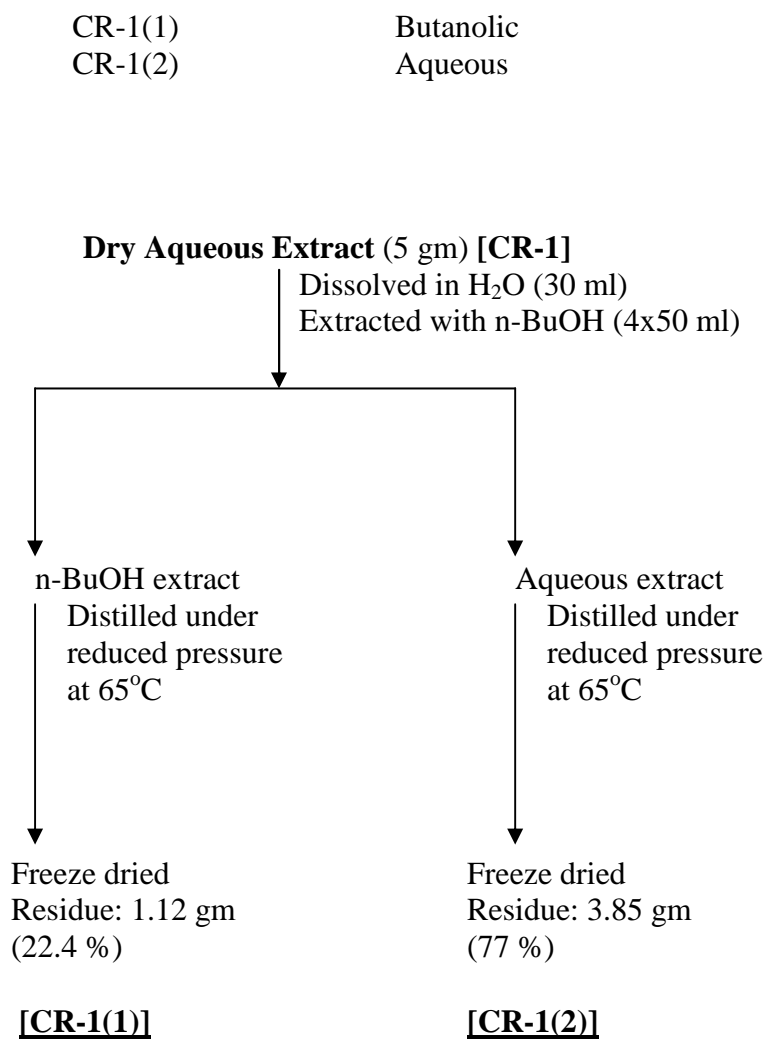


Fig. 11. Flow Chart-D

Activity profile of each CR-1 fraction was investigated as described below.

Experimental design: A total of 12 rats were divided into 2 groups (6 rats/group) and treated with the doses derived from the extractive yield of the respective fractions.

Gr	Treatment (p.o.)
I	RIF, 40 mg/kg + INH, 30 mg/kg + PZA, 90 mg/kg + CR-1(1) (4 mg/kg)
II	RIF, 40 mg/kg + INH, 30 mg/kg + PZA, 90 mg/kg + CR-1(2) (10 mg/kg)

Collection and analysis of plasma samples was done as described in **Study 1A**. The results summarized in **Table 13** showed that CR-1(1) was the active fraction. CR-1(1) was taken for further fractionation. The HPLC finger print profile of CR-1(1) is shown in **Fig. 12**.

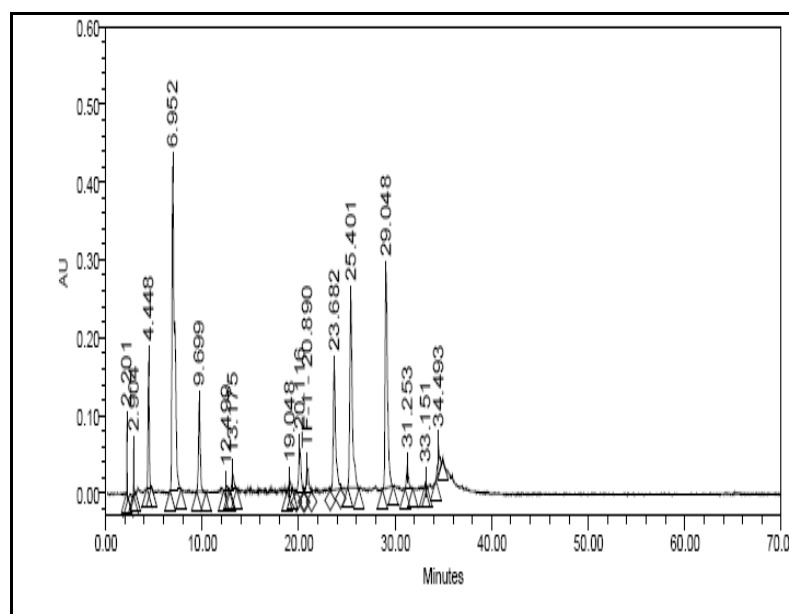


Fig. 12. HPLC finger print of CR-1(1)

Sub-fractionation of CR-1(1).

CR-1(1) was sub-fractionated using preparative HPLC as described below: CR-1(1) was dissolved in de-ionized water to prepare a solution (15 mg/ml). The CR-1(1) solution was filtered through 0.45 μ filter and analyzed using preparative HPLC. The following conditions were used for preparative HPLC: Mobile phase: MeOH:HPLC

grade water (Gradient elution); Flow rate: 10 ml/min and detection wavelength: 254 nm. The three sub-fractions [coded as Sub-Fr. 2 (0-25 min), Sub-Fr. 2D (25-38 min) and Sub-Fr. 3 (38-45 min)] were obtained. HPLC finger print profiles are shown in

Fig. 13A-C.

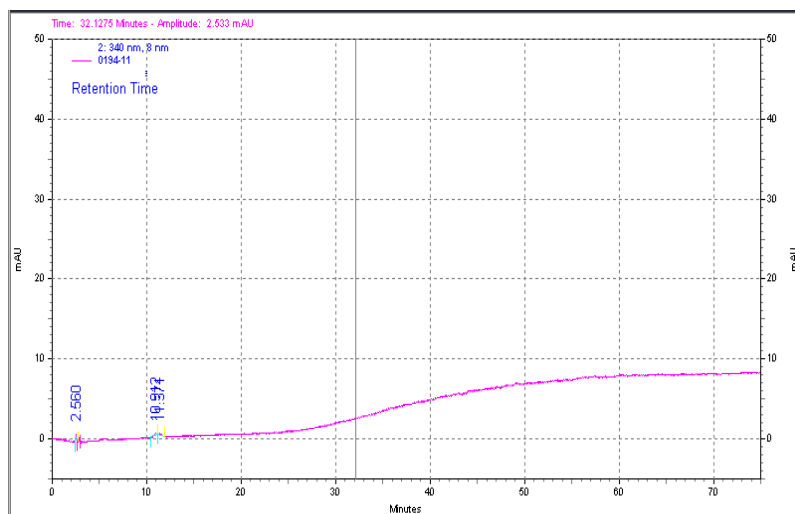


Fig. 13A. Finger print of CR-1(1) Sub-Fr. 2

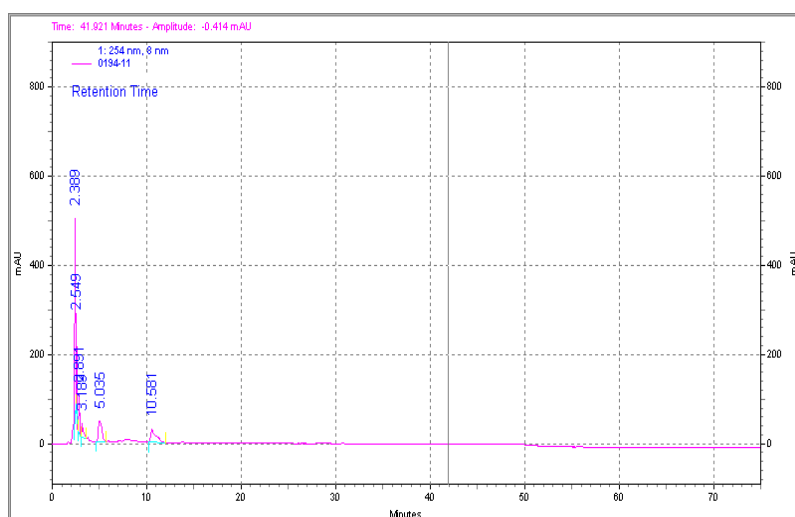


Fig. 13B. Finger print of CR-1(1) Sub-Fr. 2D

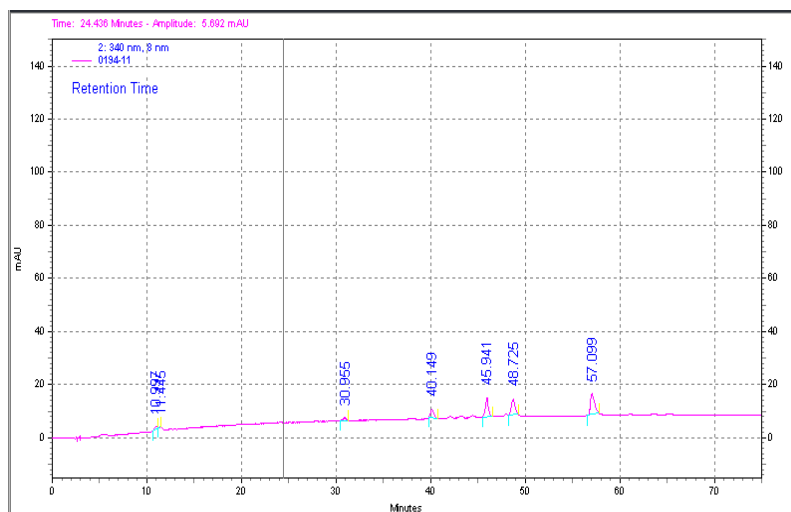


Fig. 13C. Finger print of CR-1(1) Sub-Fr. 3

Study 5. Bioevaluation of sub-fractions of CR-1(1).

Experimental design: A total of 18 rats were divided into 3 groups (6 rats/group) and treated as follows.

Gr	Treatment (p.o.)
I	RIF, 40 mg/kg + INH, 30 mg/kg + PZA, 90 mg/kg + CR-1(1) Sub-Fr. 2 (5 mg/kg)
II	RIF, 40 mg/kg + INH, 30 mg/kg + PZA, 90 mg/kg + CR-1(1) Sub-Fr. 2D (5 mg/kg)
III	RIF, 40 mg/kg + INH, 30 mg/kg + PZA, 90 mg/kg + CR-1(1) Sub-Fr. 3 (5 mg/kg)

In these experiments an arbitrary dose of 5 mg/kg was used. Collection and analysis of plasma samples was done as described in **Study 1A**. The results as summarized in **Table 13** showed that none of the CR-1(1) sub-fractions (2, 2D and 3) were active. Therefore a dose-dependent activity profile of CR-1(1) was undertaken by including two more doses (8 and 16 mg/kg).

Study 6. Dose-dependent study.

Experimental design: A total of 12 rats were divided into 2 groups (6 rats/group).

Test drugs along with CR-1(1) were administered per orally to various groups as follows:

Gr	Treatment (p.o.)
I	RIF, 40 mg/kg + INH, 30 mg/kg + PZA, 90 mg/kg + CR-1(1) (8 mg/kg)
II	RIF, 40 mg/kg + INH, 30 mg/kg + PZA, 90 mg/kg + CR-1(1) (16 mg/kg)

Collection and analysis of plasma samples was done as described in **Study 1A**.

The results as summarized in **Table 13**. The results showed that CR-1(1) was most active at a dose of 8 mg/kg.

Since none of the sub-fractions were found active CR-1(1) was chemically standardized as follows.

Isolation of marker(s) from CR-1(1).

CR-1(1) was dissolved in a minimum quantity of MeOH and adsorbed on silica gel (60-120 mesh). The free flowing material was charged onto a glass column (4 cm diameter) packed with silica gel in CHCl₃. The column was eluted first with CHCl₃ and then with CHCl₃:MeOH mixture by gradually increasing the percentage of MeOH. In all 500 fractions of 250 ml each were collected. TLC was run in n-BuOH (B): acetic acid (A): water (W) (4:1:5 upper layer) and patterns were visualized by freshly prepared 2-aminoethyl diphenyl borinate (1 % in methanol): PEG 4000 (5 % in ethanol) (1:1 v/v). Fractions 170-195 eluted in 5 % MeOH in CHCl₃ showed an identical TLC pattern with a single spot having R_f value 0.7 in solvent system B:A:W

(4:1:5). These fractions were pooled. Crystallization was carried out in MeOH and pale yellow residue (TF-1) was collected.

On the basis of melting point (235°C) and spectral data, TF-1 was identified as kaempferol-3-β-D galactoside (trifolin) (C₂₁H₂₀O₁₁; MW 448). HPLC chromatogram and the structure of TF-1 are shown in **Fig. 14A and 14B**.

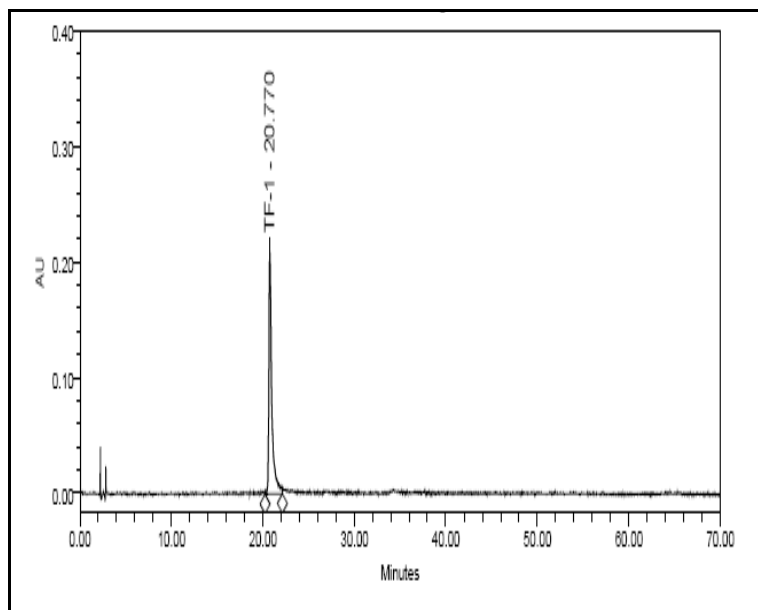


Fig. 14A. Finger print of TF-1 (Trifolin)

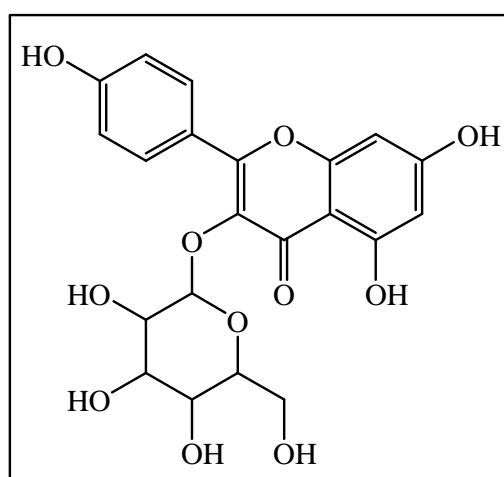


Fig. 14B. Kaempferol-3-β-D galactoside (Trifolin, TF-1)

Study 7. Bioevaluation of marker TF-1.

Experimental design: A total of 18 rats were divided into 3 groups (6 rats per group) and treated as follows.

Gr	Treatment (p.o.)
I	RIF, 40 mg/kg + INH, 30 mg/kg + PZA, 90 mg/kg + TF-1 (5 mg/kg)
II	RIF, 40 mg/kg + INH, 30 mg/kg + PZA, 90 mg/kg + TF-1 (10 mg/kg)
III	RIF, 40 mg/kg + INH, 30 mg/kg + PZA, 90 mg/kg + TF-1 (20 mg/kg)

Collection and analysis of plasma samples was done as described in **Study 1A**.

The results are summarized in **Table 13**.

4.10.1 Pharmacokinetic study (ORAL)

Experimental design: A total of 75 rats were segregated in 5 groups (15 rats/group).

Animals were treated as follows:

Gr	Treatment (p.o.)
I	RIF (40 mg/kg)
II	RIF (40 mg/kg) + FG-3 (5 mg/kg)
II	RIF (40 mg/kg) + INH (30 mg/kg) + PZA (90 mg/kg)
IV	RIF (40 mg/kg) + INH (30 mg/kg) + PZA (90 mg/kg) + FG-3 (5 mg/kg)
V	RIF (40 mg/kg) + INH (30 mg/kg) + PZA (90 mg/kg) + CR-1(1) (8 mg/kg)

Blood sampling was done as per the following scheme:

Gr	No. of rats	Sampling time (post-administration) (h)										
		0.25	0.5	1	2	3	4	6	8	12	16	24
I	5	•			•			•		•		
	5		•			•			•		•	
	5			•			•					•
II	5	•			•			•		•		
	5		•			•			•		•	
	5			•			•					•
III	5	•			•			•		•		
	5		•			•			•		•	
	5			•			•					•
IV	5	•			•			•		•		
	5		•			•			•		•	
	5			•			•					•
V	5	•			•			•		•		
	5		•			•			•		•	
	5			•			•					•

Collection and analysis of plasma samples was done as described in **Study 1A**.

4.10.2 Pharmacokinetic study (I.V.)

Rats were anaesthetized using intra-peritoneal (i.p.) injection of 25 % urethane solution in normal saline and fixed to the wooden board in a supine position. The normal body temperature was maintained at 37°C. Polyethylene tubing cannulation was made at a jugular vein for the administration of RIF (7.5 mg/kg/ml) and carotid artery for collecting blood samples. After RIF administration 500 µl of blood was collected via carotid artery in heparinized tubes at 0.25, 0.5, 1, 2, 3, 4, 6, 8, 12, 16, 24 h post-dosing. The 500 µl sterile normal saline solution was administered via jugular vein after every blood sample collection.

Blood sampling was done as per the following scheme:

Rat No	Sampling time (post-administration) (h)										
	0.25	0.5	1	2	3	4	6	8	12	16	24
1	•	•	•	•	•	•	•	•	•	•	•
2	•	•	•	•	•	•	•	•	•	•	•
3	•	•	•	•	•	•	•	•	•	•	•
4	•	•	•	•	•	•	•	•	•	•	•
5	•	•	•	•	•	•	•	•	•	•	•

Collection and analysis of plasma samples was done as described in **Study 1A**.

Pharmacokinetic analysis.

The conc. vs. time profiles of anti-TB drugs alone and in presence of FG-3 and CR-1(1) were established and pharmacokinetic parameters determined by using PK software.

4.11 In-vitro/Ex-vivo mode of action studies

Study 1. Effect of FG-3 on the passive transport of RIF.

Experimental Design:

Passive transport was investigated using parallel artificial membrane permeability assay (PAMPA) as provided by the manufacturer (Millipore, India).

Membrane of each well of 96-well multi-screen permeability plate (donor) was coated with 15 μ l hexadecane solution in hexane (5 ml of 5 % v/v). The plate was allowed to dry by keeping it into fuming hood for 4 h. The plate was ensured for dryness by visual inspection. The phosphate buffered saline (pH-5, filtered through 0.45 μ Millipore HV filter using Millipore Filtration Assembly) containing 5 % HPLC grade DMSO was prepared separately and added to each well of acceptor plate (300 μ l/well). The hexadecane pre-treated donor plate was placed onto acceptor plate in such a way that underside of membrane was in contact with buffer of acceptor plate (Fig. 15).

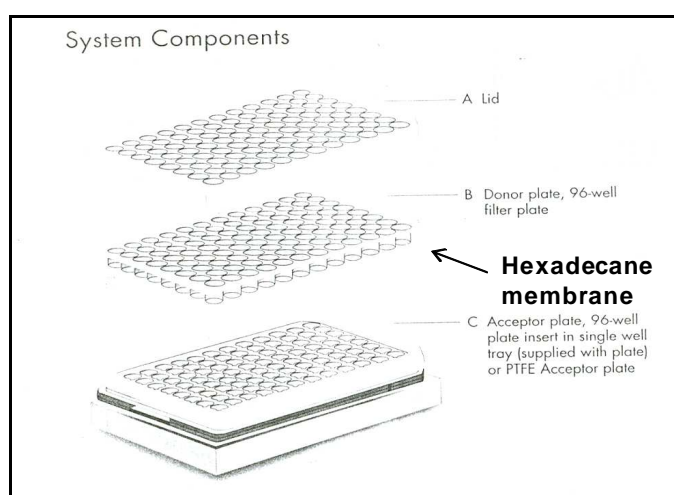


Fig. 15. PAMPA system (Millipore)

Assay procedure:

The stock solutions (10 ml of 1 mg/ml each of RIF, INH and PZA were prepared separately in HPLC grade DMSO. Two working solutions (i) RIF 10 μ M + INH 7.5 μ M + PZA 22.5 μ M (Solution A) and (ii) RIF 100 μ M + INH 75 μ M + PZA 225 μ M (solution B) were prepared from main stocks, in 5 % DMSO. FG-3 was dissolved in phosphate buffered saline (PBS) (5 ml of 1 mg/ml) and working stocks (25, 50 and 100 μ M) were prepared in PBS containing 5 % DMSO.

A volume of 150 μ l containing solution A or B was added onto each well of donor plate in absence or presence of FG-3. The lid was replaced; plate was sealed with paraffin film and covered with aluminum foil. The sealed plate was incubated in a chamber containing controlled humidity and temperature (40 % \pm 2 % and 18°C \pm 2°C respectively, Climacell Chamber; BMT Group, (Germany) for 12 h.

The various parameters like strength of RIF, pH of buffered saline, incubation temperature, and incubation time were pre-optimized before commencement of study. After completion of incubation period, the acceptor and donor plate volumes were analyzed for RIF content by HPLC.

Study 2. Effect of FG-3 on the transport of RIF (Gut Sac: mucosal-to-serosal direction).

Experimental design (Ex-vivo study):

Rats were treated with FG-3 (5 mg/kg) perorally. After 2, 3 and 4 h of treatment everted sacs (6-8 cm) of rat jejunum were prepared as described earlier [115].

For control experiments, sacs were prepared from untreated animals. Everted sacs (6-8 cm) were filled with Krebs-Ringer buffer and incubated at 37°C under constant motion in Krebs-Ringer buffer containing 0.25 mM RIF. Serosal volumes were collected during a period (0-30 min.) and samples for RIF determination by HPLC were prepared as described in **Section 4.6.8**.

Absorption characteristics were determined by quantitating the transport rate (dQ/dt) from the linear portion of conc. vs. time curves. The apparent permeability coefficient (P_{app}) was calculated using the following equation:

$$P_{app} = dQ/dt \times 1/(A \times C_o) \text{ [cm/s]}$$

where dQ/dt is the transport rate, A is the surface area of the everted sac and C_o is external mucosal load of the test drug.

Study 3. Effect of FG-3 on the efflux of Rhodamine (Rho) 123 (Gut Sac: serosal -to-mucosal direction).

Experimental design (Ex-vivo study):

Rats were treated with FG-3 (5 mg/kg) perorally. After 3 h of treatment everted sacs (6-8 cm) of rat jejunum were prepared and used as per the procedure reported earlier [116].

For control experiments, sacs were prepared from untreated animals. Sacs were filled with Krebs-Ringer buffer containing 10 μ M Rho123 (pre-optimized conc. of Rho123), and incubated at 37°C under constant motion in oxygenated 50 ml Krebs-Ringer buffer. Serosal volumes (1 ml/sampling time) were collected during a period of 0-30 min (with 10 min interval).

In parallel experiments verapamil (25 μ M) was added to both serosal and mucosal side. The Rho123 conc. was estimated by spectrofluorometer (excitation wavelength, 504 nm, and emission wavelength, 525 nm) by relating to a standard curve of Rho123.

Study 4. Effect of CR-1(1) on the transport of RIF, PZA and INH (Gut Sac: mucosal –to-serosal direction).

Experimental design (Ex-vivo study):

Rats were treated with CR-1(1) (8 mg/kg) perorally. After 3 h of treatment, everted sacs of rat jejunum were prepared as described above.

For control experiments, sacs were prepared from untreated animals. Sacs were filled with Krebs-Ringer buffer and incubated at 37°C under constant motion in Krebs-Ringer buffer containing variable external load of RIF, PZA or INH individually. In each experiment serosal samples were collected during a period 0-30 min of incubation to generate conc.-time curves and the extent of mucosal transport was quantitated from the linear portion of these curves.

Drugs were extracted and analyzed by HPLC as described earlier. P_{app} was calculated as described in **Study 2**.

Study 5. Effect of FG-3 on *in-situ* efflux of Rho123.

In-situ P-gp mediated efflux study of Rho123 was performed described earlier [117]. The rats were fasted for 16 h before experiment and were anaesthetized with sodium pentobarbital (30 mg/kg, i.p.). Rats were fixed to the wooden board in a

supine position. The normal body temperature was maintained at 37°C. Polyethylene tubing cannulation was made at a jugular vein for the administration of Rho123 and carotid artery for collecting blood samples. The whole intestinal lumen was cannulated with the help of silicon cannula (outer diameter, 5 mm; internal diameter, 3 mm) to perfuse the intestinal lumen with Dulbecco's PBS (pH 7.4) containing 25 mM glucose (Medium 1) in a single perfusion manner at a rate of 0.5 ml/min (**Fig. 16**).



Fig. 16. Experimental design of in-situ Rho123 efflux study

Rho123 (100 μ M in 5 % mannitol) was injected as a bolus dose (4.36 ml/kg), via cannulated jugular vein, and further continued as a constant infusion (2 ml/h) to attain a steady-state plasma conc. (C_{pss}) of Rho123. After 55 min of initiation of Rho123 infusion, the intestinal effluent and blood was collected at 10 min intervals for 30 min (control phase). In a similar manner samples were also collected during the treatment phase. In treatment phase Medium 1 was replaced by Medium 2A/2B

(containing FG-3, 50/100 μM), or Medium 3A/3B (containing RIF, 5/10 μM) or Medium 4, (containing 100 μM FG-3, + 10 μM RIF) or Medium 5A/5B (containing verapamil, 25/100 μM). At the end of perfusion experiment with Medium 4, Medium 1 was once again perfused to investigate the residual effect of FG-3 + RIF.

In another study this experiment was also performed in primed rats. A dose 5 mg/kg of FG-3 was administered per orally, per day, for 6 consecutive days. After one day wash out period, the perfusion experiment with Medium 1 only was carried out. The samples (blood and intestinal effluents) were collected as described above. The Rho123 conc. was estimated by spectrofluorometry as described earlier.

Study 6. Effect of FG-3 on the active transport of ^3H -benzopyrene (Intestinal epithelial cells).

Preparation of epithelial cells (guinea pig intestine):

Jejunal epithelial cells from guinea pig were prepared according to a previously published [118] method as described below.

Reagents: *Reagent A:* Solution (pH-6.8) containing 96 mM NaCl, 8 mM KH_2PO_4 , 5.6 mM Na_2HPO_4 , 1.5 mM KCl, 5 mM EGTA, 5 mM EDTA, 0.5 mM DTT, 185 mM mannitol, 5.5 mM glucose, 2 mM L-glutamine and 2.5 g/L of bovine serum albumin (BSA). *Reagent B:* incubation buffer containing 225 mM NaCl. *Reagent C:* Cell isolation buffer (pH-7.4) containing 200 mM sucrose, 19 mM KH_2PO_4 and 76 mM Na_2HPO_4 . *Reagent D:* Krebs-Ringer buffer containing 2.5 mM CaCl_2 , 1 mM dithiothreitol and 1% BSA.

Procedure:

The animal was sacrificed and abdomen opened by midline incision. The intestine was collected and divided into two segments. The intestinal segments were filled with *Reagent A*. The segments were incubated in *Reagent B* at 37°C for 5 min. After incubation, the filled solution was drained out. The intestinal segments were refilled with *reagent C* and incubated at 37°C for 5 min.

The contents of segments were collected and the process was repeated 5 times. The contents were pooled, filtered and centrifuged at 400 g for 5 min. The pellet was collected and re-suspended in *reagent D*. The viability was determined using trypan blue.

ATP dependent transport of ³H-benzopyrene was investigated according to a previously published method [119]. Cells (3×10^6) were pre-incubated in absence (control) and presence of FG-3 (25-100 μM) for 20 min in 20 mM HEPES/Tris buffer (pH 7.4). After completion of 20 min, incubations were supplemented with 270 mM mannitol, 1 mM ATP, 10 mM MgCl₂, 0.1 % (w/v) BSA, 10 mM phosphocreatinine and 100 μg/ml creatinine phosphokinase. To these incubations 0.5 mM ³H-benzopyrene (20,000 cpm) dissolved in HEPES/Tris buffer (20 mM, pH 7.4, containing 310 mM mannitol and 0.1 % BSA) was added. Incubation was continued for 10 min in final volume of 1.0 ml. At the end of the experiment, incubation mixtures were transferred over glass fiber filters and drained off with the help of a vacuum pump.

The filters were air dried and added to scintillation fluid (supplied by the manufacturer) and counted in a Rack-Beta Scintillation Counter.

Study 7. Effect of FG-3 on P-gp ATPase Activity (*in-vitro*) intestinal membrane preparations.

Preparation of intestinal membrane fractions:

Crude intestinal membrane fractions were prepared from jejunal mucosa of rats as reported earlier [120]. Fasted rats were sacrificed by cervical dislocation. After opening of the abdomen, intestinal segment (from 10 cm below duodenum) was collected and washed with ice-cold saline to remove all the luminal contents. The intestinal segment was kept on ice bath. The intestinal segment was opened with scissor to expose the mucosal surface. The mucosal layer was scrapped off with the help of glass slide and collected. The protein content was estimated by Lowry method using bovine serum albumin as standard as depicted in **Annexure II**.

Measurement of P-gp ATPase Activity:

P-gp-ATPase activity was measured by determining vanadate-sensitive release of inorganic phosphate (Pi) from ATP as reported earlier [121]. In brief, membrane preparations (15-20 µg protein/assay) were pre- incubated for 3 min in absence and presence of 10 mM *ortho*-vanadate in an assay buffer containing 100.0 mM Tris (pH 7.5), 10.0 mM NaN₃, 4.0 mM EGTA, 2.0 mM ouabain, 4.0 mM DTT, 100.0 mM KCl and 20.0 mM MgCl₂ (final volume 100 µL). An addition of 5.0 mM ATP was made in all incubations which were allowed to continue for 30 min. Reaction was stopped by adding 5 % (w/v) sodium dodecyl sulphate (SDS) and the released Pi was measured as described in the procedure. In one set of identical incubations FG-3 was added. Vanadate -sensitive activity in presence and absence of a test substance was calculated as the difference between ATPase activity obtained in presence and

absence of FG-3. In incubations not containing test materials DMSO alone (1.0-1.5 % final) was used. All incubations were done in triplicate. In parallel experiment verapamil (100 μ M) was also used. An identical reaction mixture containing 50 μ l of 3 mM sodium *ortho*-vanadate was also assayed. The final conc. of DMSO as a solvent in the assay medium was 1 % v/v. The reaction was initiated by addition of 50 μ l of 10 mM ATP. In an identical manner, two additional incubations were also carried out in the absence of test material mixtures with or without *ortho*-vanadate as control. After incubation of 30 min at 37°C, reaction was terminated by 100 μ l of 5 % SDS and the amount of Pi released was measured by a colorimetric reaction. The calibration curve (Range: 1 to 100 μ g/ml) for phosphate was found linear (>0.999) (**Annexure III**).

Study 8. Effect of FG-3 on CYP 450 3A4-mediated enzymes (rat liver microsomes).

Preparation of rat and mouse liver microsomes:

Liver microsomes from were prepared as per the procedure described earlier [122]. The animals were deeply anesthetized with the help of diethyl ether. The abdomen was opened by making mid-line incision. The liver lobes were carefully isolated, and washed with ice-cold normal saline and 0.25 M sucrose solution. The isolated livers were immediately homogenized in a 0.25 M sucrose solution to obtain 20 % homogenates. The homogenates were centrifuged at 15,000 rpm for 15 min at 4°C. The supernatants were diluted with 0.125 M sucrose solution (1:4 v/v) and 8 mM calcium chloride (CaCl₂) was added to it. After 35 min with intermittent stirring, the diluted supernatants were centrifuged at 10,000 rpm for 10 min at 4°C.

The pellets were collected, washed with washing solution (0.01 M Na₂HPO₄, 0.01 M KH₂PO₄, 0.15 M KCl, and 1 mM EDTA) and re-suspended in 0.25 M sucrose solution with the help of homogenizer. The microsomal suspension samples were stored at -80°C until use. One group of swiss and C57BL mice were treated with phenobarbital (80 mg/kg, intra-peritoneal). After 6 days liver microsomes from these animals was prepared as described above. The protein content of microsomes was estimated by Lowry method as described in **Annexure II**.

Effect of FG-3 on Testosterone hydroxylase.

The testosterone hydroxylase activity was determined by a previously reported method [123]. Microsomes (1 mg protein) were pre-incubated for 5 min at 37°C in phosphate buffer (0.1 M, pH-7.4) containing 500 µM testosterone, 6 mM MgCl₂, and 1 mM EDTA in absence (control) and in presence of FG-3 (25-100 µM). In these experiments, piperine (25-100 µM) was used as standard. Reaction was started by adding 1 mM Nicotine adenine di-nucleotide phosphate reduced (NADPH), and incubations were continued for 20 min. At the end of 20 min, samples were mixed with chilled CHCl₃ and the organic layer collected and dried. The dried samples were reconstituted in mobile phase and analyzed for testosterone by HPLC. The optimized HPLC conditions used for the estimation of testosterone were as follows: mobile phase; MeOH: 1 % acetic acid (75:25 v/v); flow rate: 1 ml/min; column: RP-18, 250 x 4.6 mm, 10 µ particle size (Merck, USA) with 50°C column oven temperature and PDA detector set at 254 nm.

The retention time of testosterone was 7.1 min. The calibration curve was prepared separately which showed good linearity (>0.999) with lowest quantification limit of 9 ng/ml. The HPLC chromatogram is depicted in **Fig. 17**.

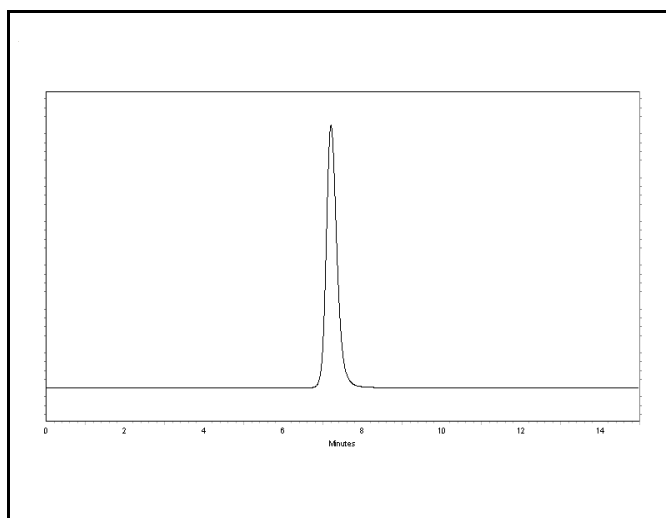


Fig. 17. HPLC chromatogram of Testosterone

Effect of FG-3 on the erythromycin demethylase.

The erythromycin demethylase activity was determined by a previously reported method [123]. Microsomes (5 mg protein) were pre-incubated for 5 min at 37°C in phosphate buffer (0.1 M, pH-7.4) containing 1 mM erythromycin, 6 mM MgCl₂, in absence (control) and in presence of FG-3 (25-100 μM). Reaction was started by adding NADPH, 1 mM, and incubations were continued for 30 min. At the end of 30 min, samples were mixed with 25 % ZnSO₄, and 0.3 N Ba(OH)₂. The samples were centrifuged and supernatants were collected. To the supernatants (350 μl), Nash reagent (150 μl) was added, mixed and incubated for 30 min at 56°C. At the end of 30 min, OD of samples was recorded at 405 nm. A standard curve of formaldehyde (HCHO) was made to determine the specific activity of the enzyme expressed as ng HCHO generated/mg protein/min.

4.12 Toxicity studies

4.12.1 Effect of FG-3 on intestinal mucosal membrane integrity.

Model: Uneverted gut sac (rat jejunum)

Uneverted sacs were prepared from jejunum as described in **Section 4.11**. These sacs were filled with Krebs-Ringer buffer with or without the test materials FG-3/CR-1(1) and incubated at 37°C under constant motion for 30 min. At the end of the experiment, luminal contents were collected, centrifuged (3500 rpm x 10 min) and used for protein determination by the method of Lowry as described in **Annexure II**.

4.12.2 Acute toxicity studies.

Animals and dosing: Male healthy wistar rats (with minimum body weight of 125 gm) were included in the study. Animals were maintained in regulated environmental conditions (Temp. $26 \pm 2^\circ\text{C}$, relative humidity $50 \pm 5\%$; 12 h light/dark cycle), according to CPCSEA guidelines. Animal experiments were approved by Institutional Animal Ethics Committee and were performed as per the Guidelines for Animal Care as recommended by the Indian National Academy, New Delhi (1992). Animals were fed with standard pelleted diet (Ashirwad Industries, Chandigarh, India) and sterilized water was provided *ad libitum*. Seven days after acclimatization, animals were used.

Test Materials:

- (i) FG-3, active molecule from cumin
- (ii) CR-1(1), active fraction from caraway

A total of 35 rats (male) received single dose of the test materials as per following experimental design.

Experimental design:

Gr	No. of rats	Treatment	Dose (p.o)
IA	5	Control	Vehicle (d.w.)
IB	5	FG-3	1 gm/ kg
IC	5	FG-3	2 gm/ kg
ID	5	FG-3	3 gm/kg
IIB	5	CR-1(1)	1 gm/kg
IIC	5	CR-1(1)	2 gm/kg
IID	5	CR-1(1)	3 gm/kg

Test materials were dissolved in distilled water for oral administration. Animals were observed for mortality for 21 days.

4.12.3 Sub-acute (4-week) toxicity studies.

Dose administration:

A total of 30 rats (15 M/15 F) were used in this investigation as per the experimental design described below. Animals received FG-3, p.o., once daily between 9:00 to 11:00 am, for 28 days consecutively.

Experimental design:

Gr	Sex	No. of rats	Treatment	Dose (p.o)
IA	M	5	Control	Vehicle (d.w.)
IB	F	5	Control	Vehicle (d.w.)
IIA	M	5	FG-3	5 mg/ kg
IIB	F	5	FG-3	5 mg/ kg
IIIA	M	5	FG-3	25 mg/kg
IIIB	F	5	FG-3	25 mg/kg

During the study period weekly body weights were recorded after every 7 days upto 28 days. At the end of study animals were sacrificed, and blood/major organs collected. Blood/serum was used for hematological/biochemical parameters.

4.12.4 Sub-chronic (8-week) toxicity studies.

FG-3: 5 mg/kg (effective dose) and 25 mg/kg

Dose administration:

A total of 30 rats (15 M/15 F) were used in this investigation as per the experimental design described below. Animals received FG-3, p.o., once daily between 9:00 to 11:00 am, for 60 days consecutively, as described below:

Experimental design:

Gr	Sex	No. of rats	Treatment	Dose (p.o)
IA	M	5	Control	Vehicle (d.w.)
IB	F	5	Control	Vehicle (d.w.)
IIA	M	5	FG-3	5 mg/ kg
IIB	F	5	FG-3	5 mg/ kg
IIIA	M	5	FG-3	25 mg/kg
IIIB	F	5	FG-3	25 mg/kg

During the study period after every 2 weeks, body weights were recorded upto 60 days. At the end of study animals were sacrificed, and blood/major organs collected. Blood/serum was used for hematological/biochemical parameters.

In sub-acute and sub-chronic toxicity investigation, animals were observed daily for clinical signs and mortality. Body weights were recorded every week (in sub-acute study) and after every 2 weeks (in sub-chronic study) during the study period. At the end of the studies blood samples and major organs were collected. Following parameters were recorded in blood/serum: RBC, WBC, differential leucocyte count, haemoglobin (Hb), platelet (Plt), glucose, triglyceride (TG), cholesterol, bilirubin, alanine aminotransferase (ALT: SGPT), aspartate aminotransferase (AST: SGOT),

urea, uric acid (UA) and creatinine. Measurements were made using commercial kits procured from Bayer Diagnostics, Baroda, India.

4.12.5 Statistical Analysis.

Statistical analysis was performed as described in **Section 4.3**. Data were expressed as mean \pm S.D. For significance a level of $p < 0.05$ was considered.

Bibliography

- [115] Brown J.R., Collett J.H., Attwood D., Ley R.W., Sims E.E. Influence of Monocaprin on the permeability of a diacidic drug BTA-243 across caco-2 cell monolayers and everted gut sacs. *International Journal of Pharmaceutics*. 2002, 245: 133-142.

- [116] Veau C., Leroy C., Banidel H., Daniel A., Tardivell S., Farinotti R., Lacour B. Effect of chronic renal failure on the expression and function of rat intestinal P-glycoprotein in drug excretion. *Nephrology Dialysis Transplantation*. 2001, 16: 1607-1664.

- [117] Yumoto R., Murakami T., Nakamoto Y., Hasegawa R., Nagai J., Takano M. Transport of rhodamine 123, a p-glycoprotein substrate, across rat intestine and caco-2 cell monolayers in the presence of cytochrome P-4503A related compounds. *Journal of Pharmacology and Experimental Therapeutics*. 1999, 289: 149-155.

- [118] Monaghan S.S., Mintenig G.M., Fransisco V. Outwardly rectifying Cl channel in guinea pig small intestinal villus Enterocytes: effect of inhibitors. *American*

Journal of Physiology: Gastrointestinal and Liver Physiology. 1997, 273: G1141-1152.

- [119] Penny J.I., Campbell C.F. Active transport of benzo[a]pyrene in apical membrane vesicles from normal human intestinal epithelium. *Biochimica et Biophysica Acta*. 1994, 1226: 232-236.
- [120] Yumoto R., Murakami T., Sanimasa M., Nasu R., Nagai J., Takano M. Pharmacokinetic interaction of cytochrome P450 3A related compounds with rhodamine 123, a P-glycoprotein substrate in rats pretreated with dexamethasone. *Drug Metabolism and Disposition*. 2001, 29: 145-151
- [121] Hrycyna C.A., Ramachandra M, Pastan I, Gottesman MM. Functional Expression of human P-glycoprotein from plasmids using vaccinia virus-bacteriophage T7 RNA polymerase system. *Methods in Enzymology*. 1998, 33: 456-473.
- [122] Johnson T.N., Tanner M.S., Tucker G.T. Developmental changes in the expression of enterocytic and hepatic cytochrome P4501A in rat. *Xenobiotica*. 2002, 32: 595-604.
- [123] Wang R.W., Newton D.J., Seheri T.D., Lu A.Y.H. Human cytochrome P450 3A4 catalyzed testosterone 6- β hydroxylation and erythromycin N-demethylation. Competition during catalysis. *Drug Metabolism and Disposition*. 1997, 25: 502-507.

RESULTS

5. Results

5.1 Validation of drug assay

HPLC methods for the estimation of RIF (Method A) and INH+PZA (Method B) were developed and validated as per ICH guidelines. The following optimized conditions showed best resolution of RIF and INH+PZA in terms of retention time, peak characteristics and total run time:

	Method A (RIF)	Method B (INH +PZA)
Column	RP-18, 250 x 4.6 mm; 5 μ m	RP-18, 250 x 4.6 mm; 5 μ m
Mobile phase	ACN :50 mM KH ₂ PO ₄ buffer (pH, 5) (60: 40 v/v)	ACN : 50 mM KH ₂ PO ₄ buffer (pH; 5) (40: 60 v/v)
Flow rate	1.0 ml/min	0.5 ml/min,
Column head pressure	132-142 kgf/cm ²	182-191 kgf/cm ²
Column oven temp.	40°C	40°C
Retention time	6.779 min	INH, 4.640 min; PZA, 5.067 min

A. System suitability: Results as summarized in **Table 6** showed that for both Method A and Method B, the critical parameters like retention time, area and number of theoretical plates met the acceptance criteria.

B. Recovery: Method A: The % recovery of RIF at three different conc. (0.10, 10 and 20 μ g/ml RIF spiked plasma) using pre-optimized SPE technique was in between 84.5 to 89.6 %. **Method B:** The % recovery of INH (at 0.10, 2.5 and 10 μ g/ml INH spiked plasma) was in between 81.2 to 87.3 % , whereas for PZA (0.05, 10 and 30 μ g/ml PZA spiked plasma), it was in between 91.4 to 93.5 % , using optimized LLE technique.

Table 6. System suitability test

Drug/compound	Parameter	Acceptance Criteria	Average	Low	High	%RSD	Status
Method A RIF	Retention time	%RSD < 0.5	6.773	6.768	6.779	0.122	Passed
	Peak area	%RSD < 1.5	333036	328377	337270	0.894	Passed
	No. of Plates	> 3500	4025.08	3978.01	4052.47	0.717	Passed
Method B INH	Retention time	% RSD < 1.0	4.643	4.628	4.599	0.483	Passed
	Peak area	% RSD < 2.5	140653	138449	142350	1.181	Passed
	No. of Plates	> 4000	4460	4327	4539	3.587	Passed
PZA	Retention time	% RSD < 1.0	5.062	5.089	5.102	0.401	Passed
	Peak area	% RSD < 2.5	275422	272440	277925	0.778	Passed
	No. of Plates	> 4000	6669	6589	6778	1.060	Passed

C. Linearity and range: Both the methods were found linear over the calibration range and the results showed good correlation between conc. and resulting peak areas ($r^2 > 0.999$). The linearity and calibration range results of both the methods are summarized in **Table 7**.

D. Accuracy and precision: Method A: The intra- and inter-day accuracy as well as precision results are summarized in **Table 8** and **Table 9** respectively. **RIF:** The intra- and inter-day accuracy (diff.%) was in the range of -3.34 to +3.28 and -4.87 to +2.88 respectively. The intra- and inter-day precision (% RSD) for RIF was in the range from 1.08 to 2.61 and 1.62 to 2.77 respectively. **Method B: INH:** The intra- , and inter-day accuracy (diff.%) was in the range of -8.75 to +7.58 and -9.71 to +7.68 respectively. The intra- and inter-day precision (% RSD) for was in the range of 1.07 to 4.12 and 2.01 to 5.73. **PZA:** The intra- and inter-day accuracy (diff.%) was in the range of -8.21 to +6.19 and -8.91 to +4.91 respectively. The intra- and inter-day precision (% RSD) values were in the range of 1.09 to 5.21 and 1.49 to 7.25 respectively.

E. LOQ: LOQ of RIF was 0.10 $\mu\text{g/ml}$ (**Method A**) whereas that of INH and PZA was 0.10 $\mu\text{g/ml}$ and 0.05 $\mu\text{g/ml}$ respectively (**Method B**).

F. Robustness: Minor modifications in the mobile phase composition and the pH of buffer did not significantly alter the performance of the both the methods in terms of retention time, resolution, peak characteristics and theoretical plates which suggested that the developed methods were robust.

Table 7. Details of parameters and linearity data of calibration curves

Drug	Calibration curve	Range (µg/ml)	No. of Calibrators	Slope	y-intercept	r²
Method A RIF	Set 1*	0.10-20.00	7	0.48	+2.27	> 0.999
	Set 2*	0.10-20.00	7	0.47	+2.26	> 0.999
	Set 3*	0.10-20.00	7	0.47	+2.26	> 0.999
Method B INH	Set 1*	0.10-10.00	6	0.0011	-0.6243	> 0.999
	Set 2*	0.10-10.00	6	0.0013	-0.4922	> 0.999
	Set 3*	0.10-10.00	6	0.0011	-0.5899	> 0.999
PZA	Set 1*	0.05-30.00	6	0.0005	-0.4946	> 0.999
	Set 2*	0.05-30.00	6	0.0005	-0.4940	> 0.999
	Set 3*	0.05-30.00	6	0.0005	-0.4912	> 0.999

* *The validation was performed separately in terms of sets.*

Table 8. Accuracy data of RIF, INH and PZA

Drug/Compound	Nominal Conc.	Accuracy (% bias)					
		Intra-run (n = 9)			Inter-run (n = 9)		
		Set 1*	Set 2*	Set 3*	Set 1*	Set 2*	Set 3*
Method A RIF	0.10 µg/ml	+2.66	-1.76	-2.64	+2.88	-2.38	-3.73
	10.0 µg/ml	+3.28	-2.94	+1.22	-2.44	-3.16	+1.81
	20.00 µg/ml	-3.34	+1.92	+3.08	+2.11	-2.39	-4.87
Method B INH	0.10µg/ml	+7.58	-8.75	-6.31	+7.68	-9.33	-9.71
	2.50µg/ml	+4.22	-6.04	+5.02	-3.13	-3.16	+5.17
	10.00µg/ml	-3.17	+5.62	+3.08	+2.23	-3.49	-4.86
PZA	0.05µg/ml	+6.19	-7.53	-8.21	+4.91	+4.56	+3.46
	10.00µg/ml	+2.31	-3.39	+3.13	-8.91	-6.80	+3.23
	30.00µg/ml	+1.55	+2.18	-3.44	-4.35	+3.29	-2.33

* *The validation was performed separately in terms of sets.*

Table 9. Precision data of RIF, INH and PZA

Drug/Compound	Nominal Conc.	Precision (% RSD)					
		Intra-run (n = 9)			Inter-run (n = 9)		
		Set 1*	Set 2*	Set 3*	Set 1*	Set 2*	Set 3*
Method A RIF	0.10 µg/ml	1.43	2.54	1.73	1.98	2.77	1.93
	10.0 µg/ml	1.92	2.61	1.29	2.17	1.62	1.89
	20.00 µg/ml	1.34	2.12	1.08	2.34	2.01	1.74
Method B INH	0.10µg/ml	4.11	2.29	2.88	5.73	4.16	4.03
	2.50µg/ml	4.12	3.62	3.13	2.15	2.92	3.48
	10.00µg/ml	1.49	2.02	1.07	5.37	2.01	2.59
PZA	0.05µg/ml	5.21	3.17	4.81	1.84	7.25	3.91
	10.00µg/ml	2.27	1.68	3.73	4.65	1.94	3.02
	30.00µg/ml	1.09	1.12	3.01	1.49	3.15	6.17

* The validation was performed separately in terms of Set 1, Set 2 and Set 3.

G. Specificity: Fig. 18A-C depicts chromatograms of extracted blank rat plasma, mobile phase and extracted RIF spiked plasma. Fig. 18D depicts chromatogram of simultaneously recovered INH and PZA from spiked plasma samples. No interference of plasma artefacts, mobile phase constituents and any other analyte were observed at the retention times of RIF, INH and PZA.

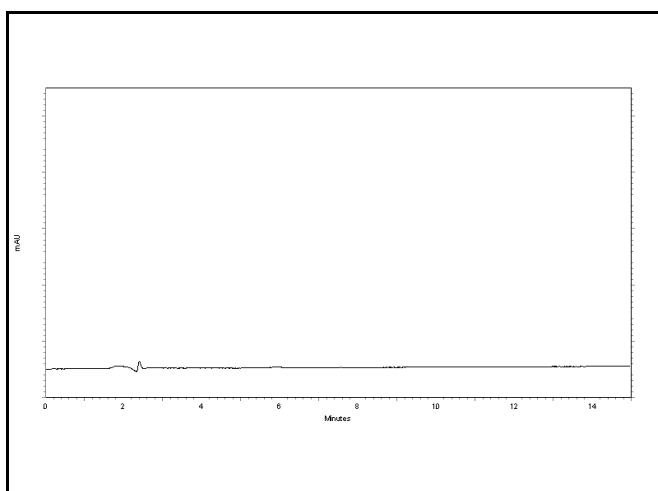


Fig. 18A. Chromatogram of blank rat plasma

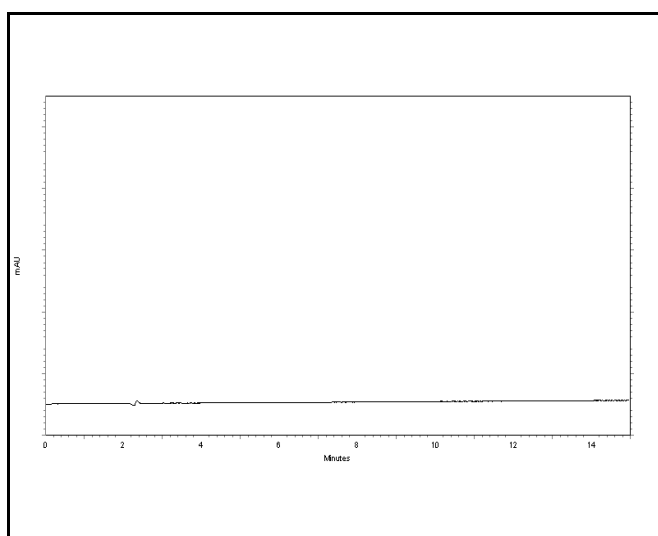


Fig. 18B. Chromatogram of mobile phase

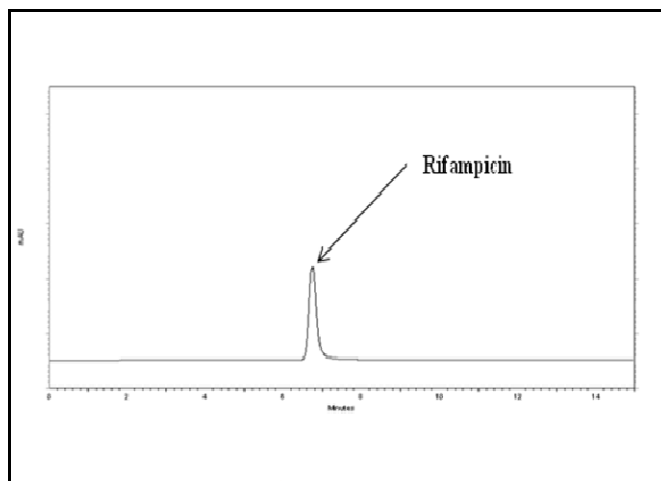


Fig. 18C. Chromatogram of plasma sample spiked with RIF

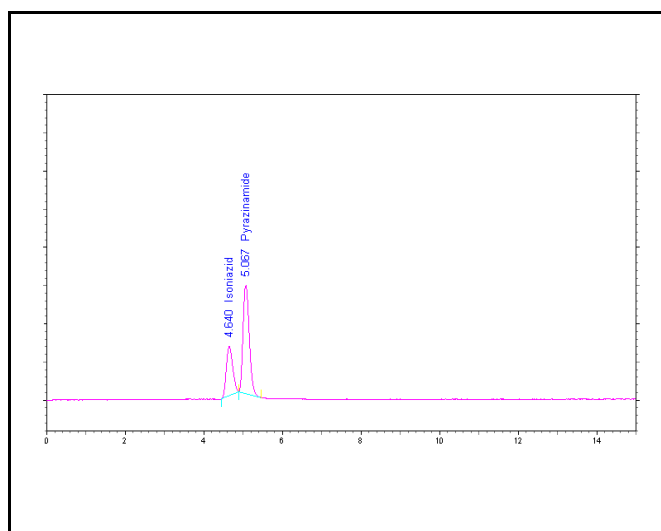


Fig. 18D. Chromatogram of plasma sample spiked with INH and PZA

H. Stability: Results showed that under various storage conditions as summarized in **Tables 10-11**, samples were stable within the acceptable limits (% RSD < 15).

Table 10. Stability data of RIF

Conditions	Theoretical Conc. (µg/ml)	% RSD
1. Storage stability in plasma (-80°C)		
0 month	0.1	9.2
	10.0	7.2
	20.0	5.1
1 month	0.1	9.6
	10.0	3.1
	20.0	4.9
2. Freeze-thaw stability		
0 cycles	10.0	7.3
3 cycles	10.0	5.9
3. Auto-sampler stability (10°C)		
0 h	10.0	6.7
24 h	10.0	4.3
4. Short-term stability in plasma at room temperature		
0 h	10.0	10.6
24 h	10.0	9.7

Table 11. Stability data of INH and PZA

Condition	Theoretical Conc. ($\mu\text{g/ml}$)	% RSD	
		INH	PZA
1. Storage stability (-80°C)			
0 month	00.10 + 00.05	9.4	7.4
	10.00 + 30.00	5.5	3.9
1 month	00.10 + 00.05	10.2	9.3
	10.00 + 30.00	6.7	4.3
2. Freeze-thaw stability			
0 cycles	00.10 + 00.05	7.9	10.1
	10.00 + 30.00	4.9	4.4
3 cycles	00.10 + 00.05	2.9	4.1
	10.00 + 30.00	3.4	4.9
3. Stability at room temperature			
0 h	00.10 + 00.05	5.1	3.2
	10.00 + 30.00	2.5	2.9
24 h	00.10 + 00.05	5.3	6.1
	10.00 + 30.00	3.2	7.3
4. Autosampler stability			
0 h	00.10 + 00.05	7.3	9.2
	10.00 + 30.00	6.1	5.8
24 h	00.10 + 00.05	6.3	5.1
	10.00 + 30.00	2.7	2.4

5.2 In vivo studies

5.2.1 Restricted Pharmacokinetics

Results for cumin herbal products are summarized in **Table 12**. The base line levels of RIF after 2, 3 and 4 h of oral administration of the drug were 5.31 ± 0.52 , 6.93 ± 0.49 , and 4.54 ± 0.31 $\mu\text{g/ml}$, respectively. The base line levels of INH after 1, 2 and 3 h of oral administration of the drug were 3.30 ± 0.34 , 4.72 ± 0.21 , and 3.22 ± 0.16 $\mu\text{g/ml}$, respectively. The base line levels of PZA after 1, 2 and 3 h of oral administration of the drug were 17.02 ± 1.43 , 26.25 ± 1.75 , and 21.0 ± 1.32 $\mu\text{g/ml}$ respectively.

Initially all extracts were tested at an arbitrary dose of 100 mg/kg dose. Among the 3 types of extracts, only aqueous extracts possessed significant activity. An aqueous extract, CM-1 enhanced the plasma levels of RIF by 61 %, 77 % and 74 % at 2, 3 and 4 h respectively. The other two extracts CM-2 and CM-3 were less active. There was no effect on the other two drugs INH and PZA.

Out of 5 fractions from the parent cumin extract (CM-1), significant activity was found located mainly in an aqueous fraction, CM-1(2). CM-1(2) enhanced the plasma level of RIF by 51 %, 78 % and 81 % at 2, 3 and 4 h respectively.

A total of 4 molecules could be isolated from the CM-1(2) (active fraction of cumin). However only one of these, i.e., a flavonoid glycoside identified as 3',5'-dihydroxyflavone-7-O- β -D-galacturonide-4'-O- β -D-glucopyranoside (FG-3) showed a significant activity. FG-3 enhanced plasma levels of RIF in a dose dependent manner. A dose of 5 mg/kg of FG-3 enhanced the RIF levels by 73 %, 89 % and 81 % at 2, 3 and 4 h respectively.

Table 12. Effect of CM test materials on plasma levels of RIF, INH and PZA

Extract Identity	Dose mg/kg	Nature	RIF ($\mu\text{g/ml}$ plasma)			INH ($\mu\text{g/ml}$ plasma)			PZA ($\mu\text{g/ml}$ plasma)		
			2 h	3 h	4 h	1 h	2 h	3 h	1 h	2 h	3 h
Control			5.31 \pm 0.52	6.93 \pm 0.49	4.54 \pm 0.31	3.30 \pm 0.34	4.72 \pm 0.21	3.22 \pm 0.16	17.02 \pm 1.4	26.25 \pm 1.75	21.00 \pm 1.32
CM-1	100	Aq.	8.54 \pm 0.61 (61%)	12.26 \pm 0.98 (77%)	7.89 \pm 0.43 (74%)	3.86 \pm 0.31	5.71 \pm 0.28	3.89 \pm 0.13	20.93 \pm 2.21	29.92 \pm 3.28	21.87 \pm 1.33
	40	Aq.	8.44 \pm 0.61 (59%)	12.26 \pm 0.88 (77%)	7.85 \pm 0.41 (73%)						
	16	Aq.	8.23 \pm 0.34 (55%)	12.05 \pm 0.71 (74%)	8.12 \pm 0.39 (79%)						
CM-1 (1)	2	But. Fr.	5.41 \pm 0.22	7.34 \pm 0.31 (6%)	4.81 \pm 0.27						
CM-1(2)	13	Aq. Fr.	8.01 \pm 0.46 (51%)	12.33 \pm 0.73 (78%)	8.21 \pm 0.39 (81%)						
FG-1	5	Aq.	5.30 \pm 0.21	7.34 \pm 0.32	4.57 \pm 0.19						
FG-2	5	Aq.	6.00 \pm 0.38	8.31 \pm 0.43 (20%)	5.03 \pm 0.31						
FG-3	10	Aq.	9.39 \pm 0.41 (77%)	13.16 \pm 0.76 (90%)	8.26 \pm 0.35 (82%)						
	7.5	Aq.	9.02 \pm 0.35 (70%)	12.82 \pm 0.71 (85%)	8.17 \pm 0.41 (80%)						
	5	Aq.	9.18 \pm 0.37 (73%)	13.09 \pm 0.81 (89%)	8.21 \pm 0.32 (81%)						
	2.5	Aq.	7.38 \pm 0.29 (39%)	10.18 \pm 0.39 (47%)	6.40 \pm 0.21 (41%)						
	1.25	Aq.	5.89 \pm 0.21	8.24 \pm 0.39	5.17 \pm 0.23						
FG-4	5	Aq.	5.32 \pm 0.38	7.48 \pm 0.29	4.90 \pm 0.23						
CM-1(3)	8	Alc.	5.30 \pm 0.21	6.95 \pm 0.32	4.55 \pm 0.22						
CM-1(4)	5	Aq-Alc	5.33 \pm 0.26	6.98 \pm 0.37	4.59 \pm 0.21						
CM-1(5)	2.5	Residue	5.32 \pm 0.19	6.91 \pm 0.31	4.49 \pm 0.13						
CM-2	100	Aq.-Alc	6.63 \pm 0.31 (25%)	8.66 \pm 0.32 (25%)	5.58 \pm 0.21 (23%)						
CM-3	100	Alc.	5.78 \pm 0.21	7.96 \pm 0.22	5.08 \pm 0.15						

Figures in parenthesis show % change vs. control

Results for caraway herbal products are summarized in **Table 13**. The base line levels of RIF after 2, 3 and 4 h of oral administration of the drug were 5.31 ± 0.52 , 6.93 ± 0.49 , and 4.54 ± 0.31 $\mu\text{g/ml}$ respectively. The base line levels of INH after 1, 2 and 3 h of oral administration of the drug were 3.30 ± 0.34 , 4.72 ± 0.21 , and 3.22 ± 0.16 $\mu\text{g/ml}$, respectively. The base line levels of PZA after 1, 2 and 3 h of oral administration of the drug were 17.02 ± 1.43 , 26.25 ± 1.75 , and 21.0 ± 1.32 $\mu\text{g/ml}$, respectively.

Initially all extracts were tested at an arbitrary dose of 100 mg/kg dose. Among the 3 types of extracts, only aqueous extracts possessed significant activity. An aqueous extract, CR-1 enhanced the plasma levels of RIF by 60 %, 79 % and 81 % at 2, 3 and 4 h respectively. Plasma levels of INH were enhanced by 60 %, 57 % and 64 % at 1, 2 and 3 h respectively. Plasma levels of PZA were enhanced by 58 %, 58 % and 68 % at 1, 2 and 3 h respectively. The other two extracts CR-2, and CR-3 were less active.

This activity remained confined mainly in butanolic fraction, CR-1(1), when tested at 4 mg/kg (based upon the extractive yield). Further dose-dependent profile showed that a dose of 8 mg/kg produced optimum effect: plasma levels of RIF were enhanced by 47 %, 70 % and 68 % at 2, 3, and 4 h respectively. Plasma levels of INH were enhanced by 52 %, 51 % and 64 % at 1, 2, and 3 h respectively. Plasma levels of PZA were enhanced by 52 %, 54 % and 64 % at 1, 2, and 3 h respectively. Sub-fractions of CR-1(1) and a molecule TF-1 were not found active.

Table 13. Effect of CR test materials on the plasma levels of RIF, INH and PZA

Extract Identity	Dose mg/kg	Nature	RIF (µg/ml plasma)			INH (µg/ml plasma)			PZA (µg/ml plasma)		
			2 h	3 h	4 h	1 h	2 h	3 h	1 h	2 h	3 h
Control			5.31 ± 0.52	6.93 ± 0.49	4.54 ± 0.31	3.30 ± 0.34	4.72 ± 0.21	3.22 ± 0.16	17.02 ± 1.4	26.25 ± 1.75	21.00 ± 1.32
CR-1	100	Aq.	8.49 ± 0.61 (60%)	12.40 ± 0.98 (79%)	8.21 ± 0.43 (81%)	5.28 ± 0.31 (60%)	7.41 ± 0.38 (57%)	5.28 ± 0.33 (64%)	20.93 ± 2.21	41.47 ± 3.99 (58%)	35.28 ± 1.33 (68%)
	40	Aq.	8.33 ± 0.61 (57%)	12.26 ± 0.88 (77%)	8.03 ± 0.41 (77%)	5.18 ± 0.21 (57%)	7.50 ± 0.33 (59%)	5.24 ± 0.21 (63%)	26.89 ± 2.63 (58%)	42.26 ± 3.68 (61%)	34.44 ± 1.13 (64%)
	16	Aq.	8.23 ± 0.34 (55%)	12.40 ± 0.71 (79%)	7.99 ± 0.39 (76%)	5.04 ± 0.24 (53%)	7.36 ± 0.21 (56%)	5.18 ± 0.34 (61%)	26.38 ± 2.51 (55%)	41.47 ± 3.01 (58%)	34.23 ± 1.29 (63%)
CR-1 (1)	4	But. Fr.	7.16 ± 0.32 (35%)	9.97 ± 0.34 (44%)	6.71 ± 0.25 (48%)	4.55 ± 0.21 (38%)	6.56 ± 0.21 (39%)	4.60 ± 0.23 (43%)	25.70 ± 1.39 (51%)	37.27 ± 1.39 (42%)	30.45 ± 2.17 (45%)
	8		7.80 ± 0.22 (47%)	11.78 ± 0.31 (70%)	7.62 ± 0.27 (68%)	5.01 ± 0.19 (52%)	7.12 ± 0.19 (51%)	5.28 ± 0.23 (64%)	23.48 ± 3.02 (38%)	40.42 ± 2.11 (54%)	34.44 ± 2.07 (64%)
	16		8.07 ± 0.22 (52%)	11.85 ± 0.31 (71%)	7.76 ± 0.27 (71%)	5.08 ± 0.26 (54%)	7.31 ± 0.41 (55%)	5.37 ± 0.22 (67%)	25.87 ± 2.62 (52%)	40.95 ± 2.68 (56%)	33.39 ± 1.57 (59%)
TF-1	5		5.36 ± 0.22	7.08 ± 0.32	4.61 ± 0.19	3.37 ± 0.12	4.81 ± 0.32	3.35 ± 0.11	26.38 ± 2.00 (55%)	26.35 ± 2.02	21.31 ± 1.16
	10		5.38 ± 0.23	7.11 ± 0.36	4.65 ± 0.19	3.49 ± 0.14	4.78 ± 0.23	3.28 ± 0.12	17.36 ± 0.32	26.97 ± 1.32	21.51 ± 1.18
	20		5.29 ± 0.21	7.11 ± 0.33	4.69 ± 0.19	3.42 ± 0.19	4.89 ± 0.18	3.35 ± 0.19	17.46 ± 0.31	27.02 ± 1.87	20.50 ± 2.01
CR-1(1)	5	Sub-Fr.2	5.57 ± 0.51	7.02 ± 0.37	4.65 ± 0.21	3.49 ± 0.14	4.77 ± 0.27	3.20 ± 0.21	17.52 ± 0.37	26.51 ± 2.39	21.25 ± 1.21
	5	Sub-Fr.2D	5.39 ± 0.24	7.20 ± 0.32	4.69 ± 0.22	3.39 ± 0.21	4.65 ± 0.12	3.29 ± 0.25	18.38 ± 1.92	27.30 ± 3.12	21.43 ± 1.32
	5	Sub-Fr.3	5.41 ± 0.21	6.91 ± 0.31	4.52 ± 0.27	3.41 ± 0.22	4.91 ± 0.41	3.42 ± 0.22	17.70 ± 1.44	27.03 ± 1.89	21.05 ± 1.07
CR-1(2)	10	Aq.	5.42 ± 0.46	7.34 ± 0.73	4.63 ± 0.39	3.44 ± 0.26	4.64 ± 0.51	3.46 ± 0.39	18.04 ± 2.11	26.32 ± 2.53	21.33 ± 1.89
CR-2	100	Aq-Alc	6.69 ± 0.22 (26%)	9.56 ± 0.31 (38%)	6.08 ± 0.31 (34%)	4.25 ± 0.11	5.99 ± 0.42 (27%)	4.21 ± 0.23	17.32 ± 1.26	33.33 ± 3.12 (27%)	27.51 ± 1.52 (31%)
CR-3	100	Alc.	5.78 ± 0.21	7.96 ± 0.22	5.08 ± 0.15	3.66 ± 0.20	5.09 ± 0.42	3.51 ± 0.17	20.93 ± 2.11 (23%)	30.18 ± 2.11	24.15 ± 1.37

Figures in parenthesis show % change vs. control

5.2.2 Pharmacokinetics (ORAL).

In order to assess the effect of FG-3 on the pharmacokinetics of RIF and in combination with INH + PZA, following conc. vs. time curves were established:

- (a) RIF (alone)
- (b) RIF + FG-3 (5 mg/kg)
- (c) RIF + INH + PZA
- (d) RIF + INH + PZA + FG-3.

In order to assess the effect of CR-1(1) on the pharmacokinetics of RIF + PZA + INH following conc. vs. time curves was established.

- (e) RIF + INH + PZA + CR-1(1)

These curves (a) to (e) are depicted in **Fig. 19A, 19B** and **19C**.

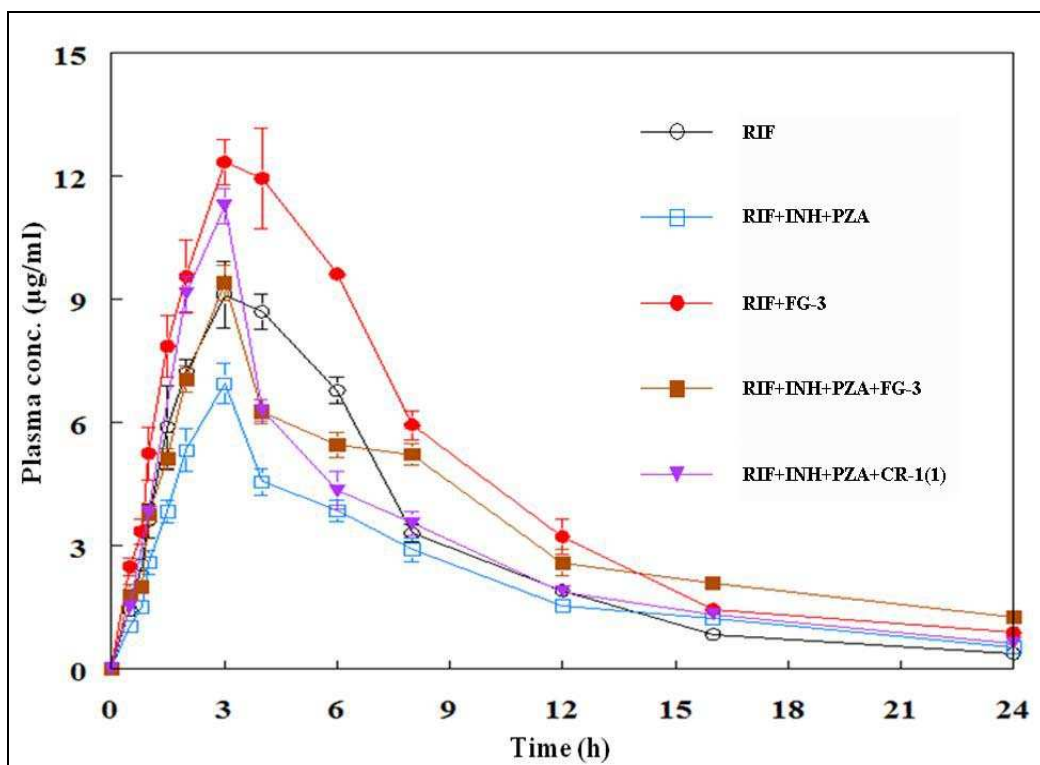


Fig. 19A. Pharmacokinetic profile of RIF (ORAL)

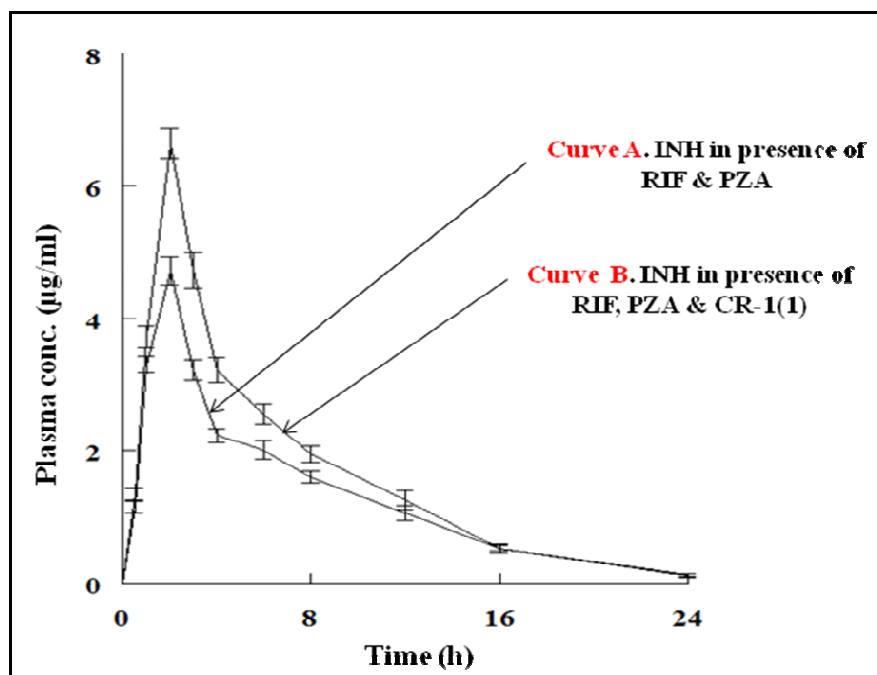


Fig. 19B. Pharmacokinetic profile of INH (ORAL)

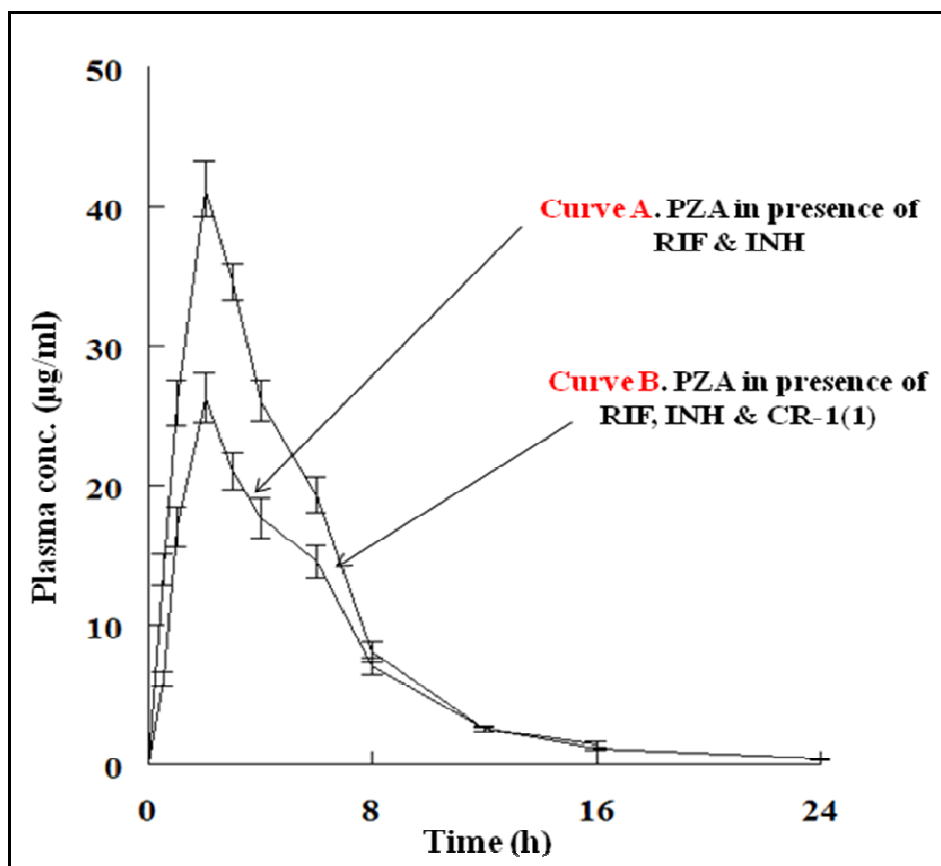


Fig. 19C. Pharmacokinetic profile of PZA (ORAL)

The pharmacokinetic parameters (C_{max} , AUC, T_{max} , $t_{1/2}$, V_d and Cl) are summarized in **Table 14A (ORAL)**.

Table 14A. Pharmacokinetic parameters of RIF, INH and PZA (Oral)

Parameter	PK Parameters of RIF Fig 19A					PK Parameters of INH Fig 19B		PK Parameters of PZA Fig 19C	
	Curve A RIF Alone	Curve B RIF + FG-3	Curve C RIF + INH + PZA	Curve D RIF + INH + PZA + FG-3	Curve E RIF + INH + PZA + CR-1(1)	Curve A RIF + INH + PZA	Curve B RIF + INH + PZA + CR-1(1)	Curve A RIF + INH + PZA	Curve B RIF + INH + PZA + CR-1(1)
C_{max} ($\mu\text{g/ml}$)	9.1	12.33	6.93	9.39	11.26	4.72	6.65	26.25	41.25
T_{max} (h)	3	3	3	3	3	2	2	2	2
AUC_{0-t} ($\mu\text{g.h/ml}$)	70.3	106.9	53.1	83.4	70.5	30.9	39.2	157.2	224.8
$t_{1/2}$ (h)	6.63	11.15	6.56	10.88	7.18	3.56	3.78	4.96	6.61
Vd (ml/kg)	5192	5326.1	6526.7	6099.9	5394.3	4908.4	4103.4	4032.4	3725.7
Cl (ml/min/kg)	542.2	330.9	689.1	388.3	520.59	953.86	752.26	562.86	390.28

A. Following inferences could be drawn with respect to **RIF** from the **Table 14A**.

EFFECT OF FG-3

- (i) C_{\max} of RIF (alone) was 9.10 $\mu\text{g/ml}$, which was increased by 35.5 % in presence of FG-3. C_{\max} of RIF in presence of other two drugs was 6.93 $\mu\text{g/ml}$, which was increased by 35.5 % in presence of FG-3 in the combination.
- (ii) AUC_{0-t} of RIF (alone) was 70.3 $\mu\text{g.h/ml}$, which was increased by 52.1 % in presence of FG-3. AUC of RIF in presence of other two drugs was 53.10 $\mu\text{g/ml}$ which was increased by 57.1 % in presence of FG-3 in the combination.
- (iii) Elimination half life ($t_{1/2}$) of RIF (alone) was 6.63 h which was increased by 68.2 % in presence of FG-3. $t_{1/2}$ of RIF in presence of other two drugs was 6.56 h which was increased by 65.9 % in presence of FG-3 in the combination.
- (iv) Clearance (Cl) of RIF was 542.2 ml/min/kg, which was decreased by 39 % in presence of FG-3. Cl of RIF in presence of other two drugs was 689.14 ml/min/kg which were decreased by 43.7 % in presence of FG-3 in the combination.
- (v) The other two parameters viz., T_{\max} and V_d were not affected by FG-3.

B. Following inferences could be drawn with respect to RIF from the **Table 14A**.

EFFECT OF CR-1(1)

- (i) C_{\max} of RIF in combination with other two anti-TB drugs was found to be 6.93 $\mu\text{g/ml}$, which was increased by 62.5 % in presence of CR-1(1).

- (ii) AUC of RIF in combination with other two anti-TB drugs was found to be 53.10 $\mu\text{g}\cdot\text{h}/\text{ml}$, which was increased by 32.8 % in presence of CR-1(1).
- (iii) Elimination half life ($t_{1/2}$) of RIF in presence of other two drugs was 6.56 h which was increased by 9.45 % in presence of CR-1(1) in the combination.
- (iv) Cl of RIF in presence of other two drugs was 689.14 ml/min/kg which were decreased by 24.45 % in presence of CR-1(1) in the combination.
- (v) The other two parameters viz., T_{max} and V_d were not notably affected by CR-1(1).

C. Following inferences could be drawn with respect to **INH** from the **Table 14A**.

EFFECT OF CR-1(1)

- (i) C_{max} of INH in combination with other two anti-TB drugs was found to be 4.72 $\mu\text{g}/\text{ml}$, which was increased by 41 % in presence of CR-1(1).
- (ii) AUC of INH in combination with other two anti-TB drugs was found to be 30.9 $\mu\text{g}\cdot\text{h}/\text{ml}$, which was increased by 26.9 % in presence of CR-1(1).
- (iii) $t_{1/2}$ of INH in presence of other two drugs was 3.56 h which was not altered in presence of CR-1(1) in the combination.
- (iv) The other two parameters viz., T_{max} and V_d were not notably affected by CR-1(1) in combination.

D. Following inferences could be drawn with respect to **PZA** from the **Table 14A**.

EFFECT OF CR-1(1)

- (i) C_{max} of PZA in combination with other two anti-TB drugs was found to be 26.25 $\mu\text{g/ml}$, which was increased by 57.1 % in presence of CR-1(1).
- (ii) AUC of PZA in combination with other two anti-TB drugs was found to be 157.20 $\mu\text{g.h/ml}$, which was increased by 43 % in presence of CR-1(1).
- (iii) $t_{1/2}$ of PZA in presence of other two drugs was 4.96 h which was increased by 33.3 % in presence of CR-1(1) in the combination.
- (iv) Cl of PZA in presence of other two drugs was 562.86 ml/min/kg which was decreased by 30.7 % in presence of CR-1(1) in the combination.

5.2.3 Pharmacokinetics (i.v).

A conc. vs. time curve of RIF (i.v.) is depicted in **Fig. 19D**. The PK parameters are summarized in **Table 14B**.

Table 14B. Pharmacokinetic parameters of RIF

From Fig. 19D

AUC _{0-t} ($\mu\text{g.h/ml}$)	20.6
$t_{1/2}$ (h)	73.9
V _d (ml/kg)	12233.6
Cl (ml/min/kg)	114.6

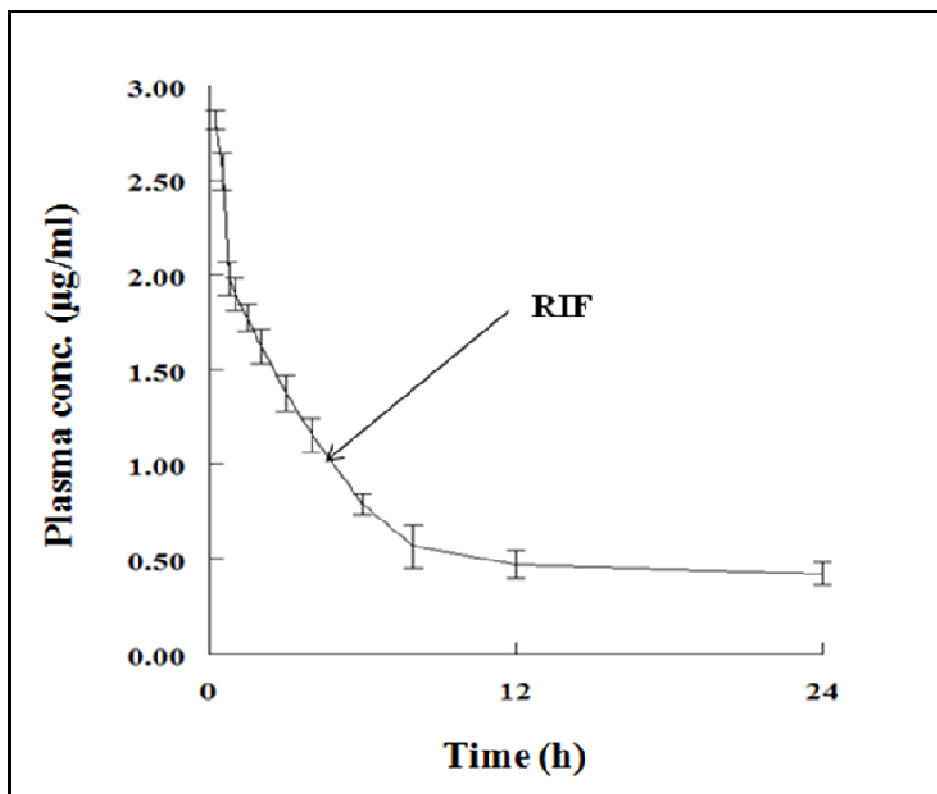


Fig. 19D. Pharmacokinetic profile of RIF (I.V.)

5.2.4 Absolute/relative bioavailability (AB/RB)

The values were calculated from **Tables 14A-B** to determine the AB by using the formula: $F_{\text{oral}} = [\text{AUC}_{\text{oral}}/\text{AUC}_{\text{i.v.}}] \times [\text{Dose}_{\text{i.v.}}/\text{Dose}_{\text{oral}}]$.

The results as summarized in **Table 15**, showed that (a) AB of RIF in presence of PZA +INH, was lower by 24 %, than the AB of RIF alone (b) AB of RIF increased by 52 % in presence of FG-1, and (c) AB of RIF in combination with PZA + INH was increased by 57 % in presence of FG-3, and (d) The relative bioavailability (RB) of RIF in combination with PZA + INH was increased by 32 % in presence of CR-1(1).

Table 15. Absolute/relative bioavailability

A. RIF alone	63.98
B. RIF + FG-3	97.29 (52 % ↑)*
C. RIF in presence of PZA + INH	48.33 (24 % ↓)**
D. RIF in presence of PZA + INH + FG-3	75.91 (57 % ↑)***
E. RIF in presence of PZA + INH + CR-1(1)	64.16 (32 % ↑)****

Values in parenthesis show % change

* vs. A; ** vs. A; *** vs. C; ****vs. C (RB), ($p < 0.001$)

5.3 Mode of action studies

5.3.1 Effect of FG-3 on the passive transport of RIF:

Results for the donor-to-acceptor plate passive transport of RIF after 12 h of incubation are depicted in **Fig. 20**. With 10 μM and 100 μM initial load of RIF, the conc. of the drug transported was $0.21 \pm 0.02 \mu\text{M}$, and $1.98 \pm 0.06 \mu\text{M}$ respectively. In presence of FG-3 (25-100 μM) RIF transport was not affected.

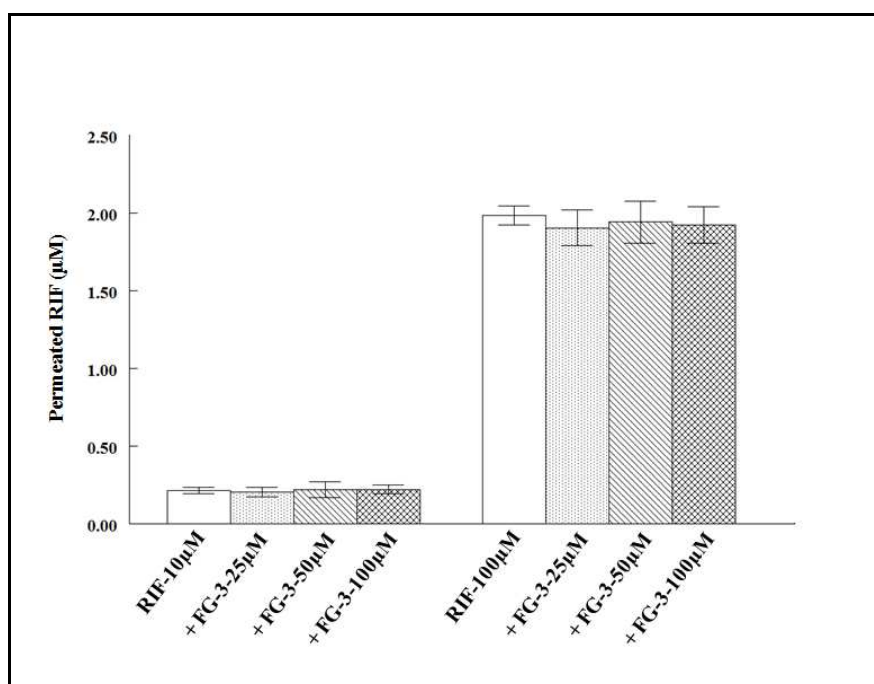


Fig. 20. Parallel Artificial membrane permeability assay (PAMPA). The experiment was carried out as described in Section 4.11 study 1. Open columns represent the amount of RIF permeated (with donor plates containing drug only). Shaded columns represent RIF permeated in presence of FG-3. Values are mean \pm SEM (n=6).

5.3.2 Effect of FG-3 on the active transport of RIF.

Results of *ex-vivo* experiment on FG-3 (everted gut sac studies) are summarized in **Table 16**. The mucosal-to-serosal transport of RIF was found to be linear against an external load of 0.25 mM during 0–30 min of incubation (optimization data not shown). From the liner transport curves the rate of RIF transport was 4.44 ± 0.08

$\mu\text{g}/\text{min}/\text{unit area}$. After 1 h and 2 h of FG-3 treatment (5 mg/kg, p.o.) mucosal-to-serosal transfer of RIF was increased by 37 % and 49 %, respectively. During the next 1 h the transport further increased by 69 % and this profile was maintained even 4 h after FG-3 treatment. The P_{app} also increased in a corresponding manner to a maximum of 69 % by 3-4 h.

Table 16. Mucosal to serosal transfer of RIF

Treatment Group	Absorption rate ($\mu\text{g RIF}/\text{min}/\text{unit area}$)	$P_{\text{app}} \times 10^{-4}$ (cm/s)
A. None	4.44 ± 0.08	1.865 ± 0.05
B. FG-3: 1 h	6.09 ± 0.05 (37 %) ^a	2.558 ± 0.09
C. FG-3: 2 h	6.66 ± 0.04 (49 %) ^a	2.798 ± 0.07
D. FG-3: 3 h	7.51 ± 0.09 (69 %) ^a	3.155 ± 0.08
E. FG-3: 4 h	7.54 ± 0.10 (69 %) ^a	3.168 ± 0.06

*The experiment was carried out as described in Section 4.11 study 2. Rats were administered with FG-3 (5.0 mg/kg, p.o.). Everted sacs from jejunum prepared at 0, 1, 2, 3 and 4 h post-treatment. Everted gut sacs were incubated against an external (mucosal) load of 0.25 mM RIF. Values are mean \pm SEM; n = 9 sacs (3 each from one rat; 3 rats used). * $p < 0.001$ vs. Group A (Dunnett's t-test).^a $p < 0.001$ vs Group A (Student's t-test).*

5.3.3 Effect of CR-1(1) on the transport of RIF, INH and PZA.

Results of *ex-vivo* experiment on CR-1(1) (everted gut sac studies) are summarized in **Fig. 21A** for RIF, in **Fig. 21B** for INH and in **Fig. 21C** for PZA. An identical pattern of mucosal to serosal transport was observed for all the drugs: as the mucosal load of the drug was increased, so did the mucosal transfer rate. In the low range of external load of the drugs, the pattern of absorption across everted gut sacs was similar in untreated and CR-1(1) treated groups. However, with gradual increase of drug load in the external medium, the extent of mucosal-to-serosal transfer of each drug was significantly high in CR-1(1) treated group compared to untreated group.

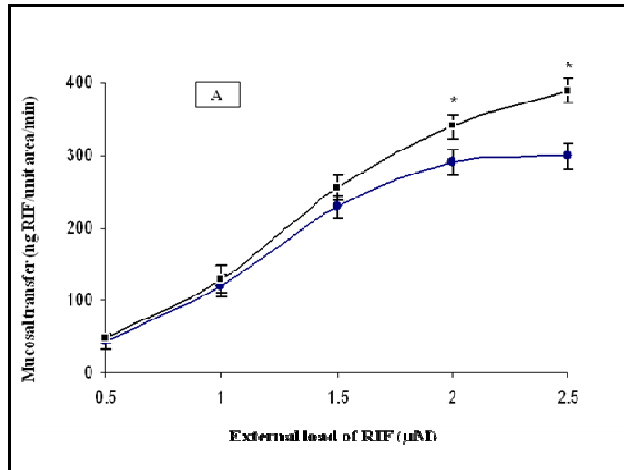


Fig. 21A. RIF. The experiment was carried out as described in Section 4.11 study 4. Rats were administered with CR-1(1) (8.0 mg/kg, p.o.). Everted sacs from jejunum prepared at 3 h post-treatment and incubated against varying external (mucosal) load of RIF. Values are mean \pm SEM; $n = 9$ sacs (3 each from one rat; 3 rats used). * $p < 0.001$ vs. Group A (Dunnett's t -test).

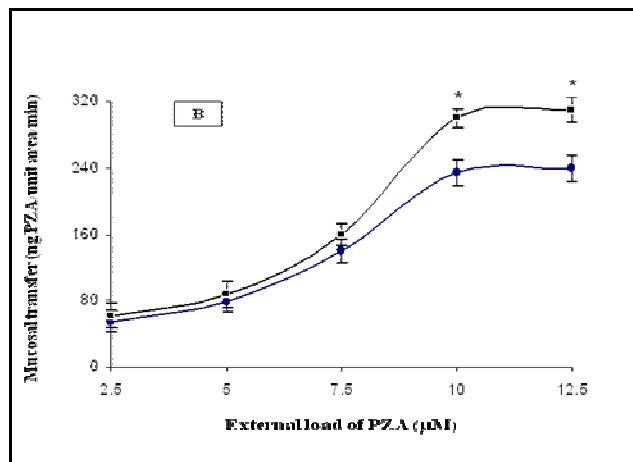


Fig. 21B. PZA. The experiment was carried out as described in Section 4.11 study 4. Rats were administered with CR-1(1) (8.0 mg/kg, p.o.). Everted sacs from jejunum prepared at 3 h post-treatment and incubated against varying external (mucosal) load of PZA. Values are mean \pm SEM; $n = 9$ sacs (3 each from one rat; 3 rats used). * $p < 0.001$ vs. Group A (Dunnett's t -test).

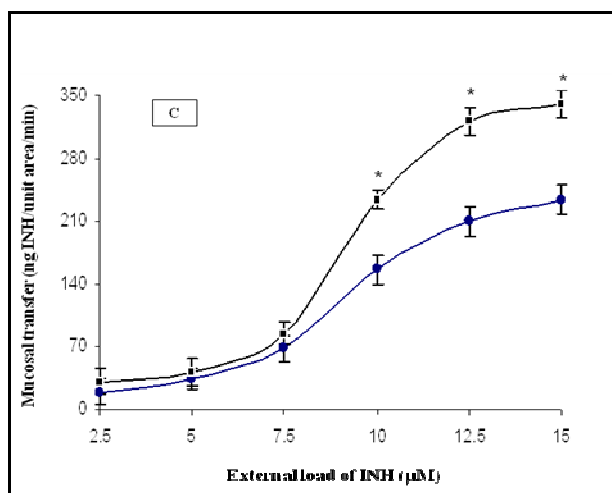


Fig. 21C. INH. The experiment was carried out as described in Section 4.11 study 4. Rats were administered with CR-1(1) (8.0 mg/kg, p.o.). Everted sacs from jejunum prepared at 3h post-treatment and incubated against varying external (mucosal) load of INH. Values are mean \pm SEM; $n = 9$ sacs (3 each from one rat; 3 rats used).* $p < 0.001$ vs. Group A (Dunnett's t -test).

CR-1(1) treatment increased the P_{app} values. In case of RIF, this was $1.198 \pm 0.003 \times 10^{-3}$ for untreated group and $1.553 \pm 0.005 \times 10^{-3}$ for treated group (1.29-fold change); for PZA, these values were $2.174 \pm 0.006 \times 10^{-3}$ for untreated group and $2.871 \pm 0.003 \times 10^{-3}$ for treated group (1.32-fold change); for INH, these values were $1.685 \pm 0.002 \times 10^{-3}$ for untreated group and $2.567 \pm 0.003 \times 10^{-3}$ for treated group (1.52-fold change).

5.3.4 Effect of FG-3 on Rho123 transport (*ex-vivo* gut sac studies).

Results are summarized in **Table 17**. The serosal to mucosal transport of Rho123 was found to be linear against an external load of 2-10 μ M during 0-30 min of incubation (optimization data not shown). From the linear transport curves the rate of

Rho123 transport was 126.37 ng/min/unit area. After 3 h, of FG-3 treatment (5 mg/kg, p.o.), serosal to mucosal transfer of Rho123 was decreased by 40 %.

Table 17. Serosal to mucosal transfer of Rho123

Treatment Group	Exsorption rate (ng Rho123/min/unit area)	$P_{app} \times 10^{-5}$ (cm/s)
A. None	210.46 ± 6.55	1.84 ± 0.11
B. FG-3: 3 h	126.37 ± 7.11(40 %↓) ^a	1.10 ± 0.01
C. Verapamil: 25 μM	111.22 ± 3.43(47 %↓) ^a	0.86 ± 0.03

*The experiment was carried out as described in Section 4.11 study 3. Rats were administered with FG-3 (5.0 mg/kg, p.o.). Everted sacs from jejunum prepared, 3 h post-treatment. Values are mean ± SEM; n = 9 sacs (3 each from one rat; 3 rats used). * p < 0.001 vs. Group A (Dunnett's t-test). ^ap < 0.001 vs. Group A (Student's t-test).*

The apparent permeability coefficient (P_{app}) was also decreased in a corresponding manner by 40% in presence of FG-3.

5.3.5 Effect of FG-3 on *in-situ* efflux of Rho-123.

Results for the net efflux of Rho123 are summarized in **Fig. 22**. Following parameters were calculated:

C_{pss} : Steady state plasma conc. of Rho123 (nmol/min)

CL_t : Total plasma clearance (ml/min/kg) = (Constant infusion rate of Rho123 in nmol/min) / C_{pss} in nmol/min);

Exsorption Rate Int.: Intestinal exsorption rate (nmol/min/kg) = (Rho123 conc. in effluent in nmol/ml) / (effluent flow rate in ml/min)

$CL_{Int.Ex.}$: Intestinal exsorption clearance (ml/min/kg) = (Intestinal exsorption rate in nmol/min/kg) / (C_{pss} in nmol/ml)

In this experiment following perfusion medium were used:

- Medium 1 : Buffer only
- Medium 2-A : Buffer containing FG-3 (50 μ M)
- Medium 2-B : Buffer containing FG-3 (100 μ M)
- Medium 3-A : Buffer containing RIF (5 μ M)
- Medium 3-B : Buffer containing RIF (10 μ M)
- Medium 4 : Buffer containing RIF (10 μ M) + FG-3 (100 μ M)
- Medium 5-A : Buffer containing verapamil (25 μ M)
- Medium 5-B : Buffer containing verapamil (100 μ M)

Results are summarized in **Fig. 22** and **Table 21**.

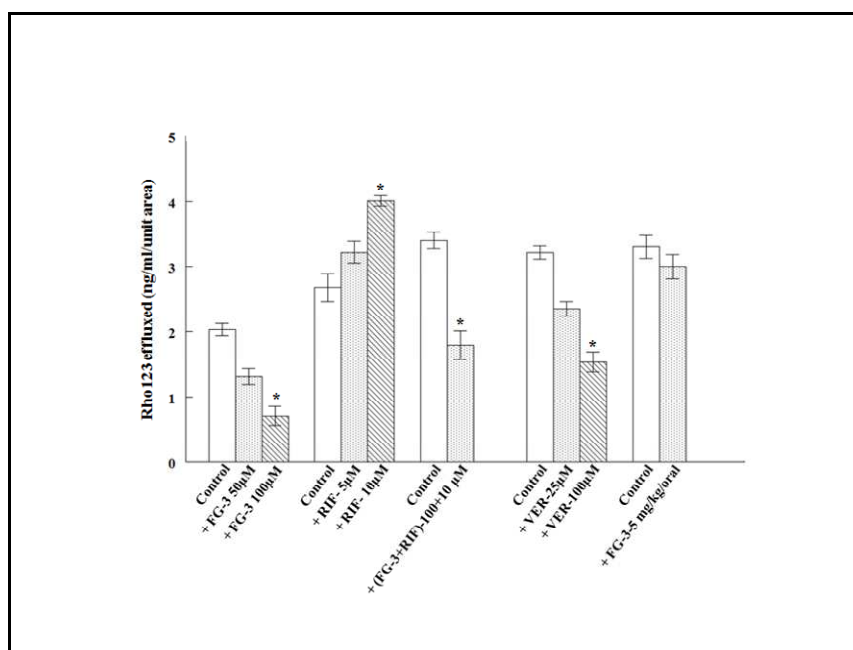


Fig. 22. Effect of test substances on Rho123 efflux. The *in situ* experiment was carried out as described in Section 4.11 study 5. Open column represent control group (perfusion medium only). Shaded columns represent treated groups. Values are mean \pm SEM from 5 independent experiments * $P < 0.05$, vs. control.

Experiment A. Net efflux of Rho123 in control (with Medium 1) was 2.0278 ng/ml/unit area. In presence of 50 μ M and 100 μ M of FG-3 in the perfusion medium (Medium 2A-B), the net efflux decreased by 35.05 % and 65.13 % respectively. The intestinal exsorption rate, and $CL_{Int.Ex}$ decreased by 65-71 % (**Fig. 22** and **Table 18**).

Experiment B. The net efflux of Rho123 in control (with Medium 1) was 2.671 ng/ml/unit area which was increased by 20.43 % and 50.14 % respectively in presence of 5 μ M and 10 μ M of RIF in the perfusion medium (Medium 3A-B). A load of 10 μ M of RIF increased the intestinal exsorption rate and $CL_{Int.Ex}$ by 52 % and 81 % respectively (**Fig. 22** and **Table 18**).

Experiment C-I: The net efflux of Rho123 in control (with Medium 1) was 3.3972 ng/ml/unit area which was decreased by 47.26 % in presence of 100 μ M FG-3 + 10 μ M of RIF in the perfusion medium (Medium 4). The intestinal exsorption rate, and $CL_{Int.Ex}$ decreased by 47 % and 54 % respectively.

Experiment C-II: After the perfusion with Medium 4 (containing FG-3 +RIF), was over, again a Medium 1 was reperfused in order to investigate the reversibility of FG-3 + RIF effect. In this experiment intestinal exsorption rate, and $CL_{Int.Ex}$ showed a decrease of 37.21 % and 44.29 % with Medium 4, but after reperfusion with Medium 1 intestinal exsorption rate was increased by 20.17% (**Fig. 23**).

Experiment D: The net efflux of Rho123 in control (with Medium 1) was 3.2146 ng/ml/unit area which was decreased by 26.99 % and 51.99 % respectively in presence of 25 μ M and 100 μ M of verapamil in the perfusion medium (Medium 5-A and B). A load of 100 μ M of verapamil decreased the intestinal exsorption rate and $CL_{Int.Ex}$ in the range of 52 %- 58 %.

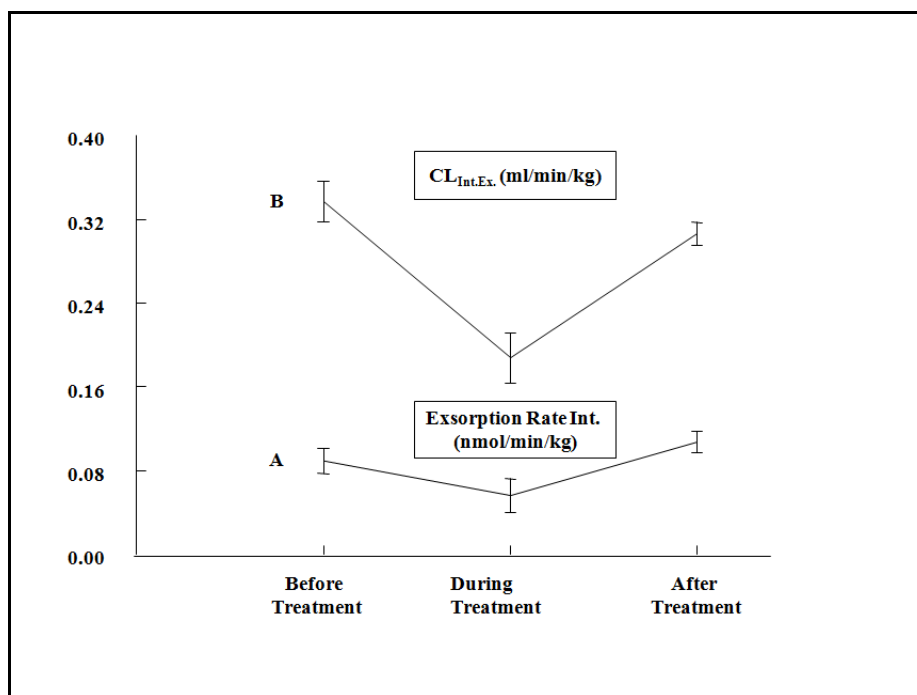


Fig. 23. Effect of FG-3 on intestinal clearance and intestinal exsorption rate of Rho123.

Experiment E, as described in section 4.11 study 5 for 3 perfusion sets: with medium 1 (a), followed by medium 4, and further reperfusion with Medium 1. y axis shows the data for intestinal exsorption rate, in line graph A, and for $CL_{int.ex.}$ in line graph B., Values are mean \pm SEM (n=5).

Experiment E: In this experiment rats pre-treated with FG-3 (5 mg/kg, p.o.) were used. The net efflux of Rho123 in control (with Medium 1) was 3.3011 ng/ml/unit area, which showed a non-significant change in the net efflux of Rho123 as well as in the C_{pss} , CL_t , intestinal exsorption rate, and $CL_{Int.Ex.}$, compared with control (perfusion with Medium 1).

Table 18. Effect of FG-3, RIF and verapamil on Rho123 clearance under steady state plasma conc. of Rho123.

Treatment	C _{pss} . (μ M)	CL _t . (ml/min/kg)	Exsorption Rate Int. (nmol/min/kg)	CL _{Int.Ex.} (ml/min/kg)
<u>A. FG-3</u>				
Control	0.198 \pm 0.02	84.24 \pm 1.79	0.096 \pm 0.01	0.487 \pm 0.03
50 μ M	0.220 \pm 0.01	75.65 \pm 1.83	0.062 \pm 0.01	0.284 \pm 0.02
100 μ M	0.239 \pm 0.01	69.56 \pm 2.05	0.033 \pm 0.00 ^a	0.140 \pm 0.01 ^a
<u>B. RIF</u>				
Control	0.259 \pm 0.01	64.33 \pm 2.38	0.125 \pm 0.03	0.483 \pm 0.03
5 μ M	0.241 \pm 0.01	68.92 \pm 2.27	0.152 \pm 0.02	0.632 \pm 0.02
10 μ M	0.216 \pm 0.02	76.88 \pm 2.11	0.190 \pm 0.01	0.879 \pm 0.02 ^a
<u>C-I. RIF+FG-3</u>				
Control	0.327 \pm 0.02.	78.0 \pm 1.92	0.161 \pm 0.02	0.493 \pm 0.03
10+500 μ M	0.377 \pm 0.01	94.0 \pm 2.31	0.085 \pm 0.02 ^a	0.225 \pm 0.03 ^a
<u>C-II. RIF+FG-3 (Reversibility)</u>				
Control	0.266 \pm 0.02.	63.45 \pm 2.52	0.089 \pm 0.01	0.337 \pm 0.01
	0.299 \pm 0.01	56.02 \pm 2.38	0.056 \pm 0.01 ^a	0.188 \pm 0.02 ^a
	0.338 \pm 0.02	49.58 \pm 2.80	0.107 \pm 0.01	0.306 \pm 0.01
<u>D. Verapamil</u>				
Control	0.310 \pm 0.02	53.651 \pm 1.99	0.152 \pm 0.02	0.4918 \pm 0.02
25 μ M	0.337 \pm 0.01	49.318 \pm 2.13	0.111 \pm 0.02	0.3301 \pm 0.02
100 μ M	0.357 \pm 0.02	46.621 \pm 2.29	0.073 \pm 0.01 ^a	0.2052 \pm 0.01 ^a
<u>E. FG-3</u>				
Control	0.3178 \pm 0.01	52.451 \pm 1.878	0.1569 \pm 0.01	0.4937 \pm 0.029
Treated	0.3275 \pm 0.01	50.902 \pm 2.03	0.1423 \pm 0.02	0.4346 \pm 0.025

Experiments were conducted as described in Section 4.11 study 5. Each value represents the Mean \pm SEM (n = 6). Infusion rate of Rho123 was 3.3333 nmol/min in each control and treatment group. ^a p < 0.05, vs. control groups.

5.3.6 Effect of FG-3 on the ³H-benzopyrene transport (Guinea pig epithelial cells, *in-vitro*)

The results are summarized in **Table 19**. The results showed that FG-3 (25-100 μM) enhanced the ³H-Benzopyrene accumulation by cells in the range of 18-21 %.

Table 19. Effect of FG-3 on the ³H-benzopyrene transport (Guinea pig intestinal epithelial cells)

Treatment	Test Conc.	³ H-Benzopyrene accumulation pmol/ 2x10 ⁶ cells/10 min
Control	-	9470 ± 166.2
FG-3	25 μM	11174 ± 234.3*
	50 μM	11458 ± 230.3*
	100 μM	11467 ± 227.9*
Verapamil	50 μM	13222 ± 11.32

*The experiment was carried out as described in Section 4.11 study 6. Values show mean ± SEM from 4 independent experiments (Each experiment was done in triplicate). Cells were incubated with 0.5 mM ³H-benzopyrene (20,000 cpm) in absence and presence of FG-3/verapamil for 10 min. Whole incubation medium was filtered using glass fiber filters, and washed. The radioactivity retained on filters, was counted as described in Section 4 study 6. * p < 0.05 vs. control (n=4).*

5.3.7 Effect of FG-3 on vanadate sensitive P-gp ATPase activity (rat jejunal membranes, *in-vitro*).

Results are summarized in **Fig. 24**. Basal P-gp ATPase activity of the freshly prepared isolated rat jejunal membrane was in the range of 4.65–5.21 nmol Pi/mg protein/min. FG-3 showed a conc. dependent effect: 25, 50 and 100 μM of FG-3

inhibited the ATPase activity by 28.3 %, 59.9 % and 78.4 % .Verapamil (25-100 μ M) inhibited the enzyme activity in the range of 19 % to 88 %.

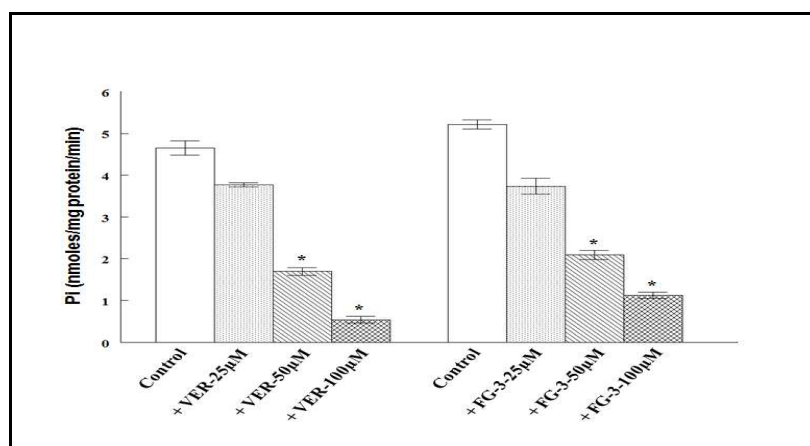


Fig. 24. Effect of test substances on P-gp ATPase activity.

*The experiment was carried out as described in Section 4.11 study 7. Open column represent ATPase activity in control (untreated membranes). Shaded columns show results with test materials. Values are mean \pm SEM from 4 independent experiments (each experiment was done in triplicate). * $P < 0.05$, vs. control.*

5.3.8 Effect of FG-3 on CYP 3A4: Testosterone hydroxylase activity (rat liver microsomes, *in-vitro*)

The specific activity of the testosterone hydroxylase enzyme was determined on the basis of the testosterone converted to 6 β -hydroxy testosterone by estimating a difference between control (without FG-3) and test incubations (containing FG-3), under the given conditions of the assay. Results are summarized in **Fig. 25**.

In control preparations the enzyme activity was found to be 6.56 nmole hydroxy-testosterone /mg protein/min. FG-3 at conc. of 25 μ M, 50 μ M and 100 μ M, inhibited testosterone hydroxylase activity by 21 %, 25 % and 34 % respectively. On the other hand, piperine (25-100 μ M) inhibited the enzyme activity by 76.8-81 %.

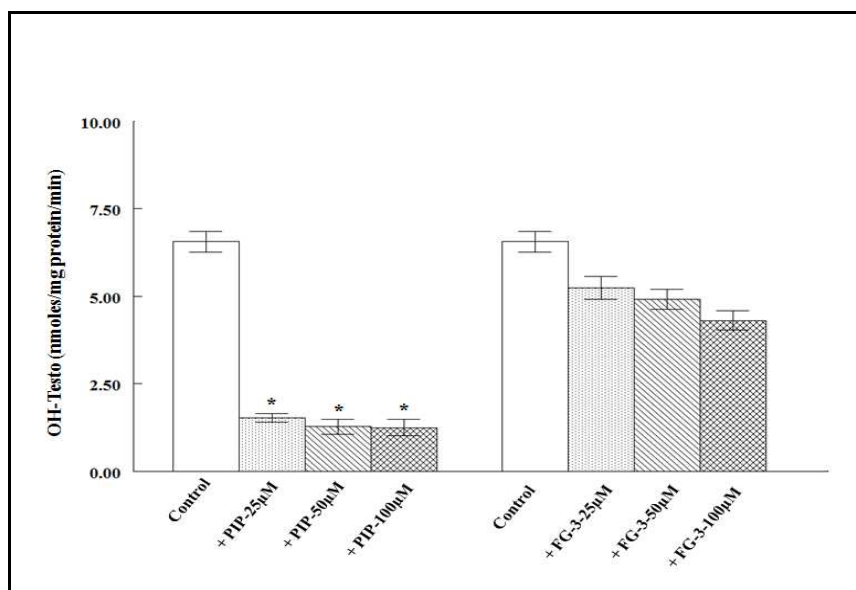


Fig. 25. Effect of test substances on testosterone hydroxylase activity.

*The experiment was carried out as described in Section 4.11 study 8. Open column represent enzyme activity in control. Shaded columns show results with test materials. Values are mean \pm SEM from 4 independent experiments (each experiment was done in triplicate). * $P < 0.05$, vs. control (*t*-test).*

5.3.9 Effect of FG-3 on CYP 3A4: Erythromycin demethylase activity (rat liver microsomes, *in-vitro*)

The specific activity of erythromycin demethylase was calculated as the difference between HCHO (nmoles/mg protein/min, generated along with demethyl-erythromycin in a ratio of 1:1), produced in the control (without FG-3) and HCHO produced in test incubations (containing FG-3). Results are summarized in **Fig. 26**.

In control (untreated) preparations the enzyme activity was found to be 3.59 nmole HCHO formed/mg protein/min. The effect of FG-3 on erythromycin demethylase activity was not statistically significant. Piperine (25-100 μ M) inhibited the activity by 19-23 %.

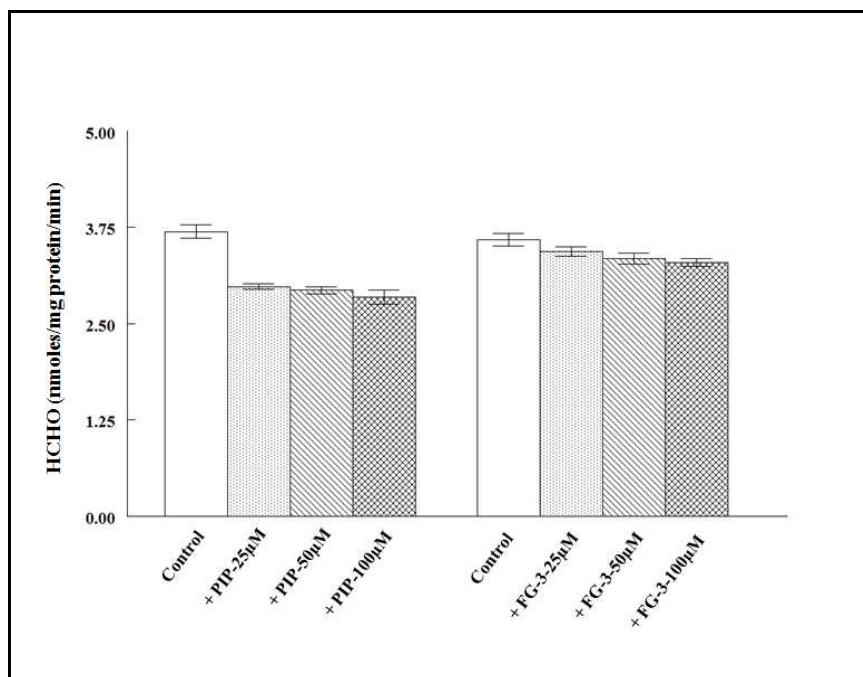


Fig. 26. Effect of test substances on erythromycin demethylase activity.

The experiment was carried out as described in Section 4.11 study 8. Open column represent enzyme activity in control. Shaded columns show results with test materials. Values are mean \pm SEM from 4 independent experiments (each experiment was done in triplicate).

5.3.10 Effect of FG-3 on CYP 3A4: Inducible erythromycin demethylase activity (mouse liver microsomes, *in-vitro*)

Results are summarized in **Fig. 27**. In control (untreated) preparations the phenobarbitone-inducible enzyme activity in *C57BL* mice was found to be 17.4 nmole HCHO formed/mg protein/min, which was 56.3 % higher compared to un-induced animals. The effect of FG-3 on inducible activity was not statistically significant.

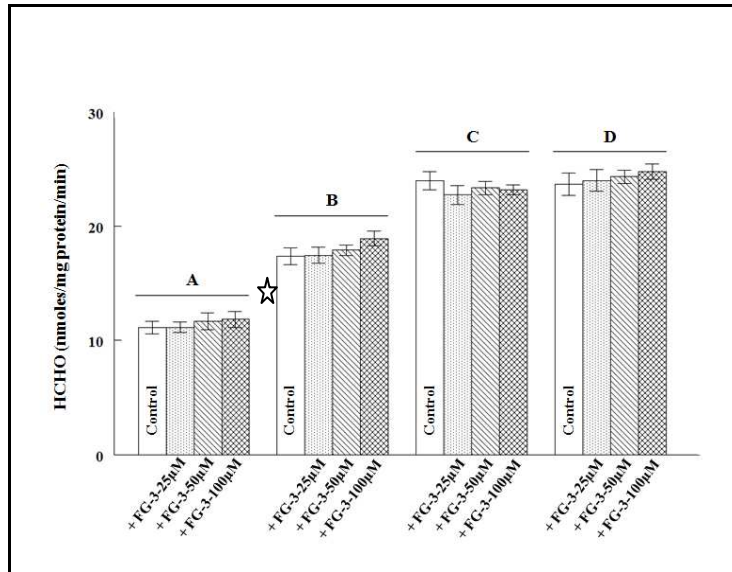


Fig. 27. Effect of FG-3 on inducible erythromycin demethylase activity.

The experiment was carried out as described in Section 4.11 study 8. Open column represent enzyme activity in control. Shaded columns show results with test materials. Values are mean \pm SEM from 4 independent experiments (each experiment was done in triplicate).

☆ $p < 0.05$, A vs. B

- A: Constitutive activity - C57BL mice
- B: Inducible activity - C57BL mice
- C: Constitutive activity - Swiss mice.
- D: Inducible activity - Swiss mice.

5.4 Toxicity studies

5.4.1 Effect of FG-3 on intestinal mucosal membrane integrity.

Results are summarized in **Table 20**. There was no significant release of protein in the luminal fluid recovered from gut sacs in presence of either FG-3 or CR-1(1).

Table 20. Effect of test materials on mucosal (luminal) protein content of un-everted sac

Incubation	mg Protein/ml/unit area
A. Buffer	0.295 ± 0.005
B. Buffer + FG-3 (10µg/ml)	0.290 ± 0.004 ^a
C. Buffer + FG-3 (30 µg/ml)	0.277 ± 0.004 ^a
D. Buffer + FG-3 (100 µg/ml)	0.286 ± 0.003 ^a
E. Buffer + CR-1(1) (10µg/ml)	0.237 ± 0.010 ^a
F. Buffer + CR-1(1) (30 µg/ml)	0.246 ± 0.006 ^a
G. Buffer + CR-1(1) (100 µg/ml)	0.241 ± 0.005 ^a

Values (mean ± SEM) (n= 9 sacs: 3 sacs derived from 3 rats).

^aNon-significant vs. control (Student's t-test).

Area of the sac = $2 \Pi r^2 \times l$, where r = radius of the intestine; L =length of the sac.

5.4.2 Acute, sub-acute and sub-chronic toxicity studies.

General observations: In acute toxicity study no mortality was observed for 21 days in control (untreated) or treated groups.

Clinical observations: There was no treatment-related mortality of animals at any dose level tested. Gross observations did not reveal any treatment-related changes and all animals both in control and treated groups appeared healthy. Any clinical symptoms of locomotor dysfunction, tremors or convulsions were absent, and all animals survived until the end of the study. Animals of both sexes in control as well as in treated groups showed identical pattern of body weight changes (**Fig. 28 A-D**).

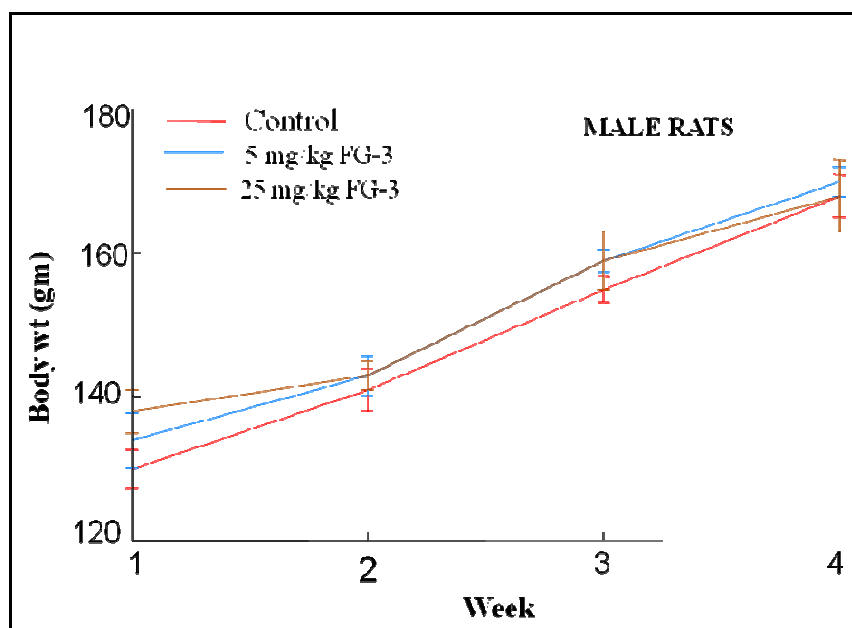


Fig. 28A. Weekly body weight (Sub-acute toxicity study in male rats)

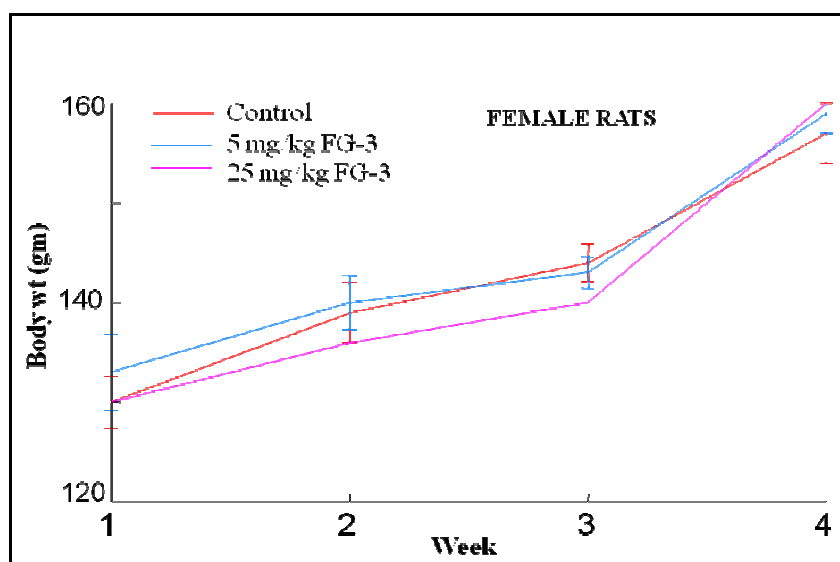


Fig. 28B. Weekly body weight (Sub-acute toxicity study in female rats)

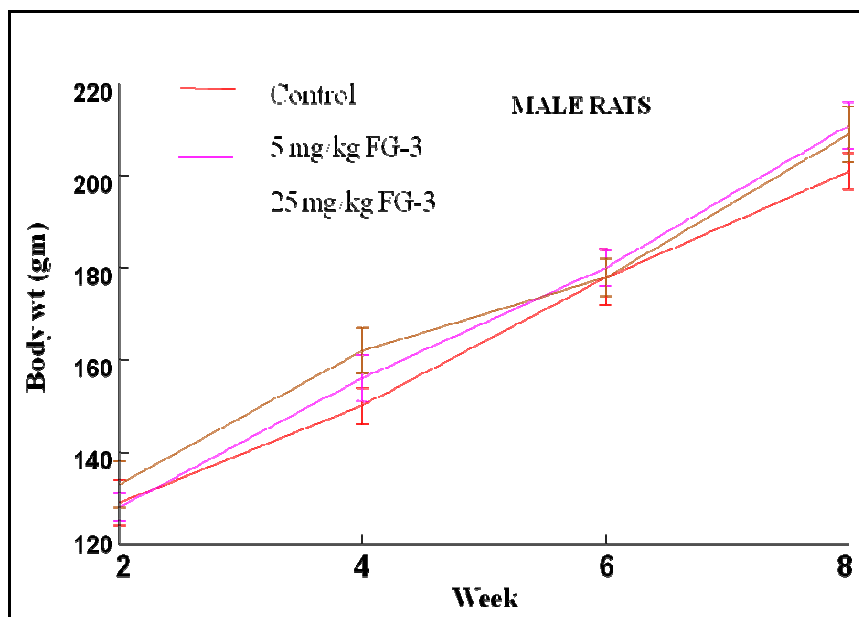


Fig. 28C. Weekly body weight (Sub-chronic toxicity study in male rats)

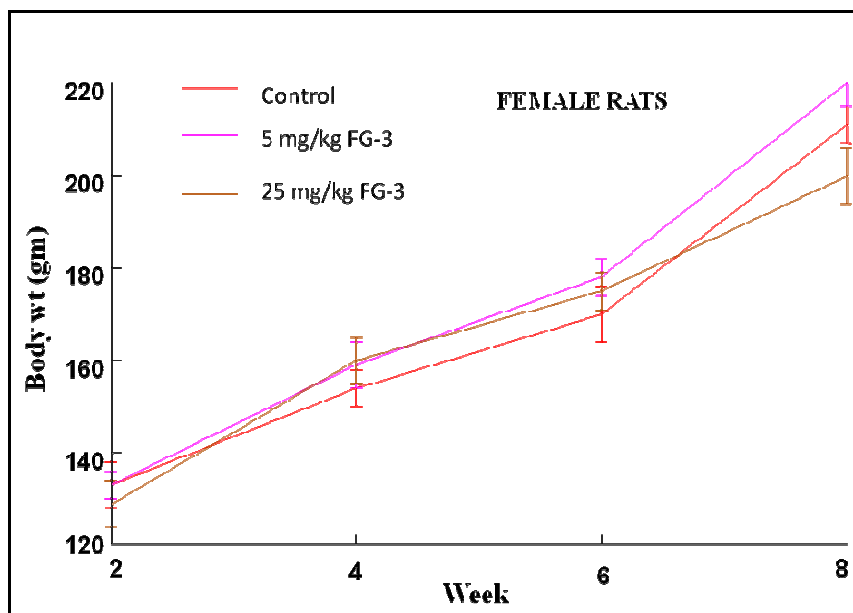


Fig. 28D. Weekly body weight (Sub-chronic toxicity study in female rats)

Hematology and serum biochemistry: The results of hematology examination are summarized in **Table 21-A** (sub-acute study) and **Table 21-B** (sub-chronic study).

There were no statistically significant difference in the values of RBC, WBC, and differential leucocyte counts. The other parameters, hemoglobin and platelet counts also showed no alteration by FG-3 treatment. Serum biochemistry parameters are summarized in **Table 22-A** (sub-acute study) and **Table 22-B** (sub-chronic study).

The levels of serum glucose, TG, cholesterol, urea, UA and creatinine in treated groups remained within the normal range. The indicators of liver function (AST, ALT and bilirubin,) were within the normal range in treated male and female rats.

Conclusion of toxicity studies:

No evaluation of the effect of the repeated dosing of any herbal product of carum/caraway is reported, prior to this study. A 4-week sub-acute toxicity testing as well as an 8-week sub-chronic toxicity are widely considered satisfactory to assess any possible health hazard, and are now considered important even for herbal supplements/natural products. The results showed that FG-3 was devoid of toxicity at its bioeffective dose as well as at 5-times higher dose. There were no treatment related clinical symptoms or organ toxicity as revealed by a normal organ to body weight ratios (**Table 23A-B**).

Table 21A. Hematological values of rats treated with FG-3 (4 weeks sub-acute toxicity study)

Male rats						
	WBC (x10⁹/l)	Lym^a. (%)	Gra^b. (%)	RBC (x10¹²/l)	Hb^c. (%)	Plt^d. (g/dl)
Control	15.9 ± 2.1	73.6 ± 5.1	22.1 ± 6.6	8.9 ± 1.1	12.1 ± 3.0	47.2 ± 7.0
FG-3Treatment						
5 mg/kg	16.3 ± 1.1	75.1 ± 2.1	24.9 ± 5.8	7.9 ± 1.4	11.6 ± 1.3	43.2 ± 4.8
25 mg/kg	16.6 ± 5.1	71.1 ± 8.2	25.1 ± 5.1	8.7 ± 1.4	12.5 ± 1.3	44.3 ± 4.9
Female rats						
	WBC (x10⁹/l)	Lym^a. (%)	Gra^b. (%)	RBC (x10¹²/l)	Hb^c. (%)	Plt^d. (g/dl)
Control	13.2 ± 1.9	69.3 ± 4.4	23.4 ± 5.5	9.1 ± 2.7	11.7 ± 2.8	43.8 ± 5.2
FG-3Treatment						
5 mg/kg	15.6 ± 1.3	73.2 ± 2.1	24.7 ± 6.5	8.2 ± 1.3	13.5 ± 1.8	47.4 ± 5.0
25 mg/kg	17.4 ± 5.6	73.6 ± 8.5	22.3 ± 5.1	8.8 ± 1.4	11.9 ± 1.1	44.3 ± 4.4

*Values are mean ± S.D (n = 5).
^alymphocytes; ^bgranulocyte; ^chemoglobin; ^dplatelets.*

Table 21B. Hematological values of rats treated with FG-3 (8 week sub-chronic toxicity study)

Male rats						
	WBC (x10⁹/l)	Lym^a. (%)	Gra^b. (%)	RBC (x10¹²/l)	Hb^c. (%)	Plt^d. (g/dl)
Control	12.3 ± 1.9	71.1 ±3.1	21.7 ± 5.5	8.2 ±1.7	11.8 ± 2.7	41.3 ± 3.5
FG-3Treatment						
5 mg/kg	14.2 ± 1.7	70.2 ± 3.1	21.2 ± 4.3	10.2 ± 1.3	10.1 ± 2.4	41.9 ± 3.8
25 mg/kg	13.2 ± 5.0	68.4 ± 7.2	22.3 ± 4.1	9.9 ± 2.3	11.2 ± 2.1	45.6 ± 3.6
Female rats						
	WBC (x10⁹/l)	Lym^a. (%)	Gra^b. (%)	RBC (x10¹²/l)	Hb^c. (%)	Plt^d. (g/dl)
Control	11.2 ± 1.9	73.4 ± 4.0	22.6 ± 3.5	8.01 ± 2.3	12.0 ± 2.3	41.2 ± 4.7
FG-3Treatment						
5 mg/kg	14.2 ± 2.6	70.9 ± 4.3	23.5 ± 4.7	9.0 ± 2.2	10.5 ± 1.1	45.8 ± 3.9
25 mg/kg	13.3 ± 3.2	71.2 ± 6.2	24.3 ± 4.3	9.5 ± 3.5	13.1 ± 1.7	46.1 ± 5.1

*Values are mean ± S.D (n = 5).
^alymphocytes; ^bgranulocyte; ^chemoglobin; ^dplatelets.*

Table 22A. Biochemical parameters of rats treated with FG-3 (4 week sub-acute toxicity study)

Male rats									
	Glu	TG	Chol	AST	ALT	Bil	Urea	Creat	UA
Control	90.4 ± 9.6	103.2 ± 13.5	51.3 ± 6.5	112.5 ± 11.9	59.2 ± 8.1	0.6 ± 0.17	51.2 ± 7.5	0.79 ± 0.13	1.12 ± 0.21
FG-3 Treatment									
5 mg/kg	98.1 ± 7.4	97.4 ± 9.8	49.4 ± 7.6	92.4 ± 8.1	54.2 ± 7.1	0.59 ± 0.13	48.7 ± 6.4	0.83 ± 0.14	0.98 ± 0.1
25 mg/kg	101.4 ± 6.7	100.1 ± 11.8	53.2 ± 6.4	90.7 ± 7.8	53.2 ± 5.5	0.49 ± 0.11	56.1 ± 4.9	0.72 ± 0.13	1.01 ± 0.1
Female rats									
	Glu	TG	Chol	AST	ALT	Bil	Urea	Creat	UA
Control	87.7 ± 5.9	89.7 ± 9.3	65.2 ± 7.1	97.3 ± 7.7	55.3 ± 7.3	0.59 ± 0.11	49.7 ± 6.1	0.88 ± 0.12	0.95 ± 0.31
FG-3 Treatment									
5 mg/kg	80.2 ± 6.8	88.5 ± 11.2	60.8 ± 8.8	87.4 ± 6.8	56.8 ± 7.4	0.63 ± 0.17	51.2 ± 6.1	0.90 ± 0.17	0.99 ± 0.11
25 mg/kg	91.5 ± 8.0	88.3 ± 7.6	56.4 ± 7.2	100.2 ± 11.1	51.8 ± 5.3	0.58 ± 0.13	53.1 ± 4.6	0.89 ± 0.18	0.88 ± 0.16

Values are mean ± S.D (n=5).

Glu= glucose (mg/dl); TG= triglyceride(mg/dl); Chol= cholesterol (mg/dl); AST= Aspartate aminotrasferase (SGOT) (IU/L); ALT=alanine aminotransferase (SGPT) (IU/L); Bil= bilirubin (mg/dl); Creat= creatinine (mg/dl); UA= uric acid (mg/dl)

Table 22B. Biochemical parameters of rats treated with FG-3 (8 week sub-chronic toxicity study)

Male Rats									
	Glu	TG	Chol	AST	ALT	Bil	Urea	Creat	UA
Control	90.4 ± 9.6	103.2 ± 13.5	51.3 ± 6.5	112.5 ± 11.9	59.2 ± 8.1	0.6 ± 0.17	51.2 ± 7.5	0.79 ± 0.13	1.12 ± 0.21
FG-3 Treatment									
5 mg/kg	91.9 ± 5.7	100.3 ± 11.2	58.5 ± 6.7	92.4 ± 10.1	62.1 ± 5.9	0.63 ± 0.14	41.1 ± 5.4	0.73 ± 0.13	0.90 ± 0.18
25 mg/kg	92.3 ± 4.4	93.4 ± 7.9	58.3 ± 4.9	89.3 ± 6.2	67.7 ± 4.8	0.50 ± 0.17	51.9 ± 4.3	0.71 ± 0.19	0.99 ± 0.14
Female Rats									
	Glu	TG	Chol	AST	ALT	Bil	Urea	Creat	UA
Control	87.7 ± 5.9	89.7 ± 9.3	65.2 ± 7.1	97.3 ± 7.7	55.3 ± 7.3	0.59 ± 0.11	49.7 ± 6.1	0.88 ± 0.12	0.95 ± 0.31
FG-3 Treatment									
5 mg/kg	80.2 ± 6.8	88.5 ± 11.2	60.8 ± 8.8	87.4 ± 6.8	56.8 ± 7.4	0.63 ± 0.17	51.2 ± 6.1	0.90 ± 0.17	0.99 ± 0.11
25 mg/kg	91.5 ± 8.0	88.3 ± 7.6	56.4 ± 7.2	100.2 ± 11.1	51.8 ± 5.3	0.58 ± 0.13	53.1 ± 4.6	0.89 ± 0.18	0.88 ± 0.16

Values are mean ± S.D (n=5).

Glu= glucose (mg/dl); TG= triglyceride (mg/dl); Chol= cholesterol (mg/dl); AST= Aspartate aminotrasferase (SGOT) (IU/L); ALT=alanine aminotransferase (SGPT) (IU/L); Bil= bilirubin (mg/dl); Creat= creatinine (mg/dl); UA= uric acid (mg/dl)

**Table 23A. Organ to body weight ratio (4-week sub-acute toxicity study)
Male rats**

	Brain	Heart	Lung	Liver	Spleen	Kidney (R)	Kidney (L)	Testis (R)	Testis (L)
Control	6.6 ± 1.1	3.4 ± 0.7	7.1 ± 0.6	43.2 ± 7.3	4.1 ± 0.6	3.9 ± 0.8	3.6 ± 0.6	6.1 ± 0.5	7.0 ± 1.1
FG-3 Treatment									
5 mg/kg	6.2 ± 0.9	3.6 ± 0.9	7.3 ± 0.6	44.2 ± 6.3	3.3 ± 0.7	4.0 ± 0.6	3.7 ± 0.7	5.9 ± 0.3	6.8 ± 0.8
25 mg/kg	7.0 ± 0.7	3.1 ± 0.6	7.2 ± 0.8	43.1 ± 0.5	4.0 ± 0.7	3.3 ± 0.8	3.6 ± 0.5	6.3 ± 0.7	6.3 ± 0.8
Female Rats									
	Brain	Heart	Lung	Liver	Spleen	Kidney (R)	Kidney (L)	Testis (R)	Testis (L)
Control	6.0 ± 1.0	3.9 ± 0.5	6.8 ± 0.4	41.1 ± 1.9	4.3 ± 0.7	4.0 ± 0.6	3.9 ± 0.7	6.4 ± 0.4	6.9 ± 9.1
FG-3 Treatment									
5 mg/kg	6.1 ± 0.8	4.1 ± 0.7	6.9 ± 0.5	43.7 ± 5.9	3.1 ± 0.8	4.2 ± 0.7	3.8 ± 0.8	6.0 ± 0.4	6.1 ± 0.6
25 mg/kg	6.7 ± 0.4	3.8 ± 0.3	7.1 ± 0.9	41.1 ± 7.3	4.2 ± 0.5	3.5 ± 0.6	3.1 ± 0.7	6.0 ± 0.5	6.7 ± 0.6

Values are mean (x 10⁻³) ± S.D (x 10⁻⁴) (n =5)

Table 23B. Organ to body weight ratio (8 weeks sub-chronic toxicity study)

Male rats

	Brain	Heart	Lung	Liver	Spleen	Kidney (R)	Kidney (L)	Testis (R)	Testis (L)
Control	6.6 ± 1.1	3.4 ± 0.7	7.1 ± 0.6	43.2 ± 7.3	4.1 ± 0.6	3.9 ± 0.8	3.6 ± 0.6	6.1 ± 0.5	7.0 ± 1.1
FG-Treatment									
5 mg/kg	6.1 ± 1.3	3.2 ± 0.77	6.9 ± 0.52	43.7 ± 5.2	3.4 ± 0.59	3.8 ± 0.52	3.8 ± 0.61	5.9 ± 0.3	6.1 ± 0.3
25 mg/kg	5.9 ± 1.1	3.7 ± 0.43	7.2 ± 0.8	40.8 ± 7.1	3.6 ± 0.44	3.7 ± 0.71	4.0 ± 0.49	6.3 ± 0.7	5.9 ± 0.7

Female rats

	Brain	Heart	Lung	Liver	Spleen	Kidney (R)	Kidney (L)	Testis (R)	Testis (L)
Control	6.0 ± 1.0	3.9 ± 0.5	6.8 ± 0.4	41.1 ± 1.9	4.3 ± 0.7	4.0 ± 0.6	3.9 ± 0.7	6.4 ± 0.4	6.9 ± 9.1
FG-3 Treatment									
5 mg/kg	6.9 ± 1.1	4.3 ± 0.66	6.8 ± 0.49	41.2 ± 5.1	4.2 ± 0.57	3.8 ± 0.53	3.9 ± 0.49	5.7 ± 0.52	6.7 ± 0.47
25 mg/kg	6.5 ± 0.47	3.9 ± 0.41	7.3 ± 0.89	39.3 ± 5.9	3.9 ± 0.43	4.0 ± 0.55	3.6 ± 0.61	5.9 ± 0.46	6.1 ± 0.29

Values are mean (x 10⁻³) ± S.D (x 10⁻⁴) (n =5)

DISCUSSION

6. Discussion

As we move ahead into the 21st century we find increasing growth in the integrative medicine which largely incorporates the use of such herbal products which are considered to produce value-addition to the existing therapies. Consequently there is a visible growth in the marketing of such herbal products world over which is largely based on the traditional and folklore use of herbs. In addition continued exploration of herbs as potential sources of new and complex bioactive molecules has added a new dimension, primarily because the conventional single molecule therapy is leading to continuous decline in cure rate especially of chronic indications. One of the most powerful arguments which favor the integrative medicine comes from their synergistic action.

Ayurveda is a widely practiced alternative system of medicine which utilizes variety of herbs. One of the most common features of these therapies is the use of multi-herb compositions containing certain plants which have been suggested to produce synergy and that remains as one of the hallmarks of such indigenous drugs. Bioevaluation of several herbal products from these plants has revealed the mechanism of a number of molecules acting together in an additive, synergistic or antagonistic manner to modify a biological response.

Recently considerable information has also become available with respect to herb-drug interactions. Numerous evidences exist for many documented Ayurvedic herbs which suggest that such interactions could produce potential effects *in-vivo* [124-130]. Prominent among the many effects of these herb-drug interactions is the drug bioavailability alteration. In these context natural products which could facilitate the bioavailability of poorly bioavailable drugs offer great promise.

BIOAVAILABILITY ENHANCING ROLE OF CUMIN/CARAWAY

In the present study an aqueous extract derived from cumin seed caused a significant enhancement of RIF bioavailability in rat. An activity guided fractionation has resulted in identifying a flavonoid glycoside, 3',5-dihydroxyflavone-7-O- β -D-galacturonide-4'-O- β -D-glucopyranoside (FG-3) from a cumin water soluble fraction, which was responsible for this effect.

On the other hand, a herbal fraction, CR-1(1), from caraway seed significantly enhanced the oral bioavailability of all the three anti-TB drugs, viz., RIF, PZA and INH when used in combination. Initially this evaluation was based on a restricted pharmacokinetic study, which included determinations within the reported peak time (1- 4 h) of these drugs [35]. For evaluation purpose the test doses of anti-TB drugs used in rats corresponded with the human doses on the basis of surface area.

The results have revealed a significant pharmacokinetic interaction of the bioactive molecule (FG-3) from cumin and of the bioactive fraction, CR-1(1) from caraway, with anti-TB drugs resulting in altered bioavailability. Assessment of bioavailability from plasma conc.-time data usually involves determining the maximum (peak) plasma drug conc. (C_{max}) and the area under the plasma conc. -time curve (AUC). The plasma drug conc. increases with the rate of absorption; therefore the most widely used general index of absorption is C_{max} . AUC is another reliable measure of bioavailability. It is directly proportional to the total amount of unchanged drug that reaches systemic circulation [5]. A comparison of plasma conc.-time curves showed that a bioactive molecule (FG-3) from cumin increased both the extent and the absorption rate profile of RIF. A similar action of bioactive fraction, CR-1(1) from caraway was also observed with respect to RIF, PZA and INH.

Although an oral route is the most preferred one, the time taken for an orally administered drug to reach the systemic circulation may cause a delay before a clinical effect is observed, and less than the total dose administered reaches the systemic circulation. Various factors reduce the availability of drugs when administered by non-i.v. routes. These include physical properties of the drug (hydrophobicity, pKa, solubility), drug formulation (immediate release, excipients used, manufacturing methods, modified release-delayed release, extended release, sustained release, etc.), fed or fasting conditions, gastric emptying rate, circadian differences, interactions with other drugs/foods, GIT factors, individual variation in metabolic differences, age, gender, disease conditions, phenotypic differences, enterohepatic circulation, and diet patterns.

The extent of systemic bioavailability is described with the pharmacokinetic term bioavailability (F). Absolute bioavailability of a drug is usually determined by comparing bioavailability by oral route against intravenous administration [7, 8]. Therefore absolute bioavailability of the oral dosage form F_{oral} is: $F = \text{AUC}_{\text{oral}}/\text{AUC}_{\text{i.v.}}$

Present investigation has shown that bioactive molecule (FG-3) from cumin enhances the bioavailability of RIF, while the bioactive fraction, CR-1(1) from caraway improves the bioavailability of all the 3 anti-TB drugs (RIF, INH and PZA). This effect was found when RIF alone or in combination with other drugs was used. A recent report has revealed that RIF has only 50% absolute bioavailability in mice [131].

Cumin and caraway seeds are reported to contain a bewildering array of compounds. However, none of these has been related to any specific pharmacological activity, prior to this investigation, in which a flavonoid glycoside from cumin has been found responsible for this specific drug bioavailability enhancing activity.

The occurrence of this molecule (FG-3) was earlier reported in cumin seed [58]. In fact, establishing the molecule-based pharmacological efficacy of herbal medicinal products (HMP) remains a formidable challenge, and since botanicals, by and large, exhibit large variations in content of their natural products, resulting in variable efficacy and medicinal benefits, there is a profound need for standardization of HMPs. The goal of standardization is, therefore, to define an HMP in terms of the identity and content of its active constituent, and such standardized extracts are defined by, and represent, the content or range limit of a chemical constituent (active constituent extract, ACE).

On the other hand chromatographic finger print profiling, as an alternative to standardization, is also acceptable and such standardized extracts are recognized by a marker compound (which may or may not be bioactive) (marker extract, ME). From an ACE, the bioactive moiety may also be isolated and there are several examples where such isolates are treated as a herbal drug (termed as phytopharmaceuticals).

On the other hand for several medicinal herbs no single active constituent is known, or considered a phytopharmaceutical, and the entire extract is treated as active. In the present investigation the bioactive cumin herbal product was found to be an ACE (due to the presence of a phytopharmaceutical, FG-3), whereas bioactive caraway herbal product was found to be a ME (standardized on the basis of a molecule-trifolin).

Tuberculosis remains the leading infectious cause of death in India, killing close to 500,000 people a year. India has far more cases of tuberculosis than any other country in the world — about 2 million new cases each year — and accounts for nearly one third of prevalent cases globally [132].

A fixed drug combination (FDC) comprising of RIF, PZA, and INH is considered frontline therapy. There has been vigorous thrust to tackle the problem of poor/variable bioavailability of RIF. Besides, WHO has also launched a collaborative effort known as “Fixed Dose Combination Project”. Despite this the problem persists. For example, the polymorphic conversion of RIF is further unable to explain as to why a satisfactory dissolution test does not guarantee acceptable RIF bioavailability. There are no reports that specify the particular aspects of GMP, which causes variations to appear. Similarly excipients and other formulation dependent factors have not resulted in satisfactory answers. An account of the problems associated with the poor/variable bioavailability and the approaches to overcome these are summarized in **Section 1 (Introduction)**. In recent studies (2006-2008), many reports further highlight this aspect.

A recent population pharmacokinetic study of rifampin in South African pulmonary tuberculosis patients, showed an interindividual variability to be 52.8 %, for clearance, and 43.4 % for volume of distribution, with possible clinical implications [133].

Drug dosage regimens are determined by two basic parameters, clearance, which determines, the dosage rate to maintain average steady state conc., and volume of distribution which determines, the amount of drug required to achieve a target conc.

Related parameters, the elimination rate constant (ratio of clearance to volume of distribution), and elimination half life ($0.693/k$), control the speed of elimination of drug from the body. They are used to estimate the time taken for a drug to be eliminated from the body and to achieve steady state on multiple dosing.

Present results have shown that in animals receiving RIF, along with FG-3 (bioactive entities from cumin), a decrease in clearance was observed. A similar pattern was also observed in animal receiving RIF, PZA and INH (in combination) along with CR-1(1) (bioactive entities from caraway). These changes along with a longer $t_{1/2}$ in bioactive moieties -treated groups compared to untreated group, suggested, that an increase in the overall rate of drug elimination, is slowed down during the terminal phase, which contribute to the observed enhancement in oral bioavailability.

Earlier it has been found that co-administration of RIF, PZA and RIF + PZA caused a significant decrease in the AUC for INH. Co-administration with PZA caused a significant increase in the AUC for hydrazine metabolite of INH and a decrease in the AUC for its acetylated product acetylhydrazine [134].

In another study co-administration of PZA along with INH caused an increase in the INH distribution volume, $t_{1/2}$ of elimination and clearance, and a decrease in the AUC. Co-administration of RIF along with INH caused an increase in the INH clearance, and a decrease in the AUC. During the concomitant administration of PZA and RIF, the AUC of RIF was decreased while its clearance was increased. The combination INH, PZA, and RIF together caused an increase in the clearance, and a decrease in the AUC of INH. Further, a strong correlation between clearance and volume of distribution has been found to cause substantial variability in bioavailability [134, 135].

There are few reports which describe the time course of the anti-TB drugs, in the animal models: some of the available reports [50, 55, 136, 137] are summarized below for comparison:

ORAL	Animal	Drug	C _{max} µg/ml	AUC _{0-∞} µg.h/ml	t _{1/2} (h)	K _{el} (h ⁻¹)	T _{max} (h)	MRT (h)
Dwivedi et al., 1996 [136]	Rat	RIF	2.30 ± 0.03	18.60 ± 0.14	10.51 ± 0.51	-	6.0	-
Karan et al., 1999 [137]	Rabbit	RIF	5.12 ± 0.14	22.53 ± 2.18	2.45 ± 0.29	0.32 ± 0.004	1.80 ± 0.08	-
Sharma et al., 2004 [50]	Rat	RIF	1.22 ± 0.23	9.7 ± 1.11	4.50 ± 0.53	0.15	2.0	-
		PZA	25.46 ± 1.86	6.23 ± 1.15	6.5 ± 1.43	0.10 ± 0.01	2.0	-
		INH	2.3 ± 1.33	10.99 ± 3.0	3.11 ± 0.53	0.21	2.0	-
Pandey et al., 2004 [55]	Guinea Pigs	RIF	-	7.0 ± 1.4	-	-	-	5.8 ± 1
		PZA	-	180 ± 15	-	-	-	72 ± 1
		INH	-	7.1 ± 1.1	-	-	-	5.0 ± 1

** Detailed parameters (software analysis) of the present investigation is appended as Annexure IV.*

POSSIBLE MODES OF ACTION OF BIOACTIVE MOIETIES OF CUMIN/CARAWAY

When a drug is administered orally, its fate is usually described in the following manner: the drug comes into contact with the contents of the gastrointestinal (GI) system, undergoes dissolution process, and then comes into contact with intestinal epithelium. It is then absorbed through the gut wall (via enterocytes lining the jejunum and ileum), and transported by the portal veins through the liver, before reaching the systemic circulation and parts of the body. When the same drug is given i.v. route, it enters the systemic circulation and is distributed throughout the body before reaching the liver for the first time. The important difference between these two modes of administration lies in the presystemic fate of the drug. The incomplete bioavailability after oral administration may principally be a result of (1) incomplete absorption from the intestine, or (2) metabolism of the drug, before it reaches the systemic circulation (presystemic metabolism).

MODULATION OF INTESTINAL PERMEATION/EFFLUX PROPERTIES

Systemic bioavailability of orally administered drugs has been considered primarily a function of physical drug absorption. The intestine particularly the small bowel represents a large surface through which a vigorous substrate exchange takes place across lumen and the blood stream in both the directions (intestinal permeation). The luminal surface of the intestine is lined with a 'leaky' epithelium, through which simple or carrier-mediated diffusion and active transport occurs. The 'intestinal permeation' determines the bioavailability of drugs and contributes significantly to the pharmacokinetics of xenobiotics. The intestinal epithelium thus presents a formidable barrier restricting the drug transport. It is now appreciated that P-glycoprotein (P-gp) also plays a major role in transporting variety of diverse substrates. P-gp is functionally expressed in the enterocytes that border the epithelium of the intestinal tract, where it plays an important role as a biochemical barrier. P-gp has been shown to limit the bioavailability of several drugs belonging to different classes.

An accurate intestinal permeability for drugs is difficult to directly study in humans. There are various transport mechanisms like simple diffusion, specific transport mechanisms such as carrier mediation via facilitated diffusion, exchange diffusion (countertransport), or the active transport. Simple physicochemical measurements to predict the ability of a drug molecule to cross the intestinal barrier are also not sufficient indices. Therefore a number of *in-vitro* and animal-derived experimental models are used which determine the intestinal absorptive potential of a drug and the mechanism of absorption. The intestine is well known for its myriad of functions- absorption, metabolism, and exsorption. Several *in-vitro* and *in-situ* experimental models used in predicting the absorption of drugs *in vivo* are available.

In the present investigation the effect of the bioactive molecule (FG-3) from cumin and the bioactive fraction, CR-1(1) from caraway, have been investigated at different levels of tissue integration: in the whole animal with the intestine *in-situ*, in the isolated gut sac (jejunal), in isolated epithelial cells (enterocytes), and in isolated membrane preparations from the jejunum. The *in-situ* model was validated by using Verapamil, a known inhibitor of intestinal P-gp function [138] and it has also been used as a standard reference in benzopyrene uptake assay (in guinea pig epithelial cell model).

The everted gut sac technique was first described by Wilson and Wiseman [139]. The principle advantage of this technique is that it exposes a large absorptive surface (the mucosal cells) to a relatively large volume of well-oxygenated and mixed nutrient medium. The reproducibility of this *in-vitro* model has made it a very useful method to compare the transport kinetics of a drug in the absence or the presence of a potential modifier. In gut sac, drug transport relates closely to the human absorption profile, since it represent a model of 'leaky' epithelia and is considered more indicative of *in-vivo* intestinal absorption [121]. In this model the bioactive molecule (FG-3) from cumin caused the rate of RIF absorption to increase which seemed due to an enhanced mucosal-to-serosal permeation of the drug. Moreover the observed increase in P_{app} sustained for a relatively longer period (upto 4 h after its oral administration), suggested a modification of permeability property of the intestine. In similar *ex-vivo* experiments, a permeation enhancing property of the bioactive fraction, CR-1(1) of caraway was also revealed, which resulted into an increase in P_{app} and also modification in the absorption mechanism of all the 3 drugs, RIF, INH and PZA into a non-saturable transport system (as depicted in **Section 5.3.3**), could contribute to enhanced intestinal permeation. Intestinal permeation refers to the

process of passage of various substances across gut wall, either in absorptive or efflux direction. 'Permeability' is the condition of the gut which governs the rate of this complex two-way process [10]. The enhanced bioavailability of anti-TB drugs could thus be related to an enhanced intestinal permeability.

Experimentally a gut sac is also considered to be a useful screening tool for studying P-gp mediated efflux [140]. In this context the observed effect of bioactive moieties seemed to be a sum of not only of its absorption enhancing effect but also to efflux inhibition effect. More direct evidences for efflux inhibition are discussed later. Earlier reports have also showed involvement of both i.e., an efflux-mediated, as well as, a saturable absorption mechanism for RIF in rat intestine using the everted sac [141]. In this study it was shown that RIF permeability was decreased in jejunum and ileum with an increase in residence time. The permeation of RIF from the serosal to the mucosal side (efflux) was significantly higher than permeation from the mucosal to the serosal side (absorption) of jejunum and ileum. Our findings corroborate this for the involvement of efflux-mediated and saturable absorption mechanisms of RIF in rat intestine, which act as barriers to the absorption of the drug. This explains the drug's poor absolute bioavailability. As P-gp varies from person to person to (2-8-fold), it can be one direct reason for the interindividual variable bioavailability shown by RIF [141]. In a clinical report, bioavailability of RIF and INH have been found to be significantly lower in TB patients due to a decrease in the functional absorptive area of the intestine in patients, causing reduced serum conc. of anti-TB drugs [142].

In further experiments the bioactive molecule from cumin, FG-3 was investigated for its possible influence on the P-gp mediated mechanism. For this purpose three probes were used. These were Rho123, RIF and benzopyrene. Rho123 is a P-gp substrate and is a typical probe to assess *in-vitro* and *in-vivo* P-gp function

[143]. RIF is a well known substrate and also an inducer of P-gp. It upregulates P-gp function in intestine after oral administration. In fact, transport of RIF by P-gp is an important element in drug activity, and variation in human expression of P-gp contributes to individual variability in RIF disposition [144, 145]. The effect of bioactive molecule FG-3 from cumin on the P-gp mediated efflux of Rho123 and RIF was investigated in an *in-situ* model.

In-situ single pass perfusion technique has generally been accepted for estimating intestinal absorption and has been suggested to produce a profile closer to oral administration. Here a compound of interest is monitored in perfusate and loss of compound (difference between inlet and outlet conc.) is attributed to permeability. Several studies have shown that the extent of absorption in humans can be predicted from single-pass intestinal perfusion technique in rat and this has shown most constant absorption rate, and also a good correlation with human data [146]. In the present investigation this model was validated by using verapamil. Verapamil is a known inhibitor of mammalian intestinal P-gp function [138]. The results have shown that bioactive molecule FG-3 from cumin, inhibited the P-gp function as evidenced by a reduced intestinal exsorption clearance and intestinal exsorption rate of Rho123. Further in this experiment, RIF was found to stimulate the P-gp function, but in presence of FG-3, RIF efflux remained inhibited. The effect of FG-3 was found to be reversible. In a primed rat model, pre-exposure of FG-3 for duration of 6 days did not modulate P-gp function, suggesting that FG-3 was not effective at the expressional level of P-gp. Therefore a direct interaction of FG-3 with this protein may be anticipated. It may be mentioned here that an increase in bioavailability indices were also found to occur without any lead-time when FG-3 was administered in pre-mixed combination with RIF.

Another probe molecule, benzopyrene transport is also reported to be regulated by P-gp [119, 147]. The effect of bioactive molecule FG-3 from cumin on the P-gp - mediated transport of benzopyrene was investigated in isolated guinea pig epithelial cells. Isolated intestinal mucosal cells have the advantage of a preparation consisting of the cells which are primarily involved in intestinal transport, and free from the other functionally inert living material. In these experiments, FG-3 enhanced the accumulation of benzopyrene by the cells, thus further highlighting its P-gp inhibitory role.

Subsequently, direct evidence was also obtained by the inhibition of P-gp-dependent ATPase activity. P-gp is an unusual ATP-driven transporter, in that it has a low affinity for ATP and exhibits a high level of constitutive or basal ATPase activity. This protein has 12 transmembrane domains contained in two homologous halves and two ATP-binding cassette domains in each half that catalyze ATP hydrolysis. One characteristic of this protein is that it couples binding and hydrolysis of ATP at the two nucleotide-binding domains to drug export by transmembrane domains. Therefore ATP hydrolysis happens to be an inherent property of P-gp. P-gp-dependent ATPase assay is a widely used *in-vitro* method to investigate the affinity of a substance for P-gp, since one interesting property of this enzyme is its vulnerability to stimulation or inhibition by a variety of chemotherapeutic agents, natural products and other xenobiotics, suggesting that there exists some type of communication, or coupling, between drug-binding sites, which are believed to reside within transporter domains of the membrane. Transport activity of P-gp is related to the amount of inorganic phosphate (Pi) that gets liberated upon hydrolysis of ATP so that this assay is able to distinguish a substrate from an inhibitor. P-gp ATPase is sensitive to vanadate, a phosphate analogue which inhibits its hydrolytic activity by forming a

complex with MgADP at catalytic site that resembles the pentacovalent phosphorus of chemical transition state. With the use of three ionic pump inhibitors, ouabain (an inhibitor of Na⁺/K⁺-ATPase), sodium azide (an inhibitor of F₀-F₁ ATPase), and EGTA (an inhibitor of Ca⁺⁺-ATPase), remaining ATPase could therefore be attributed to P-gp (cross references cited in our published paper [148]). Using this assay, a prominent inhibitory action of FG-3 on P-gp dependent ATPase could be demonstrated in isolated jejunal membrane preparations.

The experimental evidences presented above suggest that modulation of P-gp, as a limiting factor could overwhelmingly contribute in the bioavailability enhancing action of identified natural products (cumin molecule and the caraway fraction), is supported by the increasingly recognized view that P-gp efflux has a key influence on the pharmacokinetics of therapeutic agents, responsible for the low oral bioavailability [149, 150] and inhibition of P-gp activity has been considered an effective way and a useful strategy to enhance the oral bioavailability [151].

Though P-gp, as an active secretion system or as an absorption barrier [149-151] remains one of the most important factors for limiting bioavailability, but the issue of passive drug permeability also merits consideration, since absorption of majority of xenobiotics is largely facilitated by passive diffusion. In addition, P-gp efflux from the cell also competes with passive trans-membrane drug influx [152]. Consequently the inhibition of secretory transport (from the enterocyte back into the intestinal lumen) may increase permeation in the absorptive direction.

To clarify whether FG-3 affects non-carrier mediated drug absorption in the intestine, we used PAMPA (Parallel artificial membrane permeation assay). PAMPA is a sophisticated approach utilizing an inert membrane supporting a lipid bilayer. PAMPA shows definite trends in the ability of molecules to permeate membranes by

transcellular passive diffusion, and has been considered a useful prescreen test to demonstrate the ability of molecules to permeate membranes by passive diffusion [153]. The results however showed that FG-3 did not modify passive transport pattern of RIF in this assay.

Generally absorption has been considered as a major determinant of oral bioavailability. Taken together the results of this investigation suggested that while the bioactive molecule from cumin i.e., FG-3 promoted active transport and inhibited P-gp mediated efflux absorption, the bioactive fraction CR-1(1) from caraway principally enhanced the intestinal permeability. A direct effect of spices with epithelial cells is reported to affect the transport of ions and macromolecules. There are evidences which suggested that spice principles interact with enterocytes to modulate their properties [154]. Capsaicin and piperine have been found to alter intestinal drug absorption process which is mainly facilitated by passive diffusion and/or paracellular permeation [155, 156].

Further, this effect was not due to cytotoxicity. This was ascertained by measuring the release of tissue proteins from the intestinal mucosa, which was used as an index to assess tissue damage. FG-3 and CR-1(1) were not found to be associated with any mucosal toxicity or cell membrane damage. Earlier a large number of substances like surfactants, bile salts, chelating agent and fatty acids have been explored as absorption enhancers. However many such agents were found to have a narrow safety margin due to membrane damaging effects, highlighting a requirement for non-toxic permeation enhancers [1].

In a related study orally administered cumin/caraway bioactive moieties did not show any sub-acute toxicity in rats.

MODULATION OF CYP 3A4 FUNCTION

The desired therapeutic plasma levels of orally administered drugs are dependent not only on adequate intestinal absorption, but also on the extent of first pass effect. As mentioned above one another reason that has been proposed for the incomplete bioavailability after oral administration is the metabolism of the drug before it reaches the systemic circulation (presystemic metabolism). The expression 'first pass metabolism' refers to the metabolism that an ingested compound undergoes in its passage through the gut and liver before reaching the systemic circulation. It is useful concept for a drug because it provides information about the relative therapeutic effect of an orally administered drug relative to its i.v. dose (absolute bioavailability). The most versatile enzyme involved in first pass effect is CYP 3A4. The clinical significance of wide variations in CYP 3A4 are recognized as major effects on drug efficacy, drug toxicity, and hence therapeutic outcome. Marked inter-individual variability in plasma conc. of drugs after administration of a fixed dose is often related to differences in drug metabolism. Although liver is the major site for a pre-systemic metabolism, CYP 3A4 is present both in hepatocytes and enterocytes, and demonstrated to be identical. In enterocytes members of the 3A subfamily constitute greater than 70 % of the cytochrome containing enzymes.

In 1972, Herbert Remmer at the University of Tübingen was the first to describe that total human hepatic CYP 450 was markedly elevated by the new anti-TB drug RIF. These early studies, in the 1970s in Tübingen, were followed by further developments. It was realized that the cytochrome P450 isoenzyme 3A4 (CYP 3A4) is the major CYP isozyme in the human liver, metabolizing a variety of xenobiotics and endobiotics. Besides RIF is one of the most potent inducers of human CYP 3A4 gene expression. These so-called pregnane X receptors (PXR), across species, are

activated by inducers of CYP 3A4 expression. It now appears that PXR is a key mediator of complex induction processes of xenobiotic processing enzymes, which are triggered by RIF. RIF is also a nonspecific inducer of metabolism of a number of drugs and is reported to cause therapeutic failure of other co-administered drugs by modifying their pharmacokinetics. It accelerated metabolism of testosterone resulting in 6- β -hydroxylation [157].

RIF, a macrocyclic antibiotic, is a well known inducer of CYP 3A4, which is suggested to lead to auto-induction and consequently low oral bioavailability [158]. P-gp is also a major determinant of RIF-inducible expression of CYP 450 3A [159]. In TB patients showing poor bioavailability, for RIF, administration of a P-gp /CYP 3A4 blocker has resulted in enhanced RIF level suggesting a pivotal role for over-expression of P-gp/CYP 3A4 in the absorption of RIF, which may be responsible for lower or variable levels of RIF [145].

P-gp and CYP 3A4 are reported to act in concert to limit oral drug bioavailability by several mechanisms. Co-localization of P-gp and CYP 3A4 in the epithelium of the gastrointestinal tract is a recognized barrier regulating oral bioavailability. In many experimental and clinical studies application of P-gp/CYP 3A4 dual inhibitors have been shown to be a useful strategy to enhance drug bioavailability. Besides, P-gp has also been hypothesized to modulate intestinal drug metabolism by increasing the exposure of drug to intracellular CYP 450 enzymes through repeated cycles of drug absorption and efflux [149, 150, 160, 161].

Erythromycin N-demethylation and testosterone 6- β hydroxylation are *in-vitro* probes of CYP 3A4 catalytic activity. Present investigation has shown that FG-3 inhibited these enzyme activities in liver microsomes. In these experiments piperine, a known inhibitor of P-gp/CYP 3A4 has been used as standard reference [162]. A

synergistic effect of the two proteins P-gp/CYP 3A4, may reduce the intestinal absorption of dual P-gp/CYP 3A4 substrates like RIF, since the activity of P-gp antiporter is co-regulated with CYP 3A4 enzyme [160]. In this respect, potential inhibitory role of cumin/caraway active moieties could possibly contribute in the reduction of the barrier functions of the intestine, thus elevating the plasma conc. of anti-TB drugs. Role of metabolic enzymes and efflux transporters in the absorption of drugs from small intestine is well documented event [163]. A vast literature also shows that natural products interact with drugs by affecting the biological processes that regulate their absorption via P-gp function and metabolism via CYP 3A4 [164-166].

FG-3 is a flavonoid glycoside. Besides the bioactive fraction CR-1(1) from caraway also contains several such compounds. Flavonoids are widely distributed throughout plants and are known to have a wide range of biochemical and pharmacological effects; for example they inhibit oxidative drug metabolism and P-gp function [167]. In earlier reports many of these constituents especially bioflavonoids have shown a clinically meaningful interactions with CYP-mediated metabolism or P-gp-mediated efflux or both to affect the pharmacokinetic behavior of several drugs. A coordinate modulation of both these proteins by several herbs and/or their constituents are also reported in animals and human volunteers: some examples of herbs are: *Curcuma longa*, *Citrus aurantium* (Seville orange), *Hydrastis Canadensis* (Golden seal), *Gingo biloba*, *Echinacea purpurea*, *Allium sativum* (garlic), *Crataegus oxycantha* (hawthorn), *Panax ginseng* (ginseng), grapefruit juice, *Camellia sinensis* (green tea), *Silybum marianum* (milk thistle), *Hypericum perforatum* (St. John's wort), *Piper nigrum* and *Piper longum* (Black peppers), *Rosemarinus officinalis* (rosemary) and others: some examples of herbal constituents

are: quercetin, naringenin, bergamottin, green tea polyphenols, catechins, biochanin A, morin, phloretin, silybin and silymarin, kaempferol, apigenin, hyperforin, gingenoside, genistein, and berberin etc. [124, 168]. It has been documented that flavonoid-mediated inhibition of P-gp and other ATP binding cassette (ABC) transporters affect the bioavailability of drugs [169].

CONCLUDING REMARKS

In conclusion this investigation has shown that absolute bioavailability (AB) of RIF in presence of PZA + INH was lower by 24 %, than the AB of RIF when given alone. However the AB of RIF increased by 52 % in presence of some herbal products and a flavonoid glycoside isolated from cumin. The glycoside molecule from cumin also enhanced the AB of RIF in combination with PZA + INH by 57 %. On the other hand another herbal product from caraway, enhanced the relative bioavailability of all the 3 drugs (RIF, INH and PZA).

The active flavonoid glycoside isolated from cumin was identified as 3',5-dihydroxyflavone-7-O- β -D-galacturonide-4'-O- β -D-glucopyranoside (FG-3). A potential inhibitory role of FG-3 on the two proteins, P-gp/CYP 3A4, along with its potentiation of intestinal permeability were identified as possible mechanisms of action of the molecule. On the other hand the main effect of herbal product from caraway was its ability to modulate intestinal permeation property. Thus the overall improvement in the bioavailability of the anti-TB drugs in presence of the identified moieties could be related to their absorption enhancing profile, while preventing their

inactivation, during transit from intestine to the systemic circulation through the liver. The bioactive herbal moiety from caraway was not found to significantly modulate P-gp/CYP 3A4 activity (data not included). An orally administered FG-3 and CR-1(1) at their bioeffective doses or at 5 times higher doses did not show any adverse effect in a sub-acute and a sub-chronic toxicity study in wistar rats.

These findings could be of profound clinical relevance with a possibility of their application as an adjunct to drug therapy. The use of bioavailability enhancers of herbal origin seem to offer a significant advantage, in the development of reformulated drug dosage regimen, for their improve bioavailability profile: the bioenhancers of herbal origin offer significant advantage precluding toxicity concerns, since such medicinal/culinary herbs-derived bioactive products have long tradition of human use.

Bibliography

- [124] Zhou S., Lim L. Y., Chowbay B. Herbal modulation of P-glycoprotein. *Drug metabolism and Disposition*. 2004, 36: 1-48.
- [125] Bhattaram V.A., Graefe U., Kohlert C., Veit M., Derendorf. Pharmacokinetics and bioavailability of herbal medicinal products. *Phytomedicine*. 2002, 1-33.
- [126] Barnes J. Herbal interactions. *The Pharmaceutical Journal*. 2003, 270: 118-121.
- [127] Haller C.A. Clinical approach to adverse events and interactions related to herbal and dietary supplements. *Clinical toxicology*. 2006, 44: 605-610.

- [128] Fugh-Berman A., Ernst E. Herb-drug interactions: review and assessment of report reliability. *British Journal of Clinical Pharmacology*. 2001, 52: 587–595.
- [129] Izzo A.A. Herb-drug interactions: an overview of the clinical evidence. *Fundamental Clinical Pharmacology*. 2005, 19: 1-16.
- [130] Ioannides C. Pharmacokinetic interactions between herbal remedies and medicinal drugs. *Xenobiotica*. 2002; 32: 451–478.
- [131] Mariapan T.T., Singh S., Pandey R., Khullar G.K. Determination of absolute bioavailability of rifampicin by varying the mode of intravenous administration and the time of sampling. *Clinical research and regulatory affairs*. 2005, 11: 119-128.
- [132] Khatri G.R. Controlling tuberculosis in India. *The New England Journal of Medicine*. 2002, 347: 1420-1425.
- [133] Wilkins J.J., Savic R.M., Karlsson M.O., Langdon G., McIlleron H., Pillai G.C., Smith P.J., Siminsson U.S. Population pharmacokinetics of rifampin in pulmonary tuberculosis patients including a semi-mechanistic model to describe variable absorption. *Antimicrobial Agents and Chemotherapy*. 2008: Online April 7.
- [134] De Rosa H.J., Baldan H.M., Brunetti I.L., Ximenes V.F., Machado R.G. The effect of pyrazinamide and rifampicin on isoniazid metabolism in rats. *Biopharmaceutics and Drug Disposition*. 2007, 28: 291-296.
- [135] Jain A., Mehta V.L., Kulshreshtha S. Effect of pyrazinamide on rifampicin kinetics in patients with tuberculosis. *Tuberculosis and Lung Disease*. 1993, 74: 87-90.

- [136] Dwivedi A., Rastogi R., Singh S., Dhawan B.N. Effect of picroliv on the pharmacokinetics of rifampicin in rats. *Indian Journal of Pharmaceutical Sciences*. 1996, 58: 28-31.
- [137] Karan R.S., Bhargava V.K., Garg S.K. Effect of Trikatu, an Ayurvedic prescription, on the pharmacokinetic profile of rifampicin in rabbits. *Journal of Ethnopharmacology*. 1999, 64: 159-264.
- [138] Paul-Magnus C., Von Richter O., Burk O. Characterization of the major metabolites of Verapamil as substrates and inhibitors of P-glycoprotein. *Journal of Pharmacology and Experimental Therapeutics*. 2000, 293: 376-382
- [139] Wilson T.H., Wiseman G. The use of sacs everted of small intestine for study of transference of substance from mucosal to serosal surface. *The Journal of Physiology*. 1954, 123: 116-125.
- [140] Carrino-Gomez B., Duncan R. Everted rat intestinal sacs: a new model for the quantitation of P-glycoprotein mediated-efflux of anti-cancer agents. *Anticancer Research*. 2000, 20: 3157-3161.
- [141] Mariappan T.T., Singh S. Evidence of efflux-mediated and saturable absorption of rifampicin in rat intestine using the ligated loop and everted gut sac techniques. *Molecular Pharmacology*. 2004, 1: 363-367.
- [142] Pinheiro V.G., Ramos L.M., Monteiro H.S., Barroso F.C., Bushen O.Y., Facanha M.C., Peloquin C.A., Guerrant R.L., Lima A.A. Intestinal permeability and malabsorption of rifampin and isoniazid in active pulmonary tuberculosis. *Brazilian Journal of Infectectious Disease* . 2006,10:374-379.
- [143] Kageyama M., Fukushima K., Togawa T., Fujimoto K., Taki M., Nishimura A., Ito Y., Sigioka N, Shibata N., Takada K. Relationship between excretion clearance of rhodamine 123 and P-glycoprotein inducers (Pgp) expression induced by representative Pgp inducers. *Biological and Pharmaceutical Bulletin* 2006. 29: 779-784

- [144] Rae J.R., Johnson M.D., Lippman M.E., Flockhart D.A. Rifampicin is a selective pleiotropic inducer of drug metabolism genes in human hepatocytes: studies with cDNA and oligonucleotide expression arrays, *Journal of Pharmacology and Experimental Therapeutics*. 2001, 299: 849-857.
- [145] Prakash J., Velpandian T., Pande J.N., Gupta S.K. Serum Rifampicin Levels in Patients with Tuberculosis : Effect of P-Glycoprotein and CYP3A4 Blockers on its Absorption. *Clinical Drug Investigation*. 2003, 23: 463-472.
- [146] Zakeri-Milania P., Valizadeha H., Tajerzadehc H., Azarmia Y., Islambolchilara Z., Barzegara S., Barzegar-Jalalia M. Predicting Human Intestinal Permeability using Single-pass Intestinal Perfusion in rat. *Journal of Pharmacy and Pharmaceutical Science*. 2007 ,10(3) : 368-379.
- [147] Yeh G.C., Lopaczynska J., Poore C.M., Phang J.M. A new functional role of P-glycoprotein: efflux pump for benzo(alpha) pyrene in human breast cancer MCF-7 cells. *Cancer Research*. 1992, 52: 6692-6695.
- [148] Najar I.A., Sachin B.S., Sharma S.C., Satti N.K., Suri K.A., Johri R.K., Modulation of P-glycoprotein ATPase activity by some phytoconstituents. *Phytotherapy Research*. 2009, 24: 454-458.
- [149] Benet L.Z., Cummins C.L. The drug-efflux alliance: Biochemical aspects. *Advanced Drug Delivery Reviews*. 2001, vol: S3-S11.
- [150] Wacher V.J., Salpheti L., Benet L.Z. Active secretion and enterocyte drug metabolism barriers to drug absorption. *Advanced Drug Reviews*. 2001, 46: 89-102.
- [151] Stephans R.H., Neill C.A., Bennet J., Humphrey M., Henry B., Rowland M, Warhurst G. Resolution of P-glycoprotein and non-P-glycoprotein effects on drug permeability using intestinal tissues from *mdr 1a (-/-)* mice. *British Journal of Pharmacology*. 2002, 135: 2038-2046.

- [152] Tolle-Sander S., Jarkko R., Wring S., Polli J.W., Polli J.E. Midazolam exhibits characteristics of a highly permeable P-glycoprotein substrate. *Pharmaceutical Research*. 2003, 20: 757-764.
- [153] Fearn R.A., Hirst B.H. Predicting oral drug absorption and hepatobiliary clearance: Human intestinal and hepatic in vitro cell models. *Environmental Toxicology and Pharmacology*. 2006, 21: 168–178.
- [154] Jensen-Jarolim E., Gajdzik L., Haberl I., Kraft D., Scheiner O., Graf J. Hot spices influence permeability of human intestinal epithelial monolayers. *Journal of Nutrition*. 1998, 128: 577-581.
- [155] Komori Y., Aiba T., Nakai C., Sugiyama R., Kawasaki H., Kurosaki Y. Capsaicin-Induced Increase of Intestinal Cefazolin Absorption in Rats, *Drug Metabolism and Pharmacokinetics*. 2007, 22: 445–449.
- [156] Johri R.K., Thusu N., Khajuria A., Zutshi U. Piperine-mediated changes in the permeability of rat intestinal epithelial cells. The status of γ -glutamyltranspeptidase activity, uptake of amino acids and lipid peroxidation. *Biochemical pharmacology*. 1992, 43: 1401-1407.
- [157] Lamba J., Strom S., Venkataramanan R., Thummel K.E., Lin Y.S., Liu W., Cheng C., Lamba V., Watkins P.B., Schuetz E. MDR1 genotype is associated with hepatic cytochrome P450 3A4 basal and induction phenotype. *Clinical Pharmacology and Therapeutics*. 2006, 79: 325-338.
- [158] Magnarin M., Morelli M., Rosati A., Bartoli F., Candussio L., Giraldi T., Decorti G. Induction of proteins involved in multidrug resistance (P-glycoprotein, MRP1, MRP2, LRP) and of CYP 3A4 by rifampicin in LLC-PK₁ cells. *European Journal of Clinical Pharmacology*. 2004, 483:19-28.
- [159] Ehret M.J., Levin G.M., Narashimhan M., Rathinavelu A. Venlafaxine induces P-glycoprotein in human Caco-2 cells. *Human Psychopharmacology*. 2007, 22: 49-53.

- [160] Cummins C.L., Jacobson W., Benet L.Z. Unmasking the Dynamic Interplay between Intestinal P-Glycoprotein and CYP 3A4. *Journal of Pharmacology and Experimental Therapeutics*. 2002, 300: 1036-1045.
- [161] Kivisto K.T., Niemi M., Fromm M.F. Functional interaction of intestinal CYP 3A4 and P-glycoprotein. *Fundamental and Clinical Pharmacology*. 2004, 18: 621- 626.
- [162] Bhardwaj R.K., Glaeser H., Becquemont L., Klotz U., Gupta S.K., Fromm M.F., Piperine, a major constituent of black pepper, inhibits human Pgp and CYP 3A4. *Journal of Pharmacology and Experimental Therapeutics*. 2002, 302: 645-650.
- [163] Watkins P.B. The barrier function of CYP 3A4 and P-glycoprotein in the small bowel, *Advanced Drug Deliver Reviews*. 1997, 27: 161-170.
- [164] Marchetti S., Mazzanti R., Beijnen J.H., Schellens J.H.M. Concise review: clinical relevance of drug-drug and herb-drug interactions mediated by the ABC transporter ABCB1 (MDRI, P-glycoprotein). *The Oncologist*. 2007, 12: 927-941.
- [165] Pal D., Mitra A.K. MDR- and CYP 3A4-mediated drug-herbal interactions. *Life Sciences*. 2006, 78: 2131-2145.
- [166] Venkataramanan R., Komoroski B., Strom S. In vitro and in vivo assessment of herb drug interactions. *Life Sciences*. 2006, 78: 2105-2115.
- [167] Yoo H.H., Lee M., Chung H.J., Lee S.K., Kim D.H. Effect of Diosmin, a flavonoid glycoside in citrus fruits, on P-glycoprotein-mediated drug efflux in human intestinal caco-2 cells. *Journal of Agricultural and Food chemistry*. 2007, 55: 7620-7625.

- [168] Deferme S., Augustijns P. The effect of food components on the absorption of P-gp substrate: a review. *Journal of Pharmacy and Pharmacology*. 2003. 55: 153-162.
- [169] Brand W., Schutte M.E., Williamson G., Van Zanden J.J., Cnubben N.H.P., Groten J.P., Van Bladeren P.J., Rietjens I.M.C.M. Flavonoid-mediated inhibition of intestinal ABC transporters may affect the oral bioavailability of drugs, food-borne toxic compounds and bioactive ingredients. *Biomedicine and Pharmacotherapy*. 2006, 1-12.

CONCLUSION

7. Conclusion

A fixed dose combination (FDC) comprising of rifampicin (RIF), isoniazid (INH) and pyrazinamide (PZA) is considered frontline therapy for tuberculosis. However RIF shows poor/variable oral bioavailability especially when administered in combination with INH and PZA. In the present investigation some herbal products from cumin/caraway and a herbal phytochemical derived from cumin seeds are proposed as novel drug bioavailability bioenhancers.

This investigation has shown that absolute bioavailability (AB) of RIF in presence of PZA + INH was lower by 24 %, than the AB of RIF when given alone. However the AB of RIF increased by 52 % in presence of some herbal products and a flavonoid glycoside isolated from cumin. The glycoside molecule from cumin also enhanced the AB of RIF in combination with PZA + INH by 57 %. On the other hand another herbal product from caraway enhanced the relative bioavailability of all the 3 drugs (RIF, INH and PZA).

There are overwhelming evidence to suggest that CYP 450 3A4 and P-gp are the major biochemical regulators of absorption and disposition of many compounds. Both these proteins are co-localized in intestinal absorptive cells (enterocytes) and act in concert to limit oral drug bioavailability. Thus, inhibition of these proteins has been regarded as a useful strategy to improve bioavailability of drugs which are given by oral route. RIF is a well know inducer of P-gp/CYP 3A4 and accelerates its own metabolism. Besides RIF also exhibits efflux-mediated and saturable absorption in the intestine.

The results of the present investigation have shown that some herbal products from cumin enhance the rat plasma levels of co-administered RIF (alone or in presence of INH + PZA). An activity guided fractionation has resulted in locating this

activity in a flavonoid glycoside, namely, 3',5'-dihydroxyflavone-7-O- β -D-galacturonide-4'-O- β -D-glucopyranoside. In this investigation caraway seed was also investigated, since it bears a phylogenetic relationship with cumin. The herbal products from caraway enhanced the rat plasma levels of all the 3 anti-TB drugs when given in combination. The active bioactive fraction of caraway was standardized on the basis of the presence of 0.35% (v/v) trifolin (kaempferol glycoside).

In order to arrive at these observations, the work components included (a) development of S.O.P for the determination of anti-TB drugs (alone and in combination) by HPLC (b) solvent extraction to make herbal products, (c) activity guided fractionation (d) finger print profiling of active herbal moieties (e) optimization of in vitro and animal-derived protocols for investigating the passive and active transport/ P-gp function/CYP 3A4 enzymes. The models included in these studies were intestinal everted gut sac, intestinal single pass in situ perfusion, and guinea pig epithelial cells to determine transport of P-gp mediated active efflux of RIF. The probe molecules (P-gp substrates) used was RIF, Rho123 and ^3H -benzopyrene. For comparison known inhibitors like piperine/verapamil were used. Rat liver microsomes were used for CYP 3A4 enzyme activities (testosterone hydroxylase/erythromycin demethylase). Rat intestinal membranes were used for P-gp dependent ATPase activity.

The results showed that bioactive moieties modulated these cellular events in rat intestine/liver. A plasma conc. vs. time curves for the drugs alone and in presence of isolated molecule from cumin/herbal products from caraway showed a meaningful pharmacokinetic interaction, resulting in the enhancement of bioavailability indices (C_{max} /AUC) of RIF when used alone or in combination with other two drugs, INH and PZA.

In conclusion it may be suggested that observed increase in RIF bioavailability, by the herbal products from cumin/caraway and a flavonoid glycoside from cumin could be via enhancement of its intestinal absorption, prevention of rapid efflux, and rapid degradation via CYP mediated Phase I metabolism, during its transit from intestine to the systemic circulation through the liver. The bioactive moieties have not shown any mucosal toxicity. In acute, sub-acute and sub-chronic toxicity study, no adverse effects of FG-3 (cumin molecule) were observed.

SPECIFIC CONTRIBUTION

Specific Contribution of the Present Work

Poor/variable bioavailability of clinically important drugs has remained an area of major concern, which has drawn enormous attention. There have been continued efforts to find the pharmaceutical strategies in order to overcome this problem.

The present investigation presents a pharmacological approach, whereby some herbal/natural products derived from reputed Indian spice/medicinal herbs, namely, *Cuminum cyminum* (white jeera), and *Carum carvi* (black jeera), showed the ability to enhance the bioavailability of rifampicin.

The identified herbal/natural products from these herbs have shown a significant interaction with key biochemical regulators of oral bioavailability, resulting in meaningful pharmacokinetic modulation of the drug.

The use of herbal/natural bioenhancers has a profound role in the development of reformulated regimen of drugs, such as rifampicin, and others, which present poor/variable bioavailability.

FUTURE SCOPE

Future scope of the work

The present piece of work is the part of plant based bioenhancer screening programme of IIIM, Jammu wherein the extracts/fractions/sub-fractions/pure isolates of cumin and caraway found to enhance the rifampicin bioavailability when co-administered. The possible mode by which these materials act as bioenhancer for rifampicin is also established. The pre-clinical toxicity studies showed sufficient evidences that these materials are non-toxic.

The future scope of work includes the following work components

- A. Rifampicin dose reduction studies and pre-clinical bio-equivalence studies using drug and promising material of cumin and caraway so as to minimize the toxicity events.
- B. Pharmacokinetic studies of promising material of cumin (FG-3).
- C. Long term (chronic) toxicity studies of promising materials of cumin and caraway.
- D. Formulation development studies of rifampicin and promising materials of cumin and caraway including stability studies.
- E. In future, the effect of promising material(s) on the bioavailability of the rifampicin can be assessed in healthy human volunteers as the material(s) is a dietary constituent and is being used as spice since long. The efficacy/safety of the said material(s) can be re-established/studied in healthy humans.

APPENDICES

Annexure I
US Patents on the use of drug bioavailability enhancers

Sr.	Year	Title	No.	Inventors
1	2008	Anti-first- pass effect compounds	7,378,534	Harris et al.
2	2007	Use of bioactive fraction from cow urine distillate (Gomutra) as a bio-enhancer of anti-infective, anti-cancer agents and nutrients	7,235,262	Khanuja et al.
3	2007	Antibiotic pharmaceutical composition with lysergol as bio-enhancer and methods of treatment	2007/ 0060604	Khanuja et al.
4	2007	Anti-first pass effect compound	7,230,027	Harris et al.
5	2007	Cytochrome P450 3A inhibitors and enhancers	7,169,763	Hu et al.
6	2006	Method , composition and kits for increasing the oral bioavailability of pharmaceutical agents	7, 041,640	Broder et al.
7	2006	Method of improving bioavailability of orally admin. drugs, a method of screening for enhancers of such bioavailability and novel pharmaceutical com-positions for oral delivery of drugs	7, 030,132	Schellens et al.
8	2005	Composition comprising pharmaceutical /Nutraceutical agent and a bioenhancer obtained from <i>Glycyrrhiza Glabra</i>	6,979,471	Khanuja et al.
9	2005	Oral pharmaceutical compositions containing taxanes and methods of treatment employing the same	6,964,946	Gutierrez-Rocca et al.
10	2005	Use of bioactive fraction from cow urine distillate ('Gomutra') as a bio-enhancer of anti-infective, anticancer agent and nutrients	6,896,907	Khanuja et al.
11	2005	Pharmaceutical compositions including ACE/ NEP inhibitors and bioavailability enhancers	6,890,918	Burnside et al.
12	2005	Nitrile glycoside useful as a bio-enhancer of drugs and nutrients, process of its isolation from <i>Moringa Oleifera</i>	6,858,588	Khanuja et al.
13	2005	Method of increased bioavailability of nutrients and pharmaceutical preparation with tetrahydropiperine /and its analogues and derivatives	6,849,645	Majeed et al.

14.	2005	Microcapsule matrix microspheres, absorption-enhancing pharmaceutical compositions and methods	6,849,271	Vaghefi et al.
15.	2004	Method, Composition and kits for increasing the oral bioavailability of pharmaceutical agents	6,803,373	Schellens et al.
16	2004	Method and compositions for administering taxanes orally to human patients	6,730,698	Broder et al.
17.	2003	Anti First Pass Effect compounds	6,660,766	Harris et al.
18.	2003	Process for preparation of pharmaceutical composition containing antiretroviral protease inhibitor with improved bioavailability	WO 03/084462	Khamar et al.
19.	2003	Composition having improved bioavailability	6,579,898	Humphry et al.
20.	2003	Composition and method for treating the effects of diseases and maladies	6,576,267	Gelber et al.
21.	2003	Method, Compositions and kits for increasing the oral bioavailability of pharmaceutical agents	6,610,735	Broder et al.
22	2002	Anti-First-Pass Effect compounds	6,476,066	Harris et al.
23	2002	Pharmaceutical composition containing cow urine distillate and an antibiotic	6,410,059	Khanuja et al.
24	2002	Process for extraction of piperine from piper species	6,365,601	Gaikar et al.
25	2000	Process for making high purity piperine for nutritional use	6,054,585	Majeed et al.
26	2002	Combinations for use in increasing the potency of a substrate for multidrug resistance related protein	6,413,937	Cylnes et al.
27	2002	Formulations for the treatment of gastro-oesophageal reflux	6,348,502	Gardiner et al.
28	2001	Triglyceride free compositions and methods for enhanced absorption of hydrophilic therapeutic agents	6,309,663	Patel et al.
29	2001	Herbal composition and method of manufacturing such composition for the management of gynecological disorders	2001/0055625	Katiyar et al.
30	2001	Multi-component biological vehicle	2001/0006983	Jia et al.
31	2001	Anti-first pass effect compounds and citrus extract	6,255,337	Harris et al.
32	2001	Anti-first pass effect compounds	6,248,776	Harris et al.

33	2001	Method, compositions and kits for increasing the oral bioavailability of pharmaceutical agents	6,245,805	Broder et al.
34	2001	Bio-enhancer	6,228,265	Henderson et al.
35	2001	Use of gallic acid esters to increase bioavailability of orally administered pharmaceutical compounds	6,180,666	Wacher et al.
36	2000	Anti-first pass effect compounds	6,162,479	Harris et al.
37	2000	Anti-first pass effect compounds	6,124,477	Harris et al.
38	2002	Chemo sensitizer	WO 02/00164	Khamar et al.
39	2000	Anti-first pass effect compounds	6,063,809	Harris et al.
40	2000	Pharmaceutical composition containing at least one NSAID having increased bioavailability	6,017,932	Singh et al.
41	2000	Anti-first pass effect compounds	6, 054,477	Harris et al.
42	2000	Process for making high purity piperine for nutritional use	6, 054,585	Majeed et al
43	1999	Anti-first pass effect compounds and citrus extract	5,990,154	Harris et al.
44	1999	High temperature extraction of spices and herbs	5,985,352	Todd et al.
45	1999	Use of piperine as a bioavailability enhancer	5,972,382	Majeed et al.
46	1999	Citrus extract	5,962,044	Harris et al.
47	1999	Propyl gallate to increase bioavailability of orally administered pharmaceutical compounds	5,962,522	Wacher et al.
48	1999	Use of benzongum to inhibit p-glycoprotein-mediated resistance of pharmaceutical compounds	5,916,566	Benet et al.
49	1998	Method for the preparation of a first-pass effective citrus derived substance and product thereof	5,820,915	Harris et al.
50	1998	Use of piperine as a bioavailability enhancer	5,744,161	Majeed et al.
51	1998	Use of essential oils to increase bioavailability of oral pharmaceutical compounds	5,716,928	Benet et al.
52	1997	Use of essential oils to increase bioavailability of oral pharmaceutical compounds	5,665,386	Benet et al.
53	1997	Compositions containing piperine	5,616,593	Patel

				et al.
54	1996	Screening method for the identification of bio-enhancers through the inhibition of P-Glycoprotein transport in the gut of a mammal	5,567,592	Benet et al.
55	1996	Use of piperine to increase the bioavailability of nutritional compounds	5, 536,506	Majeed et al.

Annexure II

Protein estimation by Lowry method

(Lowry O.H., Rosebrough N.J., Farr A.L., Randell R.J. Protein measurement with Folin phenol reagent. Journal of Biological Chemistry. 1951, 193: 265-275).

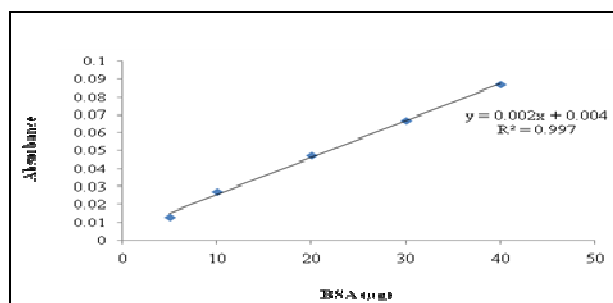
- Reagent A: Na_2CO_3 2 g in 100 ml of 0.1 N NaOH.
- Reagent B: CuSO_4 500 mg in 1 % sodium tartarate (freshly prepared).
- Reagent C: 98 ml of reagent A mixed with 2 ml of reagent B just before use.
- Folin's reagent: Folin ciocalteu reagent diluted with distilled water (1:4 v/v)
- Protein standard: Bovine serum albumin (BSA), 5 mg/10 ml of distilled water.

Assay

Addition	Blank	Test	Standard BSA
Test sample	1.0 ml	1.0 ml	0-50 $\mu\text{g/ml}$
Reagent C	5.0	5.0	5.0
Incubated at room temp. for 10 min			
Folin's Reagent	500 μl	500 μl	500 μl

After 30 min, OD of the samples was recorded at 650 nm against blank by using spectrophotometer.

Calibration curve of BSA



Annexure III

Pi estimation by Fiske- Subbarow Method

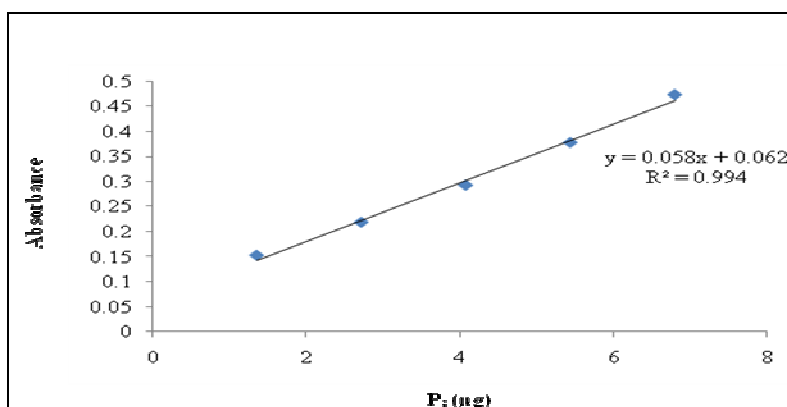
- **Potassium phosphate:** 1 mM
- **SDS:** 5%
- **P_i reagent:** 1 % ammonium molybdate in 2.5 N H₂SO₄ and 0.014% antimony potassium tartarate ; Ascorbic acid: 1%

Assay

Addition	Blank	Test	Standard Pi
Test sample	100 µl	10-100 µl	0-100 µg/ml
d.w	1.0 ml	1.0 ml	100-0 µl
SDS	100 µl	100 µl	100 µl
Pi reagent	400 µl	400 µl	400 µl
Vortex for 10 min.			

OD of the samples was recorded at 660 nm against blank by using spectrophotometer.

Calibration curve of Pi

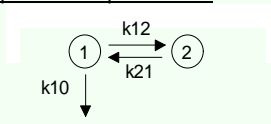


Annexure IV: PK software Data

Pharmacokinetic Data from Summit 2 PK Software

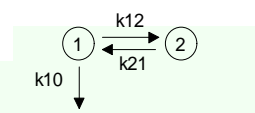
Description: enter description RIF
 RIF Alone

Adjust Number of Terms to Use →		3 <input type="text" value="3 terms"/>	1	2	3	
Routes	Pharmacokinetic Parameters	Total Curve	E Phase	D/A Phase	A Phase	
	<u>General disposition parameters:</u>					
iv, oral	Dose Amount	µg	40000.0			
iv, oral	Dosage	µg/kg	40000.0			
oral	Fraction dose absorbed (F)		1.00			
iv, oral	Intercept	µg/ml	4.412	6.575	-5.133	
iv, oral	Slope	1/hr	-0.045	-0.085	-0.085	
iv, oral	Rate	1/hr	0.104	0.196	0.195	
iv, oral	Half-life	hr	6.636	3.544	3.548	
	<u>Descriptive curve parameters:</u>					
iv	C initial (iv)	µg/ml	5.9	4.4	6.6	-5.1
oral	Cmax (obs)	µg/ml	9.1			
oral	Tmax (obs)	hr	3.0			
oral	Cmax (calculated)	µg/ml	n/a			
oral	Tmax (calculated)	hr	n/a			
oral	Lag time	hr	n/a			
	<u>Curve area calculations:</u>					
iv, oral	AUC(0-t) (obs area)	µg-hr/ml	70.3			
iv, oral	AUC∞ (area)	µg-hr/ml	73.8			
iv, oral	AUC∞ (expo)	µg-hr/ml	49.6	42.2	33.6	-26.3
iv, oral	% of AUC∞ (expo)	%	100.0	85.2	67.8	-53.0
	<u>Statistical moment calculations:</u>					
iv, oral	AUMC∞ (area)	µg-hr*hr/ml	577.6			
iv, oral	AUMC∞ (expo)	µg-hr*hr/ml	442.0	404.5	172.0	-134.5
iv, oral	% of AUMC∞ (expo)	%	100.0	91.5	38.9	-30.4
iv, oral	MRT (area)	hr	7.8			
iv, oral	MRT (expo)	hr	19.8	9.6	5.1	5.1
	<u>Volume of distribution calculations:</u>					
iv	Vc (initial central comp)	ml	6832.0	9066.3	3640.5	6832.0
iv, oral	Vd (obs area)	ml	5446.5			
iv, oral	Vd (area)	ml	5192.0			
iv, oral	Vd (area) / kg	ml/kg	5192.0			
iv, oral	Vd (expo)	ml	7721.8			
iv	Vss (area)	ml	4245.5			
iv	Vss (expo)	ml	7186.4	9066.3	4005.6	7186.4
	<u>Clearance calculations:</u>					
iv, oral	CL (obs area)	ml/hr	568.804			
iv, oral	CL (area)	ml/hr	542.225			

iv, oral	CL (area) / kg	ml/hr/kg	542.225			
iv, oral	CL (expo)	ml/hr	806.422	946.832	527.171	806.422
<u>Additional calculations:</u>						
iv	Half-life from Vd and CL	hr	6.6			
<u>2-Compartment Open Model:</u>						
iv	k12		1/hr	n/a	0.014	
iv	k21		1/hr	n/a	0.141	
iv	k10		1/hr	n/a	0.145	

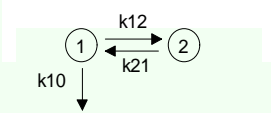
Description: RIF + FG-3

Adjust Number of Terms to Use →		3 terms <input type="button" value="v"/>	1	2	3	
Routes	Pharmacokinetic Parameters	Total Curve	E Phase	D/A Phase	A Phase	
<u>General disposition parameters:</u>						
iv, oral	Dose Amount	µg	40000.0			
iv, oral	Dosage	µg/kg	40000.0			
oral	Fraction dose absorbed (F)		1.00			
iv, oral	Intercept	µg/ml	3.863	24.201	-29.796	
iv, oral	Slope	1/hr	-0.027	-0.104	-0.306	
iv, oral	Rate	1/hr	0.062	0.239	0.706	
iv, oral	Half-life	hr	11.154	2.900	0.982	
<u>Descriptive curve parameters:</u>						
iv	C initial (iv)	µg/ml	-1.7	3.9	24.2	-29.8
oral	Cmax (obs)	µg/ml	12.3			
oral	Tmax (obs)	hr	3.0			
oral	Cmax (calculated)	µg/ml	n/a			
oral	Tmax (calculated)	hr	n/a			
oral	Lag time	hr	n/a			
<u>Curve area calculations:</u>						
iv, oral	AUC(0-t) (obs area)	µg-hr/ml	106.9			
iv, oral	AUC∞ (area)	µg-hr/ml	120.9			
iv, oral	AUC∞ (expo)	µg-hr/ml	121.2	62.2	101.3	-42.2
iv, oral	% of AUC∞ (expo)	%	100.0	51.3	83.5	-34.8
<u>Statistical moment calculations:</u>						
iv, oral	AUMC∞ (area)	µg-hr*hr/ml	1325.7			
iv, oral	AUMC∞ (expo)	µg-hr*hr/ml	1365.0	1000.9	423.9	-59.8
iv, oral	% of AUMC∞ (expo)	%	100.0	73.3	31.1	-4.4
iv, oral	MRT (area)	hr	11.0			
iv, oral	MRT (expo)	hr	21.7	16.1	4.2	1.4
<u>Volume of distribution calculations:</u>						
iv	Vc (initial central comp)	ml	-23094.3	10353.6	1425.3	-

iv, oral	Vd (obs area)	ml	6023.9			23094.3
iv, oral	Vd (area)	ml	5326.1			
iv, oral	Vd (area) / kg	ml/kg	5326.1			
iv, oral	Vd (expo)	ml	5310.1			
iv	Vss (area)	ml	3629.0			
iv	Vss (expo)	ml	3714.0	10353.6	2132.7	3714.0
<u>Clearance calculations:</u>						
iv, oral	CL (obs area)	ml/hr	374.257			
iv, oral	CL (area)	ml/hr	330.902			
iv, oral	CL (area) / kg	ml/hr/kg	330.902			
iv, oral	CL (expo)	ml/hr	329.908	643.250	244.693	329.908
<u>Additional calculations:</u>						
iv	Half-life from Vd and CL	hr	11.2			
<u>2-Compartment Open Model:</u>						
iv	k12		1/hr	n/a		0.043
iv	k21		1/hr	n/a		0.086
iv	k10		1/hr	n/a		0.172

Description: **enter description**
RIF in presence of
INH +PZA

Adjust Number of Terms to Use →			3 terms ▼	1	2	3
Routes	Pharmacokinetic Parameters	Total Curve	E Phase	D/A Phase	A Phase	
iv, oral	<u>General disposition parameters:</u>					
iv, oral	Dose Amount µg	40000.0				
iv, oral	Dosage µg/kg	40000.0				
oral	Fraction dose absorbed (F)	1.00				
iv, oral	Intercept µg/ml		6.552	0.006	-2.346	
iv, oral	Slope 1/hr		-0.046	0.147	-0.206	
iv, oral	Rate 1/hr		0.106	-0.338	0.475	
iv, oral	Half-life hr		6.563	-2.052	1.460	
<u>Descriptive curve parameters:</u>						
iv	C initial (iv) µg/ml	4.2	6.6	0.0	-2.3	
oral	Cmax (obs) µg/ml	6.9				
oral	Tmax (obs) hr	3.0				
oral	Cmax (calculated) µg/ml	n/a				
oral	Tmax (calculated) hr	n/a				
oral	Lag time hr	n/a				
<u>Curve area calculations:</u>						
iv, oral	AUC(0-t) (obs area) µg-hr/ml	53.1				

iv, oral	AUC ∞ (area)	$\mu\text{g-hr/ml}$	58.0			
iv, oral	AUC ∞ (expo)	$\mu\text{g-hr/ml}$	57.1	62.0	0.0	-4.9
iv, oral	% of AUC ∞ (expo)	%	100.0	108.7	0.0	-8.7
<u>Statistical moment calculations:</u>						
iv, oral	AUMC ∞ (area)	$\mu\text{g-hr}^2\text{/ml}$	579.8			
iv, oral	AUMC ∞ (expo)	$\mu\text{g-hr}^2\text{/ml}$	577.3	587.7	0.0	-10.4
iv, oral	% of AUMC ∞ (expo)	%	100.0	101.8	0.0	-1.8
iv, oral	MRT (area)	hr	10.0			
iv, oral	MRT (expo)	hr	8.6	9.5	-3.0	2.1
<u>Volume of distribution calculations:</u>						
iv	Vc (initial central comp)	ml	9497.2	6105.4	6100.1	9497.2
iv, oral	Vd (obs area)	ml	7131.8			
iv, oral	Vd (area)	ml	6526.7			
iv, oral	Vd (area) / kg	ml/kg	6526.7			
iv, oral	Vd (expo)	ml	6635.7			
iv	Vss (area)	ml	6884.2			
iv	Vss (expo)	ml	7085.0	6105.4	6109.2	7085.0
<u>Clearance calculations:</u>						
iv, oral	CL (obs area)	ml/hr	753.033			
iv, oral	CL (area)	ml/hr	689.140			
iv, oral	CL (area) / kg	ml/hr/kg	689.140			
iv, oral	CL (expo)	ml/hr	700.651	644.648	644.822	700.651
<u>Additional calculations:</u>						
iv	Half-life from Vd and CL	hr	6.6			
<u>2-Compartment Open Model:</u>						
iv	k12		1/hr	n/a		-0.001
iv	k21		1/hr	n/a		-0.337
iv	k10		1/hr	n/a		0.106

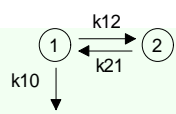
Description:

RIF in presence of INH + PZA + Fg-3

enter description

Adjust Number of Terms to Use →		3 terms	1	2	3
Routes	Pharmacokinetic Parameters	Total Curve	E Phase	D/A Phase	A Phase
iv, oral	General disposition parameters:				
iv, oral	Dose Amount μg	40000.0			
iv, oral	Dosage $\mu\text{g/kg}$	40000.0			
oral	Fraction dose absorbed (F)	1.00			
iv, oral	Intercept $\mu\text{g/ml}$		5.759	418.029	-442.712

iv, oral	Slope	1/hr		-0.028	-0.297	-0.317
iv, oral	Rate	1/hr		0.064	0.685	0.730
iv, oral	Half-life	hr		10.885	1.012	0.950
<u>Descriptive curve parameters:</u>						
iv	C initial (iv)	µg/ml	-18.9	5.8	418.0	-442.7
oral	Cmax (obs)	µg/ml	9.4			
oral	Tmax (obs)	hr	3.0			
oral	Cmax (calculated)	µg/ml	n/a			
oral	Tmax (calculated)	hr	n/a			
oral	Lag time	hr	n/a			
<u>Curve area calculations:</u>						
iv, oral	AUC(0-t) (obs area)	µg-hr/ml	83.4			
iv, oral	AUC∞ (area)	µg-hr/ml	103.0			
iv, oral	AUC∞ (expo)	µg-hr/ml	94.4	90.5	610.5	-606.6
iv, oral	% of AUC∞ (expo)	%	100.0	95.9	646.9	-642.8
<u>Statistical moment calculations:</u>						
iv, oral	AUMC∞ (area)	µg-hr ² /ml	1495.0			
iv, oral	AUMC∞ (expo)	µg-hr ² /ml	1481.4	1420.9	891.7	-831.2
iv, oral	% of AUMC∞ (expo)	%	100.0	95.9	60.2	-56.1
iv, oral	MRT (area)	hr	14.5			
iv, oral	MRT (expo)	hr	18.5	15.7	1.5	1.4
<u>Volume of distribution calculations:</u>						
iv	Vc (initial central comp)	ml	-2113.7	6945.3	94.4	-2113.7
iv, oral	Vd (obs area)	ml	7536.6			
iv, oral	Vd (area)	ml	6099.9			
iv, oral	Vd (area) / kg	ml/kg	6099.9			
iv, oral	Vd (expo)	ml	6657.4			
iv	Vss (area)	ml	5636.8			
iv	Vss (expo)	ml	6653.0	6945.3	188.2	6653.0
<u>Clearance calculations:</u>						
iv, oral	CL (obs area)	ml/hr	479.812			
iv, oral	CL (area)	ml/hr	388.349			
iv, oral	CL (area) / kg	ml/hr/kg	388.349			
iv, oral	CL (expo)	ml/hr	423.840	442.168	57.062	423.840
<u>Additional calculations:</u>						
iv	Half-life from Vd and CL	hr	10.9			
<u>2-Compartment Open Model:</u>						
iv	k12	1/hr	n/a		0.072	
iv	k21	1/hr	n/a		0.072	
iv	k10	1/hr	n/a		0.605	



Description: enter description

Rif In
presence
of
INH+PZA
+ CR-
1(1)

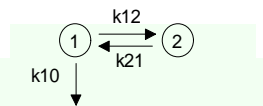
Adjust Number of Terms to Use →		3 terms <input type="button" value="v"/>	1	2	3	
Routes	Pharmacokinetic Parameters	Total Curve	E Phase	D/A Phase	A Phase	
	<u>General disposition parameters:</u>					
iv, oral	Dose Amount	µg	40000.0			
iv, oral	Dosage	µg/kg	40000.0			
oral	Fraction dose absorbed (F)		1.00			
iv, oral	Intercept	µg/ml	6.181	59.351	-60.612	
iv, oral	Slope	1/hr	-0.042	-0.243	-0.298	
iv, oral	Rate	1/hr	0.097	0.560	0.686	
iv, oral	Half-life	hr	7.181	1.238	1.011	
	<u>Descriptive curve parameters:</u>					
iv	C initial (iv)	µg/ml	4.9	6.2	59.4	-60.6
oral	Cmax (obs)	µg/ml	11.3			
oral	Tmax (obs)	hr	3.0			
oral	Cmax (calculated)	µg/ml	n/a			
oral	Tmax (calculated)	hr	n/a			
oral	Lag time	hr	n/a			
	<u>Curve area calculations:</u>					
iv, oral	AUC(0-t) (obs area)	µg-hr/ml	70.5			
iv, oral	AUC∞ (area)	µg-hr/ml	76.8			
iv, oral	AUC∞ (expo)	µg-hr/ml	81.6	64.0	106.0	-88.4
iv, oral	% of AUC∞ (expo)	%	100.0	78.5	129.8	-108.3
	<u>Statistical moment calculations:</u>					
iv, oral	AUMC∞ (area)	µg-hr*hr/ml	721.9			
iv, oral	AUMC∞ (expo)	µg-hr*hr/ml	724.0	663.6	189.3	-128.9
iv, oral	% of AUMC∞ (expo)	%	100.0	91.7	26.1	-17.8
iv, oral	MRT (area)	hr	9.4			
iv, oral	MRT (expo)	hr	13.6	10.4	1.8	1.5
	<u>Volume of distribution calculations:</u>					
iv	Vc (initial central comp)	ml	8128.6	6471.4	610.4	8128.6
iv, oral	Vd (obs area)	ml	5877.8			
iv, oral	Vd (area)	ml	5394.3			
iv, oral	Vd (area) / kg	ml/kg	5394.3			
iv, oral	Vd (expo)	ml	5076.9			
iv	Vss (area)	ml	4891.3			
iv	Vss (expo)	ml	4345.2	6471.4	1179.9	4345.2
	<u>Clearance calculations:</u>					
iv, oral	CL (obs area)	ml/hr	567.255			
iv, oral	CL (area)	ml/hr	520.591			

iv, oral	CL (area) / kg	ml/hr/kg	520.591			
iv, oral	CL (expo)	ml/hr	489.965	624.544	235.231	489.965
	<u>Additional calculations:</u>					
iv	Half-life from Vd and CL	hr	7.2			
	<u>2-Compartment Open Model:</u>					
iv	k12		1/hr	n/a		0.131
iv	k21		1/hr	n/a		0.140
iv	k10		1/hr	n/a		0.385

Description:

INH in presence of RIF + PZA

Adjust Number of Terms to Use →		3 terms <input type="button" value="v"/>	1	2	3
Routes	Pharmacokinetic Parameters	Total Curve	E Phase	D/A Phase	A Phase
iv, oral	<u>General disposition parameters:</u>				
iv, oral	Dose Amount µg	30000.0			
iv, oral	Dosage µg/kg	30000.0			
oral	Fraction dose absorbed (F)	1.00			
iv, oral	Intercept µg/ml		11.620	126.806	-128.841
iv, oral	Slope 1/hr		-0.084	-0.271	-0.244
iv, oral	Rate 1/hr		0.194	0.625	0.562
iv, oral	Half-life hr		3.568	1.110	1.233
	<u>Descriptive curve parameters:</u>				
iv	C initial (iv) µg/ml	9.6	11.6	126.8	-128.8
oral	Cmax (obs) µg/ml	4.7			
oral	Tmax (obs) hr	2.0			
oral	Cmax (calculated) µg/ml	n/a			
oral	Tmax (calculated) hr	n/a			
oral	Lag time hr	n/a			

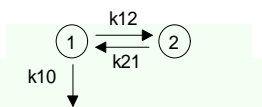
	<u>Curve area calculations:</u>							
iv, oral	AUC(0-t) (obs area)	µg-hr/ml	30.9					
iv, oral	AUC ∞ (area)	µg-hr/ml	31.5					
iv, oral	AUC ∞ (expo)	µg-hr/ml	33.7	59.8	203.0			-229.2
iv, oral	% of AUC ∞ (expo)	%	100.0	177.7	603.1			-680.8
	<u>Statistical moment calculations:</u>							
iv, oral	AUMC ∞ (area)	µg-hr*hr/ml	225.3					
iv, oral	AUMC ∞ (expo)	µg-hr*hr/ml	225.5	308.1	325.1			-407.7
iv, oral	% of AUMC ∞ (expo)	%	100.0	136.7	144.2			-180.9
iv, oral	MRT (area)	hr	7.2					
iv, oral	MRT (expo)	hr	8.5	5.1	1.6			1.8
	<u>Volume of distribution calculations:</u>							
iv	Vc (initial central comp)	ml	3129.9	2581.6	216.7			3129.9
iv, oral	Vd (obs area)	ml	4998.5					
iv, oral	Vd (area)	ml	4908.5					
iv, oral	Vd (area) / kg	ml/kg	4908.5					
iv, oral	Vd (expo)	ml	4588.5					
iv	Vss (area)	ml	6824.7					
iv	Vss (expo)	ml	5967.6	2581.6	274.9			5967.6
	<u>Clearance calculations:</u>							
iv, oral	CL (obs area)	ml/hr	970.717					
iv, oral	CL (area)	ml/hr	953.246					
iv, oral	CL (area) / kg	ml/hr/kg	953.246					
iv, oral	CL (expo)	ml/hr	891.111	501.365	114.126			891.111
	<u>Additional calculations:</u>							
iv	Half-life from Vd and CL	hr	3.6					
	<u>2-Compartment Open Model:</u>							
iv	k12		1/hr	n/a		0.062		
iv	k21		1/hr	n/a		0.230		
iv	k10		1/hr	n/a		0.527		

Description: enter description

PZA in
presence
of RIF +
INH

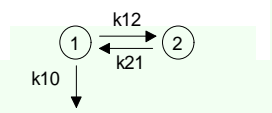
Adjust Number of Terms to Use →		3 terms <input type="button" value="v"/>	1	2	3
Routes	Pharmacokinetic Parameters	Total Curve	E Phase	D/A Phase	A Phase
	<u>General disposition parameters:</u>				

iv, oral	Dose Amount	µg	90000.0			
iv, oral	Dosage	µg/kg	90000.0			
oral	Fraction dose absorbed (F)		1.00			
iv, oral	Intercept	µg/ml		10.540	162.028	-250.016
iv, oral	Slope	1/hr		-0.061	-0.207	-0.385
iv, oral	Rate	1/hr		0.140	0.478	0.886
iv, oral	Half-life	hr		4.965	1.451	0.782
<u>Descriptive curve parameters:</u>						
iv	C initial (iv)	µg/ml	-77.4	10.5	162.0	-250.0
oral	Cmax (obs)	µg/ml	26.3			
oral	Tmax (obs)	hr	2.0			
oral	Cmax (calculated)	µg/ml	n/a			
oral	Tmax (calculated)	hr	n/a			
oral	Lag time	hr	n/a			
<u>Curve area calculations:</u>						
iv, oral	AUC(0-t) (obs area)	µg-hr/ml	157.2			
iv, oral	AUC∞ (area)	µg-hr/ml	159.9			
iv, oral	AUC∞ (expo)	µg-hr/ml	132.5	75.5	339.2	-282.2
iv, oral	% of AUC∞ (expo)	%	100.0	57.0	256.0	-213.0
<u>Statistical moment calculations:</u>						
iv, oral	AUMC∞ (area)	µg-hr*hr/ml	922.7			
iv, oral	AUMC∞ (expo)	µg-hr*hr/ml	932.4	541.0	710.0	-318.5
iv, oral	% of AUMC∞ (expo)	%	100.0	58.0	76.1	-34.2
iv, oral	MRT (area)	hr	5.8			
iv, oral	MRT (expo)	hr	10.4	7.2	2.1	1.1
<u>Volume of distribution calculations:</u>						
iv	Vc (initial central comp)	ml	-1162.1	8539.1	521.5	-1162.1
iv, oral	Vd (obs area)	ml	4100.4			
iv, oral	Vd (area)	ml	4032.4			
iv, oral	Vd (area) / kg	ml/kg	4032.4			
iv, oral	Vd (expo)	ml	4866.2			
iv	Vss (area)	ml	3248.1			
iv	Vss (expo)	ml	4780.1	8539.1	654.7	4780.1
<u>Clearance calculations:</u>						
iv, oral	CL (obs area)	ml/hr	572.348			
iv, oral	CL (area)	ml/hr	562.860			
iv, oral	CL (area) / kg	ml/hr/kg	562.860			
iv, oral	CL (expo)	ml/hr	679.246	1191.917	217.038	679.246
<u>Additional calculations:</u>						
iv	Half-life from Vd and CL	hr	5.0			
<u>2-Compartment Open Model:</u>						
iv	k12	1/hr	n/a		0.041	
iv	k21	1/hr	n/a		0.160	
iv	k10	1/hr	n/a		0.416	



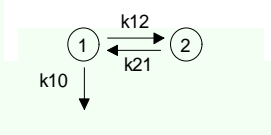
enter description
 INH in presence of
 Description: RIF +PZA + CR-1(1)

Adjust Number of Terms to Use →		3 terms ▼	1	2	3
Routes	Pharmacokinetic Parameters	Total Curve	E Phase	D/A Phase	A Phase
	<u>General disposition parameters:</u>				
iv, oral	Dose Amount μg	30000.0			
iv, oral	Dosage $\mu\text{g}/\text{kg}$	30000.0			
oral	Fraction dose absorbed (F)	1.00			
iv, oral	Intercept $\mu\text{g}/\text{ml}$		9.764	0.994	-5.161
iv, oral	Slope $1/\text{hr}$		-0.080	-0.064	-0.131
iv, oral	Rate $1/\text{hr}$		0.183	0.148	0.301
iv, oral	Half-life hr		3.780	4.669	2.304
	<u>Descriptive curve parameters:</u>				
iv	C initial (iv) $\mu\text{g}/\text{ml}$	5.6	9.8	1.0	-5.2
oral	Cmax (obs) $\mu\text{g}/\text{ml}$	6.7			
oral	Tmax (obs) hr	2.0			
oral	Cmax (calculated) $\mu\text{g}/\text{ml}$	n/a			
oral	Tmax (calculated) hr	n/a			
oral	Lag time hr	n/a			
	<u>Curve area calculations:</u>				
iv, oral	AUC(0-t) (obs area) $\mu\text{g}\text{-hr}/\text{ml}$	39.2			
iv, oral	AUC ∞ (area) $\mu\text{g}\text{-hr}/\text{ml}$	39.9			
iv, oral	AUC ∞ (expo) $\mu\text{g}\text{-hr}/\text{ml}$	42.8	53.3	6.7	-17.2
iv, oral	% of AUC ∞ (expo) %	100.0	124.4	15.6	-40.1
	<u>Statistical moment calculations:</u>				
iv, oral	AUMC ∞ (area) $\mu\text{g}\text{-hr}^2/\text{ml}$	268.1			
iv, oral	AUMC ∞ (expo) $\mu\text{g}\text{-hr}^2/\text{ml}$	278.6	290.5	45.1	-57.0
iv, oral	% of AUMC ∞ (expo) %	100.0	104.3	16.2	-20.5
iv, oral	MRT (area) hr	6.7			
iv, oral	MRT (expo) hr	15.5	5.5	6.7	3.3
	<u>Volume of distribution calculations:</u>				
iv	Vc (initial central comp) ml	5358.8	3072.4	2788.4	5358.8
iv, oral	Vd (obs area) ml	4171.9			
iv, oral	Vd (area) ml	4103.4			

iv, oral	Vd (area) / kg	ml/kg	4103.4			
iv, oral	Vd (expo)	ml	3823.0			
iv	Vss (area)	ml	5056.5			
iv	Vss (expo)	ml	4562.0	3072.4	2800.8	4562.0
<u>Clearance calculations:</u>						
iv, oral	CL (obs area)	ml/hr	764.818			
iv, oral	CL (area)	ml/hr	752.265			
iv, oral	CL (area) / kg	ml/hr/kg	752.265			
iv, oral	CL (expo)	ml/hr	700.848	563.243	500.317	700.848
<u>Additional calculations:</u>						
iv	Half-life from Vd and CL	hr	3.8			
<u>2-Compartment Open Model:</u>						
iv	k12		1/hr	n/a	0.001	
iv	k21		1/hr	n/a	0.152	
iv	k10		1/hr	n/a	0.179	

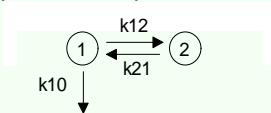
enter description
Description: PZA in presence of RIF + INH + CR-1(1)

Adjust Number of Terms to Use →		3 terms <input type="button" value="▼"/>	1	2	3
Routes	Pharmacokinetic Parameters	Total Curve	E Phase	D/A Phase	A Phase
iv, oral	<u>General disposition parameters:</u>				
iv, oral	Dose Amount µg	90000.0			
iv, oral	Dosage µg/kg	90000.0			
oral	Fraction dose absorbed (F)	1.00			
iv, oral	Intercept µg/ml		7.534	839.316	-1328.535
iv, oral	Slope 1/hr		-0.045	-0.281	-0.434
iv, oral	Rate 1/hr		0.105	0.647	1.000
iv, oral	Half-life hr		6.615	1.071	0.693
<u>Descriptive curve parameters:</u>					
iv	C initial (iv) µg/ml	-481.7	7.5	839.3	-1328.5
oral	Cmax (obs) µg/ml	41.3			
oral	Tmax (obs) hr	2.0			
oral	Cmax (calculated) µg/ml	n/a			
oral	Tmax (calculated) hr	n/a			
oral	Lag time hr	n/a			
<u>Curve area calculations:</u>					
iv, oral	AUC(0-t) (obs area) µg-hr/ml	224.8			
iv, oral	AUC∞ (area) µg-hr/ml	230.6			
iv, oral	AUC∞ (expo) µg-hr/ml	39.9	71.9	1296.9	-1328.9
iv, oral	% of AUC∞ (expo) %	100.0	180.2	3249.0	-3329.2

	<u>Statistical moment calculations:</u>						
iv, oral	AUMC ∞ (area)	$\mu\text{g}\cdot\text{hr}^2/\text{ml}$	1298.3				
iv, oral	AUMC ∞ (expo)	$\mu\text{g}\cdot\text{hr}^2/\text{ml}$	1361.2	686.5	2004.0	-1329.3	
iv, oral	% of AUMC ∞ (expo)	%	100.0	50.4	147.2	-97.7	
iv, oral	MRT (area)	hr	5.6				
iv, oral	MRT (expo)	hr	12.1	9.5	1.5	1.0	
	<u>Volume of distribution calculations:</u>						
iv	Vc (initial central comp)	ml	-186.8	11946.6	106.3	-186.8	
iv, oral	Vd (obs area)	ml	3822.2				
iv, oral	Vd (area)	ml	3725.7				
iv, oral	Vd (area) / kg	ml/kg	3725.7				
iv, oral	Vd (expo)	ml	21523.3				
iv	Vss (area)	ml	2197.3				
iv	Vss (expo)	ml	76886.7	11946.6	129.2	76886.7	
	<u>Clearance calculations:</u>						
iv, oral	CL (obs area)	ml/hr	400.396				
iv, oral	CL (area)	ml/hr	390.285				
iv, oral	CL (area) / kg	ml/hr/kg	390.285				
iv, oral	CL (expo)	ml/hr	2254.665	1251.463	65.750	2254.665	
	<u>Additional calculations:</u>						
iv	Half-life from Vd and CL	hr	6.6				
	<u>2-Compartment Open Model:</u>						
iv	k12		1/hr	n/a	0.024		
iv	k21		1/hr	n/a	0.110		
iv	k10		1/hr	n/a	0.619		

Description: RIF I.V.

Adjust Number of Terms to Use →		3 terms <input type="button" value="v"/>	1	2	3
Routes	Pharmacokinetic Parameters	Total Curve	E Phase	D/A Phase	A Phase
iv, oral	<u>General disposition parameters:</u>				
iv, oral	Dose Amount μg	7500.0			
oral	Dosage $\mu\text{g}/\text{kg}$	7500.0			
oral	Fraction dose absorbed (F)	1.00			
iv, oral	Intercept $\mu\text{g}/\text{ml}$		0.526	13.311	12.397
iv, oral	Slope 1/hr		-0.004	-0.276	-0.358
iv, oral	Rate 1/hr		0.009	0.636	0.826
iv, oral	Half-life hr		73.921	1.089	0.839
	<u>Descriptive curve parameters:</u>				

iv	C initial (iv)	µg/ml	26.2	0.5	13.3	12.4
oral	Cmax (obs)	µg/ml	26.2			
oral	Tmax (obs)	hr	0.0			
oral	Cmax (calculated)	µg/ml	n/a			
oral	Tmax (calculated)	hr	n/a			
oral	Lag time	hr	n/a			
<u>Curve area calculations:</u>						
iv, oral	AUC(0-t) (obs area)	µg-hr/ml	20.6			
iv, oral	AUC _∞ (area)	µg-hr/ml	65.4			
iv, oral	AUC _∞ (expo)	µg-hr/ml	92.0	56.1	20.9	15.0
iv, oral	% of AUC _∞ (expo)	%	100.0	61.0	22.7	16.3
<u>Statistical moment calculations:</u>						
iv, oral	AUMC _∞ (area)	µg-hr ² /ml	5999.1			
iv, oral	AUMC _∞ (expo)	µg-hr ² /ml	6035.4	5984.4	32.9	18.2
iv, oral	% of AUMC _∞ (expo)	%	100.0	99.2	0.5	0.3
iv, oral	MRT (area)	hr	91.7			
iv, oral	MRT (expo)	hr	109.5	106.7	1.6	1.2
<u>Volume of distribution calculations:</u>						
iv	Vc (initial central comp)	ml	285.9	14259.8	542.0	285.9
iv, oral	Vd (obs area)	ml	38846.5			
iv, oral	Vd (area)	ml	12233.6			
iv, oral	Vd (area) / kg	ml/kg	12233.6			
iv, oral	Vd (expo)	ml	8692.2			
iv	Vss (area)	ml	10521.1			
iv	Vss (expo)	ml	5343.6	14259.8	7607.0	5343.6
<u>Clearance calculations:</u>						
iv, oral	CL (obs area)	ml/hr	364.180			
iv, oral	CL (area)	ml/hr	114.688			
iv, oral	CL (area) / kg	ml/hr/kg	114.688			
iv, oral	CL (expo)	ml/hr	81.488	133.684	97.373	81.488
<u>Additional calculations:</u>						
iv	Half-life from Vd and CL	hr	73.9			
<u>2-Compartment Open Model:</u>						
iv	k12		1/hr	n/a	0.433	
iv	k21		1/hr	n/a	0.033	
iv	k10		1/hr	n/a	0.180	

PUBLICATIONS

List of Publications

1. **Sachin S. Bhusari**, Vandhna Bhat, Meenakshi Koul, Subhash C. Sharma, Manoj K. Tikoo, Ashok K. Tikoo, Naresh K Satti, Krishan A. Suri, Rakesh K Johri. Development and validation of a RP-HPLC method for the simultaneous determination of active ingredients of a composition containing rifampicin and a flavonoid glycoside; a novel bioavailability enhancer of the drug. Tropical journal of pharmaceutical research, 2009, 8(6): 531-537.

2. **B.S. Sachin**, P. Monica, S.C. Sharma, N. K. Satti, M K. Tikoo, A K. Tikoo, K.A. Suri, B.D. Gupta, R.K Johri. Pharmacokinetic interaction of some antitubercular drugs with caraway: implications in the enhancement of drug bioavailability. Human and experimental toxicology, 2009, 28: 175-184.

3. I.A. Najar, **B.S. Sachin**, S.C. Sharma, N.K. Satti, K.A. Suri, R.K. Johri. Modulation of P-glycoprotein activity by some phytoconstituents. Phytotherapy Research, 2009, 24: 454-458.

4. **B.S. Sachin**, S.C. Sharma, S. Sethi, S.A. Tasduq, M.K. Tikoo, A.K. Tikoo, N.K. Satti, B. D. Gupta, K.A. Suri, R.K. Johri and G.N. Qazi. Herbal Modulation of Drug Bioavailability: Enhancement of Rifampicin Levels in Plasma by Herbal Products and a Flavonoid Glycoside derived from *Cuminum cyminum*. Phytotherapy Research, 2007, 21: 157-163.

List of Presentations

NAME OF AUTHORS	YEAR	TITLE OF PAPER	NAME OF CONFERENCE	AGENCY
B.S. Sachin, SC Sharma, Tikoo MK, Tikoo AK, Satti NK, Suri KA, Johri RK	2006	Enhancement of Rifampicin plasma levels by a flavonoid glycoside	Indian Pharmacological Society, Jaipur	CSIR
B.S. Sachin, P. Monica, SC Sharma, NK Satti, MK Tikoo, AK Tikoo, KA Suri, BD Gupta, RK Johri	2007	Pharmacokinetic interactions of Anti-TB drugs with caraway: implications in the enhancement of drug bioavailability	Indian Pharmacological Society, Chandigarh	CSIR
Sachin BS, Vandhna B, Meenakshi K, Sharma SC, Satti NK, Suri KA, Johri RK	2008	Involvement of CYP3A4/ P-glycoprotein in the mode of action of a flavonoid glycoside (ex: <i>Cuminum cyminum</i>)- a drug bioavailability enhancer.	Society of Biological Chemists, Chennai	CSIR

BIOGRAPHY

Name: **SACHIN SHIVLING BHUSARI**

Address: C/o Dr. R.K. Johri
Scientist G,
PK/PD Toxicology Division
Indian Institute of Integrative Medicine, CSIR
Canal Road, Jammu-180001

Contact: 08055370136

E-mail: sachinsbhusari@gmail.com

Date of Birth: 31-12-1976

Educational Qualification: M. Pharm (BITS, Pilani) (June 2003)
Post Graduate Diploma in Clinical Research
(June 2009)

Area of Research: Pharmacokinetics

Publications: 7 No.

Patent: 1 No.

Supervisor's Biodata

Name: **Dr. R. K. JOHRI**

Present Designation: Deputy Director, Scientist G & Head

Official address: PK/PD/Toxicology Division,
IIIM (CSIR), Canal Road, Jammu-180001
(J&K), India

Telephone number: 0191-2547850

E-mail address: rakeshkjohri@rediffmail.com

Date of Birth: 23.06.1953

Broad field of research interests
with specific areas of involvement: "Herbal Drug Development/Pharmacokinetics/
Biochemistry of cell membrane"

Publications: 57 No.

Patents: 6 No.

Type of industrial and Consultancy
work done: Several sponsored projects by outside agencies
for toxicity/Pharmacokinetics/pharmacological
evaluation of candidate drugs is going on under
my supervision

Visits abroad and nature of assignment: France

Membership of professional societies: SBC, ISC, IPS

Doctoral degrees thesis already supervised: 6 No.

Number of Ph.D. candidates currently
registered under him: 6 No.